ABSTRACT

A study was made to determine the anomalous flow behaviour of very dilute solutions of polyethylene oxide, which is a very effective drag reducing agent in turbulent flow. A capillary tube viscometer was used to determine the rheological properties over low and intermediate shear stress region. Stainless steel and glass capillary tubes were used. For the tubes having $L/D < 950$, three different tube lengths were used to account for the entrance losses. Mathematical models were used to analyze the data. An attempt was made to study the influence of tube wall material on surface effects. Furthermore, the purpose of the present study was also to explain the mechanism underlying the phenomenon of turbulent drag reduction.

Both positive and negative wall effects were obtained in case of above drag reducing system. Flow curves obtained using stainless steel and glass tubes matched very closely. Anomalous layer thickness was found to be more in case of stainless steel tubes than for glass tubes.

ACKNOWLEDGEMENTS

The author is deeply indebted to his supervisor Professor W. Kozicki for his advice, guidance and constant encouragement during the course of this work. He also wishes to acknowledge other faculty members of the department, particularly Dr. F.D.F. Talbot, for permitting the use of Nova computer for the computation work. He further wishes to express his gratitude to Dr. A.R.K. Rao for his valuable assistance in conducting the experimental work.

The author is sincerely thankful to Mr. H.S. Harish for typing the manuscript and Mr. C.P. Khulbe for lettering the drawings. Author is also indebted to Mr. M.K. Dosi for his willing assistance from time to time.

TABLE OF CONTENTS

LIST OF TABLES

.....contd/...

LIST OF TABLES

LIST OF FIGURES

FIGURES PAGE

FIGURES PAGE

LIST OF COMPUTER PROGRAMS

NOMENCLATURE

A	-	Coefficient in the equation 3.B.11, dynes.sec/cm^3
A'	-	Area of the capillary tube, cm^2
A_L	-	Coefficient in the equation 3.B.15, dynes.sec/cm^2.gm
A_1	-	Coefficient in the equation 3.B.11, dynes.sec/cm^2.gm
A_2	-	Coefficient in the equation 3.B.16, dynes.sec/cm^3.gm
A_3	-	Coefficient in the equation 3.B.16, dynes.sec/cm^2.gm
B	-	Coefficient in the equation 3.B.11, dynes.sec^2/cm^3
B_L	-	Coefficient in the equation 3.B.15, dynes.sec^2/cm^2.gm^2
B_1	-	Coefficient in the equation 3.B.11, dynes.sec^2/cm^2.gm^2
B_2	-	Coefficient in the equation 3.B.17, dynes.sec^2/cm^3.gm^2
B_3	-	Coefficient in the equation 3.B.17, dynes.sec^2/cm^2.gm^2
$Ci(L,R)$	-	Coefficient in the equation 3.B.1
$C_{io}(R)$	-	Coefficient in the equation 3.B.3
$C_{i1}(R)$	-	Coefficient in the equation 3.B.3
D	-	Diameter of the capillary tube, cm.
G	-	Average mass flow rate, gm/sec
g	-	Acceleration due to gravity, cm/sec^2
g_c	-	Newton's law conversion factor, gm.cm/gmf.sec^2
h_1	-	Height of the inlet of the capillary tube from the datum,c
h_a	-	Height of the exit of the capillary tube from the datum,cm
k_c	-	Entrance losses correction factor
L	-	Length of the capillary tube, cm
L'	-	Liquid head above the capillary tube inlet, cm
L_e	-	Entrance length, cm
n	-	Entrance length correction factor, dimensionless

n' - Dimensionless factor for circular conduits

P_a - Atmospheric pressure, dynes/cm^2

P_1 - Pressure at the inlet of the capillary tube, dynes/cm^2

P_{gas} - Pressure applied by gas, dynes/cm^2

ΔP - Pressure drop across the capillary tube, dynes/cm^2

R - Radius of the capillary tube, cm

r_h - Hydraulic radius, cm

$\langle u \rangle$ - Average velocity, cm/sec

U_w - Effective slip velocity at the wall, cm/sec

α - Coefficient in the equation 3.C.10, dynes.sec/cm^2

α' - Slip coefficient, cm^3/dynes.sec

α'' - Modified slip coefficient cm^4/dynes.sec

α_1 - Angle between the tube and the vertical axis

α_2 - Kinetic energy correction factor, dimensionless

β - Coefficient in the equation 3.C.10, dynes.sec^2/cm^2

ξ - Slip coefficient, cm^3/dynes.sec

η - Non-Newtonian viscosity, gm/cm.sec

η_w - Non-Newtonian viscosity at the wall gm/cm.sec

ρ - Density, gm/cm^3

δ - Anomalous layer thickness, cm

μ_s - Solvent viscosity, gm/cm.sec

τ - Shear stress, dynes/cm^2

τ_c - Critical shear stress, dynes/cm^2

τ_w - Shear stress at the wall, dynes/cm^2

ω - $\frac{2(\langle u \rangle - U_w)}{r_h} = \frac{8(\langle u \rangle - U_w)}{D}$, sec^{-1}

τ_w' -Difference between the shear stress in the developing flow region and the shear stress in fully developed flow region.

CHAPTER I

INTRODUCTION

Reduction of drag and the power required to overcome the resistance to flow arising from the solid boundaries in contact with the fluid stream, has been the main concern in many practical fluid flow problems. Several means have been studied to reduce drag, but of these, the use of dilute polymer solutions has been the most effective and most widely investigated one. Toms (1,2) in 1948 observed considerable reduction in the frictional losses in turbulent pipe flow of dilute solutions of polymethyl methacrylate in monochlorobenzene. He also reported the presence of wall effects in laminar flow of these solutions. In spite of numerous studies, no acceptable explanation of the mechanism of drag reduction has yet been agreed upon.

The purpose of the present work was to determine anomalous flow behaviour near the solid surface using dilute solutions of a drag reducing polymer. The study was conducted on stainless steel and glass tubes using very dilute solutions of polyethylene oxide (polyox), which is a most effective drag reducing agent. Experimental

measurements were confined to laminar flow regime. The entrance losses were accounted experimentally for each solution* and valuable data was obtained by applying all corrections necessary in a capillary tube viscometer. It was found that different flow curves result for different diameters of capillary tubes on account of anomalous behaviour in the vicinity of the wall of the tube. Due to the presence of the wall effects, the values of shear rate calculated in the normal manner are erroneous and hence a correction was necessary. This involved the determination of the effective velocity, U_w of the fluid at the wall, which is caused by the interaction between the wall of the capillary tube and the polymer molecules in the solution. In the present work a comparitively simple and entirely new procedure was used to determine the true rheological curve.

The problem undertaken becomes particularly challenging when the comparitive study of flow curves for glass and steel tubes is made. A comparison of anomalous layer thickness was made for tubes of approximately the same diameter for the two tube materials. The values of the non-Newtonian viscosity were also compared using both glass and steel tubes for a given concentration.

It was further hoped that this study might

* Except for 20 ppm polyox solution (glass tubes)

furnish some additional information which could help in obtaining an understanding of the phenomena responsible for drag reduction.

CHAPTER II

LITERATURE SURVEY

The phenomenon of "slippage" has long been recognized (3,4,5,6,7), but relatively little work has been done which provides information on the distinct behaviour exhibited by the fluids in the vicinity of the solid surfaces. Schofield and Scott Blair (8) and Oldroyd (9) tried to detect the anomalous behaviour near the tube wall and have received considerable attention. Toms measurements indicated the existence of a thin layer with anisotropic rheological properties near the tube wall whose overall effect could be characterized by a positive effective velocity of slip at the wall. Subsequently Maude and Whitmore (10) and Jastrzebski (11), who studied characteristics of concentrated suspensions and Astarita (12), who studied gravity flow of CMC solutions along the inclined plane surfaces, also detected a wall effect represented by an effective velocity of slip at the wall. Morrison and Harper (13) reported direct visual measurements of slip velocity with a coaxial cylinder viscometer for fibrous suspensions.

On the other hand Luce and Robertson (14) and Koral, Ullmand and Eirich (15) reported adsorption of polyvinyl acetate from solutions by water swollen bleached sulphite pulps and metallic powders respectively. Similar

studies have been made by Hobden and Jellinek (16), Frish, Hellman and Lundberg (17) and Yurzhenko and Maleyev (18). At the same time Sadowski (19,20) and Kozicki et al. (21) in packed bed studies and Ohrn (22), Kozicki et al.(23), and Arunachalam and Fulford (2^4) in capillary flow studies of polymer solutions reported evidence of polymer adsorption on the solid surface. By an extension of Oldroyds analysis Kozicki et al. further showed that polymer adsorption or gel-formation leads to a negative effective velocity on the surface. They have demonstrated the applicability of the analysis to their data (25) and have also proposed a model which explains polymer adsorption and transition to the separation phenomena observed in tubes of different diameters under varying shear stress. It was postulated that polymer molecules adsorbed on the tube wall give rise to a less mobile, more viscous layer in the vicinity of the solid surface which results in decreased flow rates (22). Polymer adsorption seems to be more prominent in the lower shear stress region. As the shear stress is increased, the polymer molecules tend to uncoil and hence the molecules are distorted to elongated ellipsoids. These molecules then tend to align in the direction of flow near the solid boundary. This gradual change in structure to rod-like particles results in a less viscous layer near the solid boundary, as a result of which the flow rate increases. This separation

phenomenon results in a positive effective velocity of slip.

A direct consequence of separation or gel-formation in the vicinity of wall is the observed change in flow rate through the tube compared to that which would occur if the wall effects were absent. Hence a correction must be applied to obtain the true shear rate. This involves determination of anamolous flow behaviour of the fluid near the wall. The problem becomes more interesting with the use of polyox, which is an excellent drag reducing polymer. After the discovery of the Toms phenomenon numerous papers have been published reporting the phenomenon of drag reduction, and several mechanisms have been proposed to explain it. As already mentioned Oldroyd attributed the drag reduction simply to positive wall effects. Kozicki et al. (26) investigated some aspects of wall effects and postulated that the cause of drag reduction was the increased laminar sublayer in turbulent flow attributable directly to the presence of long polymer molecules. Savins (27) suggested that the drag reduction might be a result of delayed laminar to turbulent transition, which possibility was also considered by Kozicki et al. (26). Lumley (28) on the other hand defined drag reduction as a property of fully developed turbulent flow only, completely rejecting the hypothesis of delayed transition. Shin (29) recognized the possibility of anisotropic viscosity in a flowing polymer solution.

However at present no direct experimental evidence of anisotropic viscosities in very dilute polymer solutions exists. Metzner and Park (30) attributed drag reduction to viscoelasticity. Arunachalam and Fulford (24) postulated that drag reduction is due to free hanging loops of adsorbed molecules which damp turbulent eddies originating at the wall. In spite of a very large number of attempts to understand the mechanism underlying the Toms phenomena, it is not yet understood. However, some properties of drag reducing polymers are found to be of importance to understand the phenomena of drag reduction. A brief review of these properties is given below.

Hoyt and Fabula (31) and many others have established that most effective polymers are those with a linear chain structure having no side chains. Merrill et al. (32) found that the number of monomer units in the main chain rather than the molecular weight itself, is the important factor. The drag reduction effect is a direct function of the individual molecule and not of the mean value. From the work of Shin (33) it appears that the additive effect is monotone in chain flexibility. Hershey and Zakin (34) established that polyisobutylene was found to be more effective in reducing drag in a good solvent than in a poor solvent. A good solvent is the one in which polymer-solvent interactions are favoured over polymer-polymer interactions so that the polymer chain is

relatively extended in solution (35). Most of the polymer-solvent combinations that display drag reduction in very dilute solutions also display viscoelastic effects at much higher concentrations and solutions such as carbopol that do not display viscoelastic effects at any concentration do not produce drag reduction either. It is often assumed that elasticity is essential for drag reduction. However it does not mean that existence of viscoelasticity is a sufficient condition for drag reduction. On the contrary, in view of some investigators it is not even a necessary condition. For the concentration ranges involved in drag reduction studies, the solution viscosity never exceeds the solvent value by more than a few percent. These polymer solutions are commonly observed to have a soapy feeling which might not always be felt, specially at very low concentrations. There is no clear evidence as to what property of the polymer causes this. It has been suggested that some sort of lubricating phenomenon takes place when distance between the fingers is of the order of the effective molecular diameter.

Very dilute solutions of polyox in distilled water were used as the drag reducing polymer solutions. Ethylene oxide polymers of high molecular weight probably have the simplest structure among water soluble polymers, yet their water solutions exhibit this unusual behaviour.

The chemical structure of this flexible, high molecular weight linear, thermoplastic polymer can be represented by (36)

$$-\left[CH_2 - CH_2 - O\right]_n$$

Although polyethyleneoxide is completely soluble in water at room temperature, it exhibits an inverse solubility temperature relation in water (37). Dilute solutions of high molecular weight polyox display considerable structural and molecular interaction, and an enormous dependence of viscosity on shear rate.

CHAPTER III

ANALYSIS

(A) Evaluation of Shear Stress

The capillary tube data consists of flow rates for given imposed pressure gradients collected for different values of the tube diameter as a parameter. This information is utilized to determine the flow curve of the fluid i.e. shear stress vs. shear rate behaviour. This necessitates consideration and allowance for the following effects (38).

1. Head of fluid above the tube exit.
2. Kinetic energy effects.
3. Tube entrance effects.
4. Effective slip near the tube wall.

A simplification of the mechanical energy balance equation for flow in the reservoir and cappilary tube results in the following expression for the frictional pressure drop across the capillary tube in fully developed flow

$$\Delta p = (p_{gas} - p_a) + (L+L') \cdot \rho \cdot \frac{g}{g_c} - \frac{\rho \cdot \langle u \rangle^2}{g_c}\left(\frac{1}{2\alpha_2} + \frac{Kc}{2}\right) \quad \ldots \quad 3.A.1.$$

In the case of Newtonian fluids α_2 has the value of 1/2. The scraping of the cut ends of the capillary tube was done with the help of a very sharp edged, round

smooth file to remove the burr at the inside edge. This results in a slightly rounded entrance and for such cases Foust et al. (39) have suggested a value of 0.23 for Kc for Newtonian materials. The net expression for the pressure gradient for Newtonian fluids in a capillary tube would therefore be

$$\frac{\Delta p}{L} = \frac{P_{gas}-P_a}{L} + \left(\frac{L+L'}{L}\right)\rho \frac{g}{g_c} - \frac{1.12\ \rho\ \langle u\rangle^2}{L.g_c} \quad .... \quad 3.A.2$$

For time independent non-Newtonian fluids it has been indicated (40,41) that the combined correction for kinetic energy effects and entrance effects is the same as that for Newtonian materials. Equation 3.A.2 is therefore suggested (42) to obtain true pressure gradient. Uncertainties in the correction term $- 1.12.\rho.\ \frac{\langle u\rangle^2}{g_c}$ are reduced by having L/D as large as possible. Equation 3.A.2 was used for the tubes of small diameters for which L/D was larger than 950*. In this case τ_w, the shear stress at the wall was determined using the expression

$$\tau_w = \frac{R.\Delta P}{2L} \quad ..... \quad .... \quad .... \quad 3.A.3$$

For the tubes of large diameters for which L/D was less than 950, a correction for an entrance region of undeveloped flow was applied as follows. Writing

* Except for capillary tube 3S

the force balance across the ends of the capillary tube, we get

$$[A'.L.\rho.g.\cos\alpha_1 + (p_1-p_a).A'] = \pi.D[\int_0^{L_e}(\tau_w+\tau_w')dx + \int_{L_e}^{L}\tau_w.dx]$$

where $A' = \frac{\pi}{4}.D^2$, $L.\cos\alpha_1 = h_1 - h_a$

$$\frac{\pi}{4} D^2[\rho.g.\cos\alpha_1 + (p_1-p_a)] = \pi D [\int_0^{L_e}\tau_w' dx + L.\tau_w]$$

substituting $P = p + \rho gh$, we get

$$\frac{D}{4}(P_1-P_a) = [L.\tau_w + \tau_w.R\int_0^{L_e}\frac{\tau_w'}{\tau_w} d(\frac{x}{R})]$$

$$\frac{R}{2}.\Delta P = \tau_w [L+R\int_0^{L_e}\frac{\tau_w'}{\tau_w} d(\frac{x}{R})]$$

substituting $n = \int_0^{L_e}\frac{\tau_w'}{\tau_w} d(\frac{x}{R})$ 3.A.4

$$\frac{R}{2}.\Delta P = \tau_w (L + nR).$$

$$\tau_w = \frac{R.\Delta P}{2(L+nR)} \quad \ldots\ldots \quad \ldots\ldots \quad \ldots\ldots \quad 3.A.5$$

This is the modified form of equation 3.A.3 for the evaluation of the shear stress in the region of fully developed flow. A correction for an entrance length effect is made by assuming an effective capillary length, (L+nR). The same equation was suggested by Bagley (43).

Equation 3.A.5 can be rewritten as

$$\Delta P = 2.\tau_w \left(\frac{L}{R} + n\right) \quad \ldots\ldots \quad \ldots\ldots \quad 3.A.6$$

This equation suggests that the pressure drop required to produce a particular shear stress for a tube of given diameter should be a linear function of length of the tube. The slope of this straight line gives the value of τ_w and the intercept gives the value of n. Three tube lengths were used for a particular tube diameter.

(B) Evaluation of $\frac{8\langle u\rangle}{D}$

In the present analysis, we assume that ΔP, the pressure drop across the tube can be expressed as a polynomial in the average velocity $\langle u\rangle$, in the tube i.e.

$$\Delta P = \langle u\rangle c_1(L,R) + \langle u\rangle^2 c_2(L,R) + \langle u\rangle^3 c_3(L,R) + \text{---} \quad \ldots 3.B.1$$

where the coefficients $c_i(L,R)$ are functions of the length and the radius of the tube. Comparing the equations 3.A.6 and 3.B.1 we obtain

$$\langle u\rangle c_1(L,R) + \langle u\rangle^2 c_2(L,R) + \langle u\rangle^3 c_3(L,R) + \text{---} = 2.\tau_w\left(\frac{L}{R} + n\right) \quad \ldots 3.B.2$$

If the velocity in a tube of radius R is fixed at a constant value $\langle u\rangle$, then the shear stress in the

region of fully developed flow, τ under these conditions will be constant and the R.H.S. of this equation will be a linear function of L. The L.H.S. can also be made a linear function of L by expressing the $c_i(L,R)$ as follows

$$C_i(L,R) = C_{io}(R) + L\,C_{il}(R) \quad \ldots \quad 3.B.3$$

giving

$$L(\langle u\rangle C_{11}(R)+\langle u^2\rangle C_{21}(R)+\langle u^3\rangle C_{31}(R)+ \text{----}) + (\langle u\rangle C_{10}(R)+\langle u^2\rangle C_{20}(R)+\langle u^3\rangle C_{30}(R))$$

$$= 2\,\frac{\tau}{R}L + 2\,\tau n \quad \ldots \quad 3.B.4$$

Equating coefficients of like terms yields

$$\frac{2\tau}{R} = \langle u\rangle C_{11}(R)+ \langle u^2\rangle C_{21}(R)+ \langle u^3\rangle C_{31}(R) + \text{----} \quad \ldots\ 3.B.5$$

and $$2.\tau n = \langle u\rangle C_{10}(R)+\langle u^2\rangle C_{20}(R)+\langle u^3\rangle C_{30}(R) + \text{---} \ \ldots\ 3.B.6$$

combining the later equations yields the following explicit relation for n

$$nR = \frac{\langle u\rangle C_{10}(R)+\langle u^2\rangle C_{20}(R)+\langle u^3\rangle C_{30}(R) + \text{---}}{\langle u\rangle C_{11}(R)+\langle u^2\rangle C_{21}(R)+\langle u^3\rangle C_{31}(R) + \text{---}} \quad \ldots \quad \ldots\ 3.B.7$$

It was found that P could very satisfactorily be expressed as a quadratic function of velocity. There-

fore, from equation 3.B.5 we get

$$\frac{2\tau}{R} = \langle u\rangle C_{11}(R) + \langle u\rangle^2 C_{21}(R) \quad \ldots \quad \ldots \quad 3.B.8$$

or $$\frac{2\tau}{R} = \frac{8\langle u\rangle}{D} \cdot C_{11}(R)\,\frac{D}{8} + \left(\frac{8\langle u\rangle}{D}\right)^2 \cdot C_{21}(R)\left(\frac{D}{8}\right)^2 \quad \ldots \quad 3.B.9$$

setting $$\frac{D}{8} C_{11}(R) = A$$

$$\left(\frac{D}{8}\right)^2 C_{21}(R) = B$$

we obtain

$$\frac{2\tau}{R} = A\,\frac{8\langle u\rangle}{D} + B\left(\frac{8\langle u\rangle}{D}\right)^2 \quad \ldots \quad \ldots\ldots \quad 3.B.10$$

A & B are constants for a given tube.

For the tubes of small diameter, where the entrance length corrections were not necessary because of high L/D ratio (>950), values of $\frac{8\langle u\rangle}{D}$ at a given shear stress were calculated directly from the experimental data. A quadratic equation of the following form was found to represent the data with a very good accuracy.

$$\tau = A_1 \cdot G + B_1 \cdot G^2 \quad \ldots \quad \ldots \quad \ldots \quad 3.B.11$$

This equation was further modified to the following form which is analogous to the equation 3.B.10.

$$\frac{2\tau}{R} = \left[\frac{2}{R} \cdot A_1\left(\frac{\pi}{4} D^2\rho \cdot \frac{D}{8}\right)\right]\frac{8\langle u\rangle}{D} + \left[\frac{2B_1}{R} \cdot \left(\frac{\pi}{4} D^2 \cdot \rho\frac{D}{8}\right)^2\right]\left(\frac{8\langle u\rangle}{D}\right)^2 \quad 3.B.12$$

comparing equations 3.B.10 and 3.B.12 we get

$$A = \frac{2}{R} \cdot A_1 \left(\frac{\pi D^3 \rho}{32}\right) \quad \ldots\ldots \quad \ldots\ldots \quad 3.B.13$$

$$B = \frac{2}{R} \cdot B_1 \left(\frac{\pi D^3 \rho}{32}\right)^2 \quad \ldots\ldots \quad \ldots\ldots \quad 3.B.14$$

For the tubes of large diameter where the entrance length corrections were necessary due to low L/D ratio (<950), P, the pressure drop was expressed a function of G, the mass flow rate as follows:

$$\Delta P = A_L.G + B_L.G^2 \quad \ldots\ldots \quad \ldots\ldots \quad 3.B.15$$

This relation is similar to the equation 3.B.8. In the equation 3.B.15 the variable is G, the mass rate of flow instead of $\langle u \rangle$, the average velocity. Analogous to 3.B.3, A_L and B_L are further expressed as linear functions of L as given below:

$$A_L = A_2L + A_3 \quad \ldots\ldots \quad \ldots\ldots \quad 3.B.16$$

$$B_L = B_2L + B_3 \quad \ldots\ldots \quad \ldots\ldots \quad 3.B.17$$

Variable G in the equation 3.B.15 was changed to $\frac{8\langle u \rangle}{D}$ as indicated in the equation 3.B.12 and an equation analogous to the equation 3.B.10 was obtained.

Knowing A and B, $\frac{8\langle u \rangle}{D}$ can be obtained for any given τ, and the value is given by the relation

$$\frac{8\langle u \rangle}{D} = \frac{-A + \sqrt{A^2 + 4B.\frac{2\tau}{R}}}{2B} \quad \ldots \quad \ldots \quad 3.B.18$$

$$= \frac{-A + \sqrt{A^2 + \frac{8B\tau}{R}}}{2B} \quad \ldots \quad \ldots \quad 3.B.19$$

The values of n were calculated at a given shear stress and $\frac{8\langle u\rangle}{D}$ with the help of following equation, which is analogous to the equation 3.B.7, obtained from the equations 3.A.6, 3.B.15, 3.B.16 and 3.B.17.

$$n = \frac{A_3\left[\frac{\pi}{4}.D^2\ \rho.\ \frac{D}{8}\right]\left(\frac{8\langle u\rangle}{D}\right) + B_3\left[\frac{\pi}{4}.D^2\ \rho.\frac{D}{8}\right]^2\left(\frac{8\langle u\rangle}{D}\right)^2}{2\tau} \quad \ldots \quad 3.B.20$$

(C) Evaluation of $\frac{8\ U_w}{D}$

Several attempts have been made to explain clearly the cause of slippage at the wall associated with interaction between the wall of the capillary and the polymer molecules in the solutions. The mathematical expression derived by Oldroyd (9,44) can be expressed as

$$\frac{8\langle u\rangle}{D} = \frac{8\ U_w\ (\tau_w)}{D} + \frac{4}{\tau_w 3}\int_0^{\tau_w} \tau^2 f(\tau)\, d\tau \quad \ldots \quad \ldots \quad 3.C.1$$

Oldroyd (9) defined the velocity of slip by the following relation

$$U_w = \tau.\ \xi\ (\tau) \quad \ldots \quad \ldots \quad \ldots \quad 3.C.2$$

where $\xi(\tau)$ is effective slip coefficient.

Similar results have been reported by Mooney (45), Schofield and Scott Blair (7). Kozicki et al. (21) have used a plot of $\frac{8\langle u\rangle}{D}$ vs. 1/D to evaluate U_w for a given shear stress, of course the inherent assumption in this method is

that U_w is independent of diameter being only a function of τ_w. Toms successfully used equivalent methods (8,9) of detecting wall effects in the laminar flow of linear polymer solutions. However Oldroyd's method did not work satisfactorily for Jastrzebski's data on capillary tube viscometer. His data on concentrated suspensions indicated that slip coefficient is not only a function of shear stress but also varied inversely with tube radius. A careful study by Kozicki et al. (23) on a Natrosol 250G solution in a capillary tube viscometer indicated that slip coefficient is not only a function of shear stress and the tube diameter but there also exists a critical shear stress τ_c which marks the transition from a negative effective velocity at the wall to a positive effective velocity of slip at the wall for values of wall shear stress greater than critical shear stress. According to this analysis slip coefficient was defined as

$$\alpha'(\tau_w.D) = \frac{U_w}{\tau_w - \tau_{c(D)}} \quad \ldots \quad \ldots \quad 3.C.3$$

where

$$\alpha' = \frac{\alpha''(\tau_w)}{D} \quad \ldots \quad \ldots \quad 3.C.4$$

τ_c, the critical shear stress in the above equation is a new parameter, and is a function of tube diameter. Physically it determines the behaviour of the polymer molecules in the vicinity of the tube. 'Polymer adsorption' or 'Gel-Formation' takes place when the shear stress at the

wall is less than critical shear stress and 'separation phenomena' or possible polymer alignment takes place when the applied shear stress is greater than critical shear stress. Using above equations the expression for effective velocity can be written as

$$U_w = \frac{\alpha'' (\tau_w) [\tau_w - \tau_c (D)]}{D} \quad \ldots \quad \ldots \quad 3.C.5$$

Using this analysis the equation 3.C.1 derived by Oldroyd can be rewritten as

$$\frac{8\langle u\rangle}{D} = \frac{8\, U_w (\tau_w, D)}{D} + \frac{4}{\tau_w^3} \int_0^{\tau_w} \tau^2 f(\tau)\, d\tau \quad \ldots \quad \ldots \quad 3.C.6$$

It has been observed that distinct curves are obtained when $\frac{8\langle u\rangle}{D}$ is plotted against τ_w for different tube diameters. This is attributed to the wall effects. According to the equation 3.C.6 a unique relationship exists between $\frac{8(\langle u\rangle - U_w)}{D}$ and τ_w which is independent of the tube diameter.

In the present analysis an entirely new mathematical approach has been used to determine the effect slip velocity. Differenciating the equation 3.C.6 partially w.r.t. 1/D for a given value of τ_w, we obtain

$$\left[\frac{\partial(\frac{8\, u}{D})}{\partial(1/D)}\right]_{\tau_w} = \left[\frac{\partial(\frac{8\, U_w (\tau_w, D))}{D}}{\partial (1/D)}\right]_{\tau_w} + 0 \quad \ldots \quad 3.C.7$$

or $\left[\frac{8\,U_w}{D}\right]_{\tau_w,1/D} - \left[\frac{8\,U_w}{D}\right]_{\tau_w,0} = \int_0^{1/D} \left[\frac{\partial(\frac{8\,u}{D})}{\partial(1/D)}\right]_{\tau_w} d(1/D)$ .. 3.C.8

$\left[\frac{8\,U_w}{D}\right]_{\tau_w,0}$ tends to zero when 1/D tends to zero i.e. when D tends to infinity. The equation 3.C.8 then reduces to

$$\left[\frac{8\,U_w}{D}\right]_{\tau_w,1/D} = \int_0^{1/D} \left[\frac{\partial(\frac{8\,u}{D})}{\partial\,1/D}\right]_{\tau_w} d(1/D) \quad \ldots \qquad 3.C.9$$

The equation 3.C.9 is used to determine $\frac{8\,U_w}{D}$ for a given τ_w.

A plot of $\frac{8\langle u\rangle}{D}$ vs. 1/D is first constructed with shear stress as a parameter. The slope of this curve i.e. $\left[\frac{\partial\frac{8\langle u\rangle}{D}}{\partial(1/D)}\right]_{\tau_w}$ at different values of 1/D is determined. Now another plot of $\left[\frac{\partial(\frac{8\langle u\rangle}{D})}{\partial(1/D)}\right]_{\tau_w}$ vs. 1/D is constructed. The area under this curve is then determined with 1/D varying from 0 to the value of 1/D corresponding to that particular tube diameter for which $\frac{8\,U_w}{D}$ is to be determined. It is to be noted that $\left[\partial(8\langle u\rangle/D)/\partial(1/D)\right]_{1/D=0} \neq 0$ at all the shear stresses. Thus, for each tube, the value of $\frac{8\,U_w}{D}$ is determined at different values of shear stress. One can now correct the average velocity and calculate the quantity $\frac{8(\langle u\rangle - U_w)}{D}$ for each tube. These corrected values of $\frac{8(\langle u\rangle - U_w)}{D}$ for each tube at a given shear stress must now coincide according to the equation 3.C.6.

An attempt was made here to relate shear stress as a function of $\frac{8(<u> - U_w)}{D}$ as it was done for $\frac{8<u>}{D}$. Once again it was found that a quadratic relationship does exist as shown below

$$\tau_w = \alpha . \left[\frac{8(<u> - U_w)}{D} \right] + \beta \left[\frac{8(<u> - U_w)}{D} \right]^2 \quad \ldots \quad 3.C.10$$

(D) Determination of Non-Newtonian Viscosity

For inelastic time independent non-Newtonian liquids Kozicki et al. (46) modified Rabinowitsch and Mooney equation (47) to include the effective velocity of slip and further rearranged it in the following form which is analogous to the equation given by Metzner and Reed (48)

$$-\left(\frac{du}{dr}\right)_w = 3/4 \left[\frac{2(<u> - U_w)}{r_h} \right] + \frac{1}{4} \left[\frac{2(<u> - U_w)}{r_h} \right] \left[\frac{d \ln \frac{2(<u> - U_w)}{r_h}}{d \ln \tau_w} \right]$$

$\ldots\ldots$ 3.D.1

If the derivative in the above equation is denoted by $1/n'$ then one obtains

$$f(\tau_w) = -\left(\frac{du}{dr}\right)_w = \frac{3n' + 1}{4n'} \left[\frac{2(<u> - U_w)}{r_h} \right] \quad \ldots\ldots \quad 3.D.2$$

$$\text{where } n' = \frac{d \ln \tau_w}{d \ln \left[\frac{2(<u> - U_w)}{r_h} \right]} \quad \ldots\ldots \quad \ldots \quad \ldots \quad 3.D.3$$

As suggested by the equation, n' can be evaluated as the slope of the logarithmic plot of τ_w vs. $\frac{8(<u> - U_w)}{D}$.

at a given wall shear stress.

Setting $\omega = \frac{8(\langle u \rangle - U_w)}{D} = \frac{2(\langle u \rangle - U_w)}{r_h}$ ... 3.D.4

equations 3.C.10, 3.D.2 & 3.D.3 can be reduced respectively to:

$$\tau_w = \alpha . \omega + \beta . \omega^2 \quad .... \quad .... \text{ 3.D.5}$$

$$f(\tau_w) = \frac{3n' + 1}{4n'} . \omega \quad .... \quad .... \text{ 3.D.6}$$

and $$n' = \frac{d \ln \tau_w}{d \ln \omega} \quad .... \quad .... \text{ 3.D.7}$$

Differentiation of the equation 3.D.5 yields

$$d \tau_w = (\alpha + 2\beta \omega) d\omega$$

or $$d \ln \tau_w = \frac{d\tau_w}{\tau_w} = \left(\frac{\alpha + 2\beta \omega}{\alpha\omega + \beta\omega^2}\right) d\omega$$

$$= \frac{\alpha + 2 \beta \omega}{\alpha + \beta \omega} . \frac{d\omega}{\omega}$$

$$= \frac{\alpha + 2 \beta \omega}{\alpha + \beta \omega} . d \ln \omega$$

Therefore $$n' = \frac{d \ln \tau_w}{d \ln \omega} = \frac{\alpha + 2 \beta \omega}{\alpha + \beta \omega} \quad .... \quad .... \text{ 3.D.8}$$

Now substituting the value of n' in the equation 3.D.6, we get

$$f(\tau_w) = \frac{3\left(\frac{\alpha + 2\beta \omega}{\alpha + \beta \omega}\right) + 1}{4 \left(\frac{\alpha + 2\beta \omega}{\alpha + \beta \omega}\right)} . \omega$$

$$= \left(\frac{4\alpha + 7 \beta \omega}{4\alpha + 8 \beta \omega}\right) . \omega \quad .... \quad .... \text{ 3.D.9}$$

For non-Newtonian materials f (τ) is related to

non-Newtonian viscosity as follows

$$f(\tau) = \frac{\tau}{\eta}$$

or $$\eta = \frac{\tau}{f(\tau)} \quad \ldots \quad \ldots \quad 3.D.10$$

Substituting the values of τ and $f(\tau)$ one obtains

$$\eta = \frac{\alpha\ \omega + \beta\ \omega^2}{\left(\frac{4\ \alpha + 7\ \beta\ \omega}{4\ \alpha + 8\ \beta\ \omega}\right) \cdot \omega}$$

$$= \frac{(\alpha + \beta\ \omega)(4\alpha + 8\ \beta\ \omega)}{(4\alpha + 7\ \beta\ \omega)} \quad \ldots \quad 3.D.11$$

Knowing α and β, the non-Newtonian viscosity can be easily evaluated at any given value of ω i.e. $\frac{8(\langle u \rangle - U_w)}{D}$

(E) Estimation of Anomalous Layer Thickness

The method of estimation of anomalous layer has already been reported in literature (23,25).

Following equation is used for the estimation of anolamous layer thickness when the phenomenon of separation takes place

$$U_w = \delta \cdot \tau_w \left[\frac{1}{\mu_s} - \frac{1}{\eta_w}\right] \quad \ldots \quad \ldots \quad 3.E.1$$

In case of polymer adorption, the expression for anomalous layer thickness is given by

$$\delta = -\frac{U_w \cdot \eta_w}{\tau_w} \quad \ldots \quad \ldots \quad 3.E.2$$

CHAPTER IV

EXPERIMENTAL

(A) Capillary tube Viscometers

The purpose of a capillary tube viscometer is to measure the frictional pressure drop associated with steady laminar isothermal flow of a fluid through a smooth, long, cylindrical tube of known dimensions. Knowing the pressure gradient and volumetric flow rate one can find the relationship between shear stress and shear rate indirectly. The capillary tube viscometer used in the present study was prepared in the laboratory, which is a very common practice (49,50). The viscometer consists of the following main units.

1. Jacketed fluid reservoir.
2. Means of applying known driving force on the fluid.
3. A thermoregulating device.
4. Capillary tubes.

1. The viscometer in figure 1, consists of two plexiglass concentric pipes laid horizontally, and closed at the sides with the help of plexiglass flanges. The inner pipe acts as a reservoir for the experimental fluid and the annulii between the two pipe acts as the jacket for the reservoir. The fluid from the constant temperature bath B, is circulated through this jacket.

Plexiglass was chosen as the material of construction because of the obvious property of transparency, low cost and ease of machining and fabrication. The reservoir is 19 cms in diameter 60.5 cms long and .65 cms thick. The outer jacket is 34 cms in diameter 60.5 cms long and .32 cms thick. Since the reservoir, R was to be pressurized a thicker pipe was chosen for the reservoir than for the jacket. The bottom portion of the reservoir was connected with the help of a plexiglass tube to the outer jacket and a circular disc with an internal bore was glued at the lower end of the tube so that the capillary tubes of different lengths and diameters could be fastened. Brass connections (made in workshop), rubber o-rings standard sleeves and male glands for ermeto connections were used. The left hand side plexiglass flange held connections necessary for introducing compressed air, experimental fluid, and the liquid from the constant temperature bath and the flange on the right hand side had the connections leading to manometer, and the constant temperature bath. The cylinderical reservoir was kept in horizontal position to minimize the variation of liquid level in it. The size of the reservoir was chosen on the basis that even with the largest tube the fall in the fluid level was less than 1.00 cm for a complete run. This was verified from time to time

during the runs with the help of cathetometer. The liquid head above the tube entrance was measured accurately with the help of the cathetometer.

2. The pressure was applied by means of a compressed air cylinder C, fitted with a line regulator, L_R (range 0-60 psi). A by-pass valve was fitted on this line to release pressure from the reservoir. The pressure ($p_{gas}-p_a$) was measured with the help of a mercury manometer, M.

3. A constant temperature bath (D.W. Brookfield Ltd. Cooksville, Ont.) was used to control the temperature of the fluid in the reservoir. Water from the constant temperature bath was circulated through the head tank H, and the jacket around the reservoir of the viscometer. A magnetic thermo regulator provided with the bath was capable of controlling the temperature of the circulating fluid to within $\pm$ 0.01 C.

4. Several glass and stainless steel capillary tubes were used in the present study. Glass tubes obtained from Wilmad Glass Co. Inc., New Jersy and special hyperdermic needle tubings of type 304 austenitic chromium nickel stainless steel, supplied by Superior Tube, Norristown, Pa., were used. For large diameter tubes, three tube lengths were used so that the entrance length corrections could also be evaluated experimentally. Since the stainless steel tubes were flexible because of the large lengths used, they were enclosed

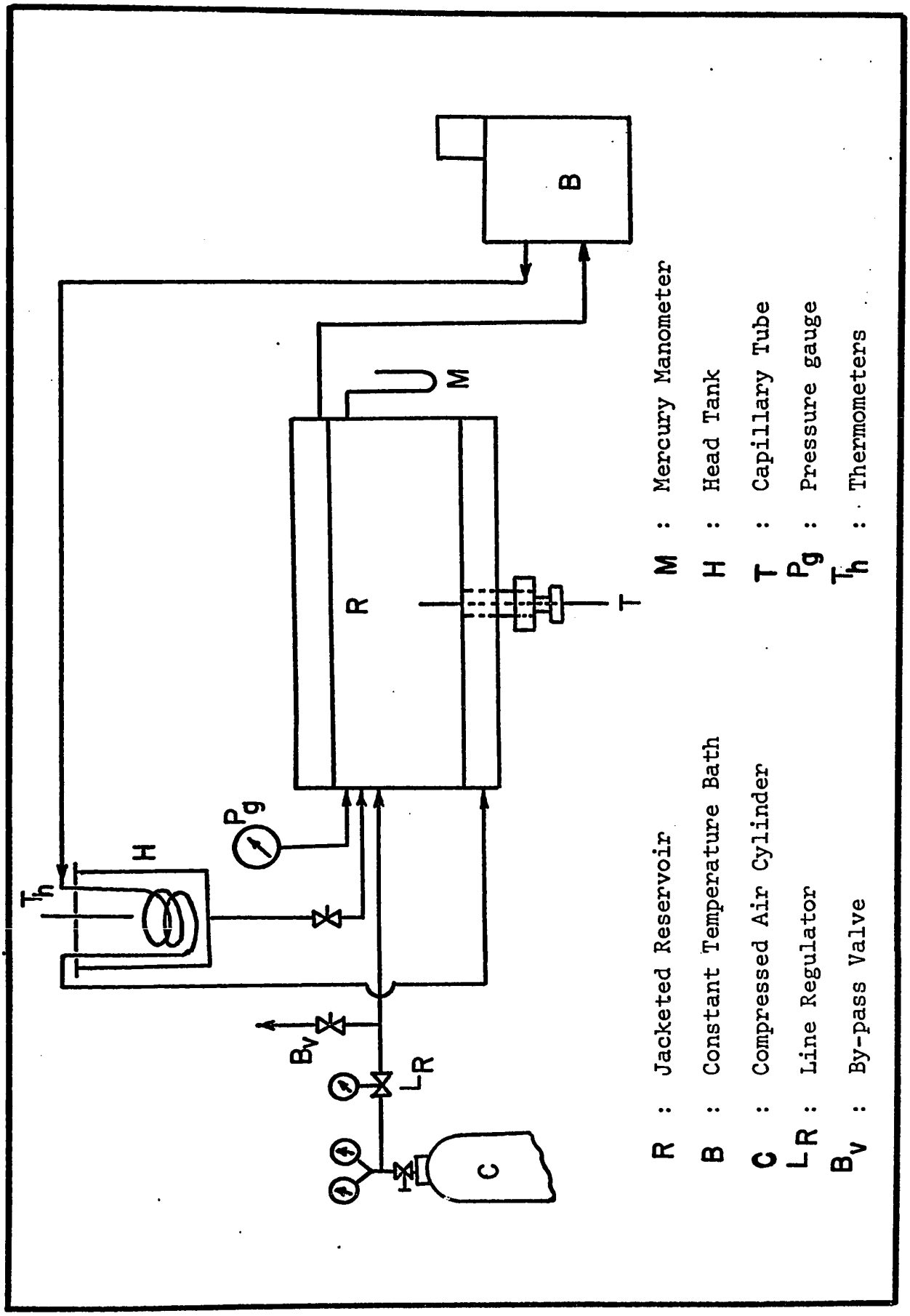

Fig.1. Schematic Diagram of the Experimental Set-Up

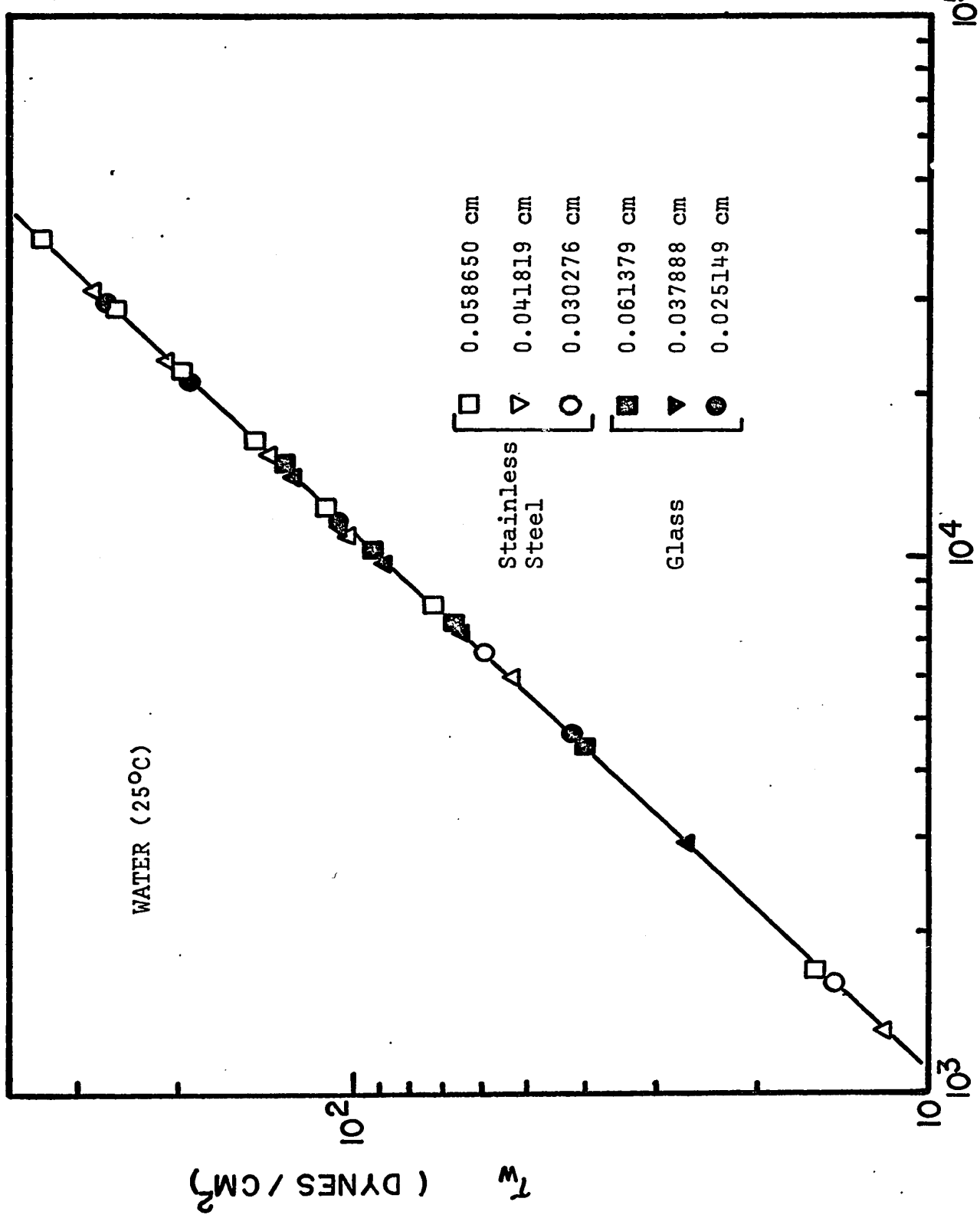

Fig. 2. Shear stress vs. shear rate curve for water at 25°C.

by protective stainless steel tubes. These were soldered near the end of the capillary tubes. The lengths varied from 28.9 cms to 84.4 cms for glass tubes and 25.3 cms to 84.4 cms for stainless steel tubes. The diameters varied from 0.02515 cms to 0.11887 cms for glass tubes and 0.03028 cms to 0.11227 cms for stainless steel tubes. Specifications of the capillary tubes used in the present study are given in Table I. The tubes were calibrated using water. The deviations of calibrated diameters from the diameters reported by manufacturers ranged from - 2.5% to 0.7% in case of glass tubes and a maximum of 6.2% in the case of stainless steel tubes. The L/D ratios employed were kept in the range of 250 to 2200 for the glass tubes and about 300 to 1050 for the stainless steel tubes.

The liquid resides in the capillary tube for a very short time and due to this continuous replenishment, the accumulation of heat due to viscous energy dissipation is reduced. This helps in achieving isothermal flow. Toors (51) has shown that the temperature rise due to viscous heating is negligible in this kind of viscometer.

Shear stress vs. shear rate relationship for water is shown in fig. 2. As expected this relation is linear with a slope of unity. The experimental points fall perfectly on the line. This indicates a very good reproducibility of the data and reliability of the viscometer.

(B) Fluids and their preparation

All solutions were made up in distilled water and measurements were conducted immediately (within two days) after the solutions were prepared. Solutions of polyox compounds deteriorate on standing for extended periods of time, possibily due to bacterial action. Solutions were also preserved from sunlight due to possible photo degradation. The method of mixing solutions is important for reproducible results and hence a standard procedure was used. For polyox, cold mixing was found to be most suitable and most effective for drag reducing effects (52).

To prepare a standard solution a known amount of water weighed into a container. Mixing was started with the help of a magnetic stirrer set at a proper speed. A corresponding quantity of polymer was then slowly sifted at regular intervals onto the liquid surface in the container. Extreme care was taken to avoid lump formation on the surface. A constant speed of mixing was maintained and a rigorous mixing was avoided which could lead to the breakdown of molecules. This master solution was later diluted to the required concentration.

(C) Experimental Procedure

The reservoir, fig. 1, was first filled with the polyox solution. Water was then circulated from

the constant temperature bath to the head tank and the jacket surrounding the reservoir. The temperature of the constant temperature bath was maintained at 25°C with the help of an adjustable microset magnetic thermoregulator which gives a control sensitivity of ± 0.01°C. Three different concentrations 20, 30 and 40 ppm of polyox solutions were studied. Data was taken using five different diameters with glass and stainless steel tubes. The volume rate of flow was obtained by weighing the liquid collected in a bottle of known weight over a measured time interval. Pressure drop was measured by means of a mercury manometer. Densities were determined by weighing known volumes of solutions in a pycnometer. However the densities were found to differ insignificantly from that of distilled water at all the three concentrations.

CHAPTER V

RESULTS

From the experimental data for polymer solutions G, the average mass rate of flow and corresponding pressure drop in the capillary tube were determined. For the tubes of small diameter, where entrance length corrections were not applied, the values of $\frac{8\langle u\rangle}{D}$ for a given shear stress were calculated directly from the experimental data. The data was then expressed in the form of the equation 3.B.11 using the method of least square curve fitting and values of A and B, the coefficients of the equation 3.B.10, were determined. These coefficients are tabulated in Table III.

For the tubes of large diameter ΔP, the pressure drop was expressed as a function of G, the mass flow rate as given by the equation 3.B.15. A plot of ΔP vs. G for 40 ppm. polyox solution is given in fig. 3(a) & 3(b) for #1 stainless steel and glass tubes respectively. As can be seen from the plot, the equation 3.B.15 expressed data with a very good accuracy. Summary of the viscometric results for all the three concentrations is given in Table II.

Fig. 4 shows a plot of A_L vs. L and B_L vs. L for both stainless steel and glass tubes in case of 40 ppm polyox solution. These are found to be linear as indicated by the equations 3.B.16 and 3.B.17. The coefficients

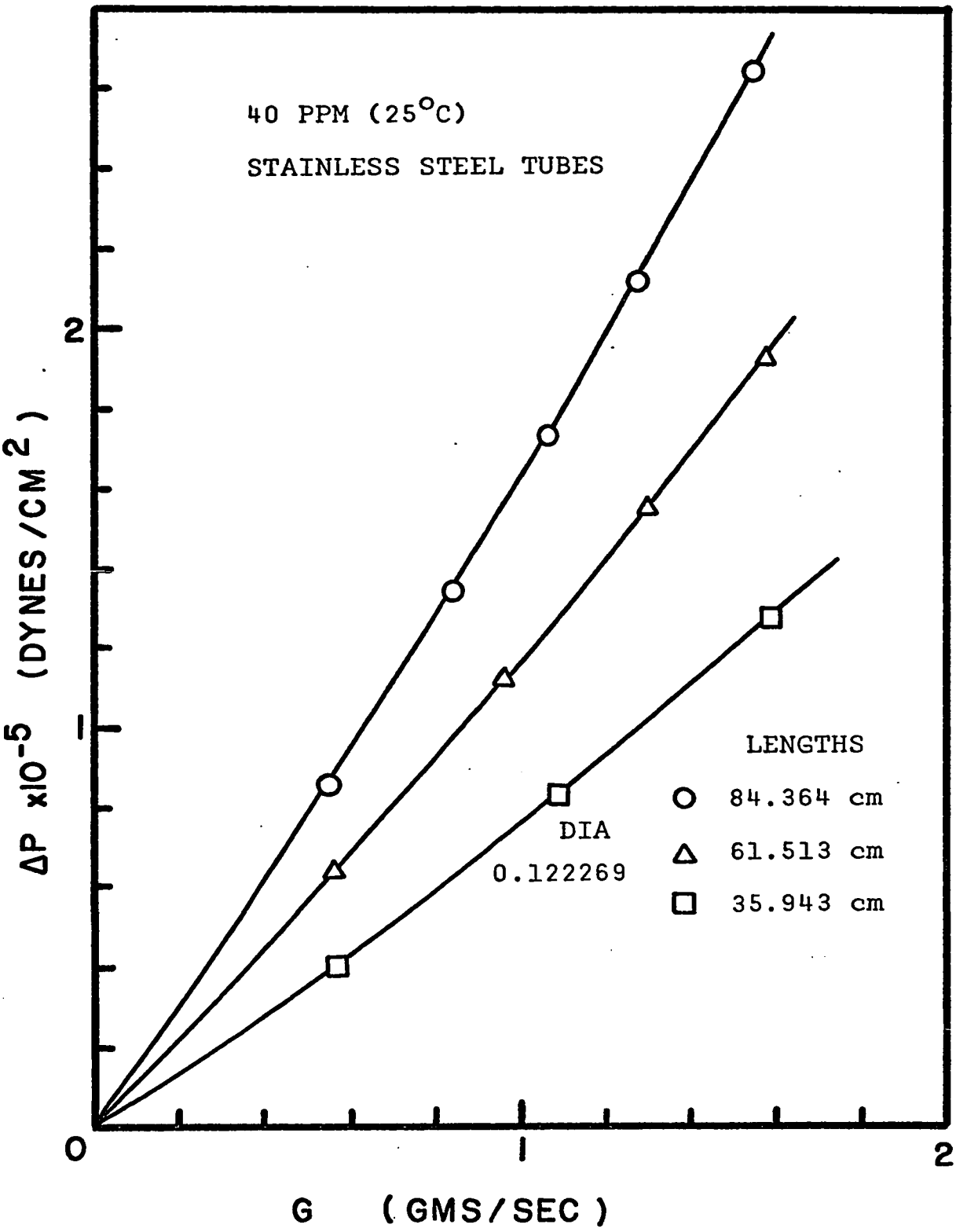

Fig. 3(a). Pressure drop vs mass flow rate for 40 ppm polyox solution at 25°C in case of #1 stainless steel capillary tubes of different lengths.

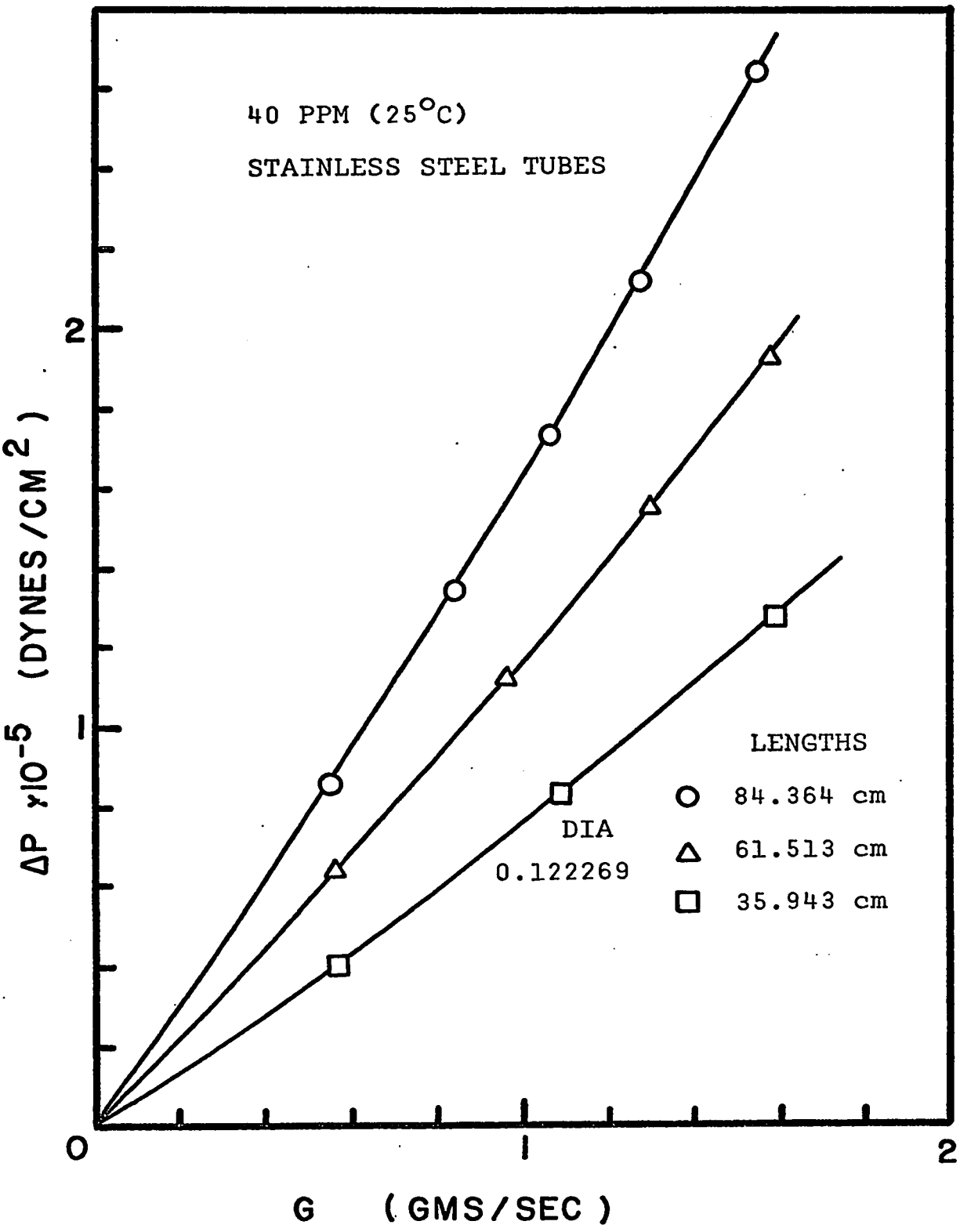

Fig. 3(a). Pressure drop vs mass flow rate for 40 ppm polyox solution at 25°C in case of #1 stainless steel capillary tubes of different lengths.

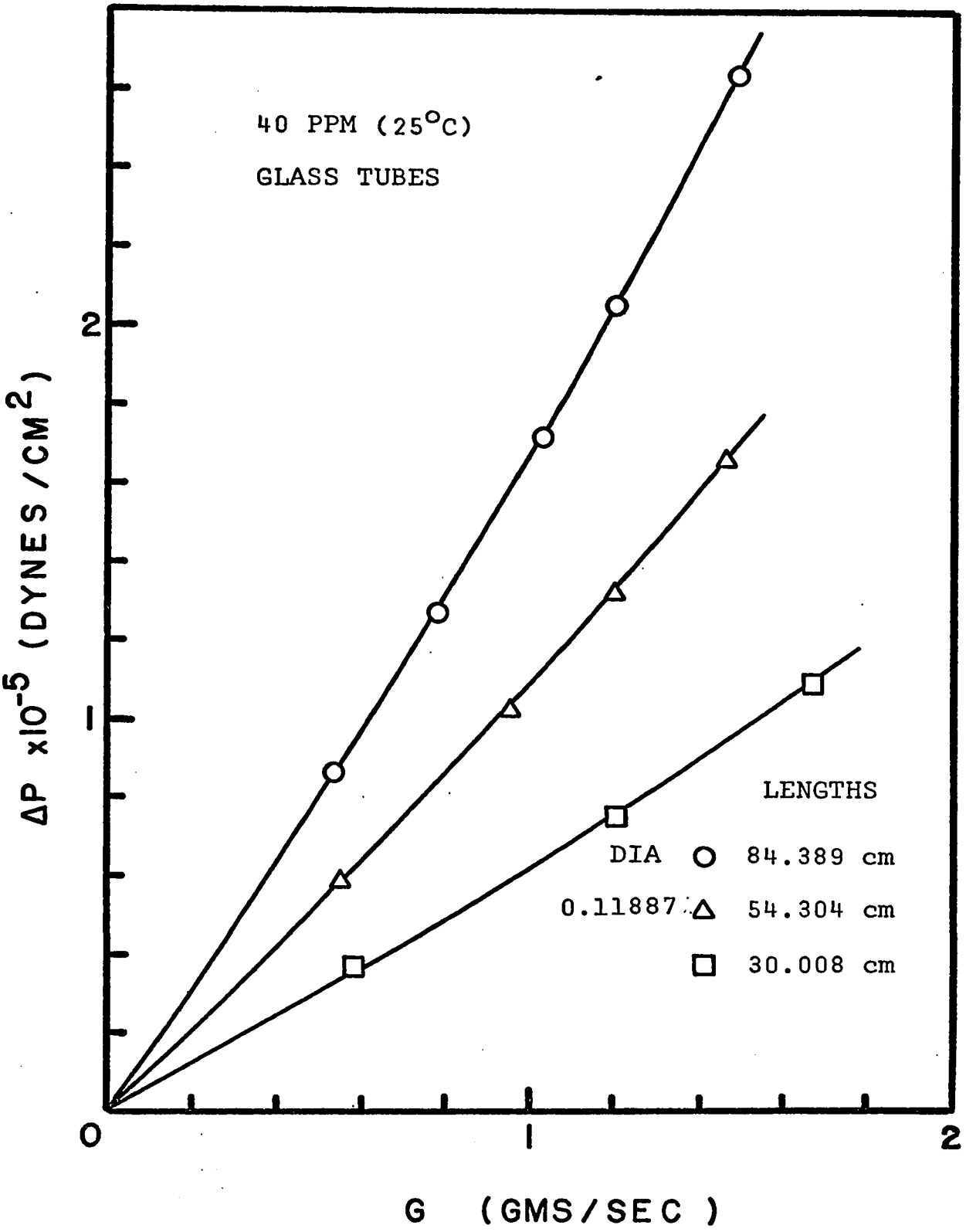

Fig. 3(b). Pressure drop vs mass flow rate for 40 ppm polyox solution at 25°C in case of #1 glass capillary tubes of different lengths.

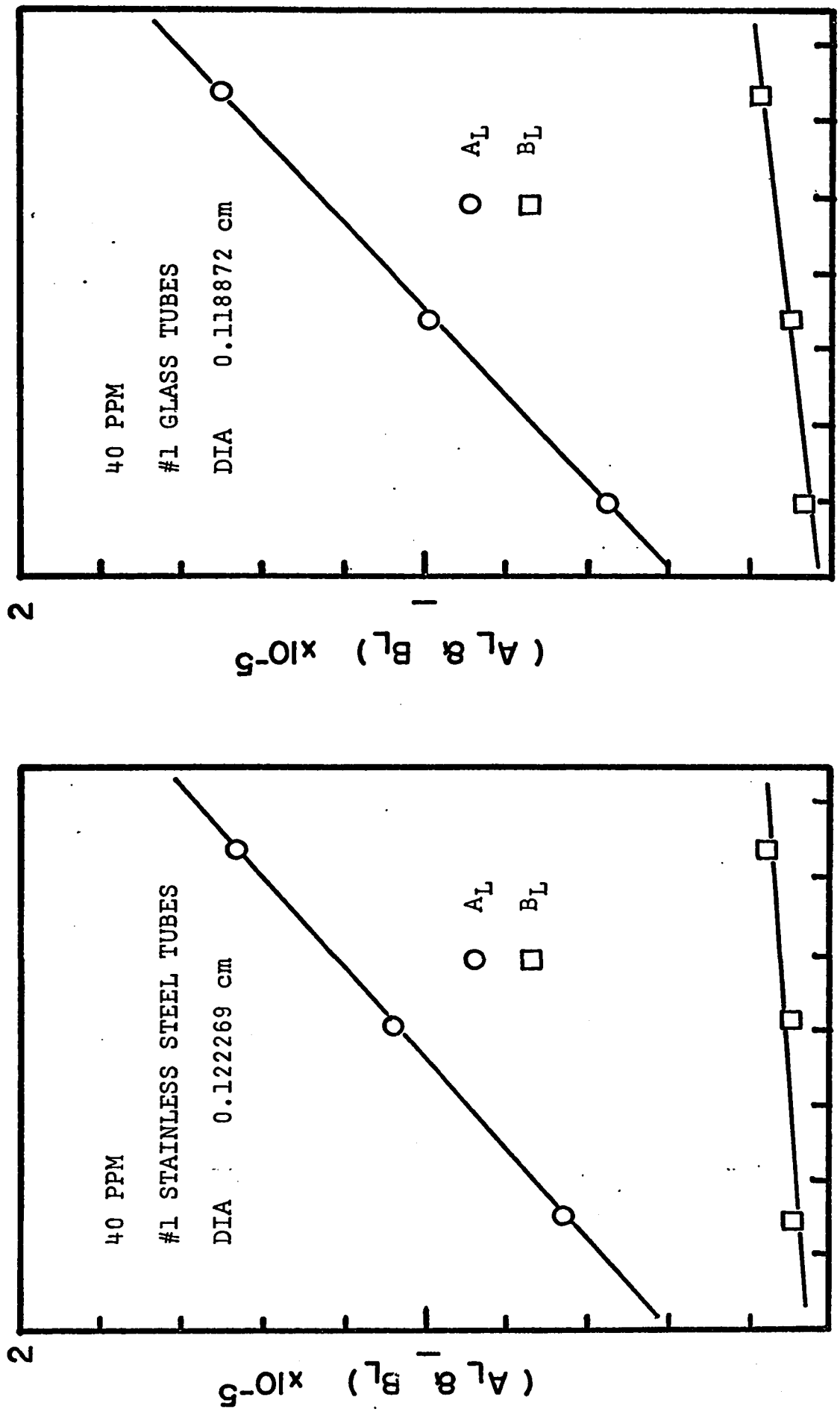

Fig. 4. Coefficients A_L and B_L vs L for 40 ppm polyox solution at 25°C.

A_L, B_L, A_2, A_3, B_2, B_3 and A and B are listed in Table IV. & V. Knowing A and B the values of $\frac{8\langle u\rangle}{D}$ at a given shear stress for a particular tube were calculated using equation 3.B.19. These results are presented in Table 1.

Based on the analysis in chapter 3 the values of n were evaluated using the equation 3.B.20. The values are given in Table VI.

A plot of n vs. $\frac{8\langle u\rangle}{D}$ was constructed for #1 glass and stainless steel tubes as shown in fig. 5 with concentration as a parameter. For stainless steel tubes values of n were found to be positive with an increasing trend with increasing $\frac{8\langle u\rangle}{D}$. However, for glass tube n decreased with increasing $\frac{8\langle u\rangle}{D}$ and in some cases the values were even found to be negative.

Fig. 6 shows the plot of τ_w vs. $\frac{8\langle u\rangle}{D}$ for 40 ppm. polyox solution in case of stainless steel tubes. Considerable separation is observed in the high shear stress region, however curves for different tubes tend to merge into the flow curve for water in low shear stress region.

Logarithmic plots of τ_w vs. $\frac{8\langle u\rangle}{D}$ were constructed separately for glass and stainless steel tubes at all the three concentrations as shown in figs. 7 to 12. Separate curves were obtained for each tube, however the curves merge into a line at low shear stresses. The curves also have a tendency to intersect each other. Dotted line indicates the final curve, which shall be explained later.

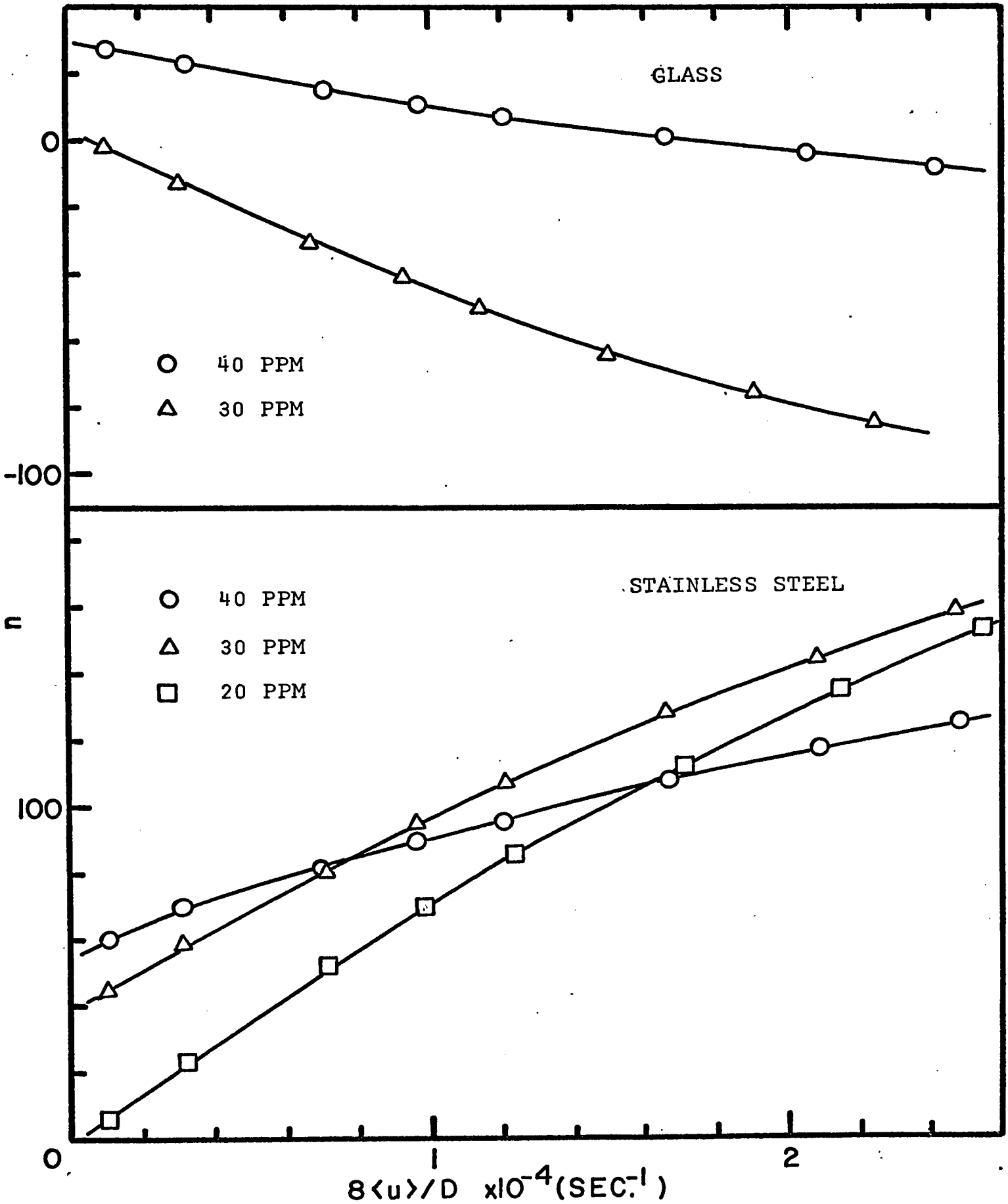

Fig. 5. n vs $\frac{8\langle u\rangle}{D}$ for #1 capillary tubes for different polyox solutions at 25°C

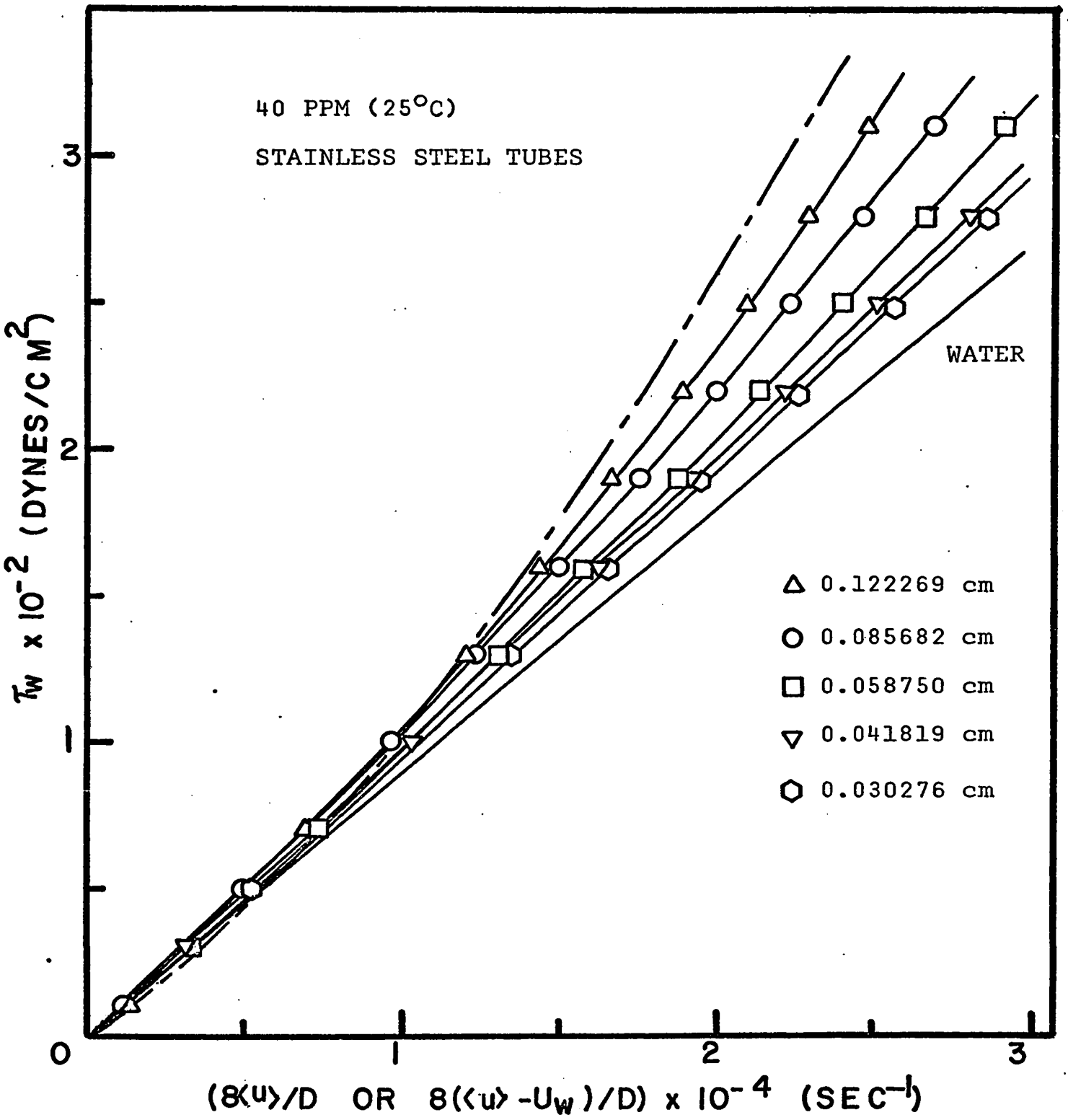

Fig. 6. Shear stress vs $\frac{8\langle u\rangle}{D}$ or $\frac{8(\langle u\rangle - U_w)}{D}$ for 40 ppm polyox solution at 25°C (Stainless Steel tubes)

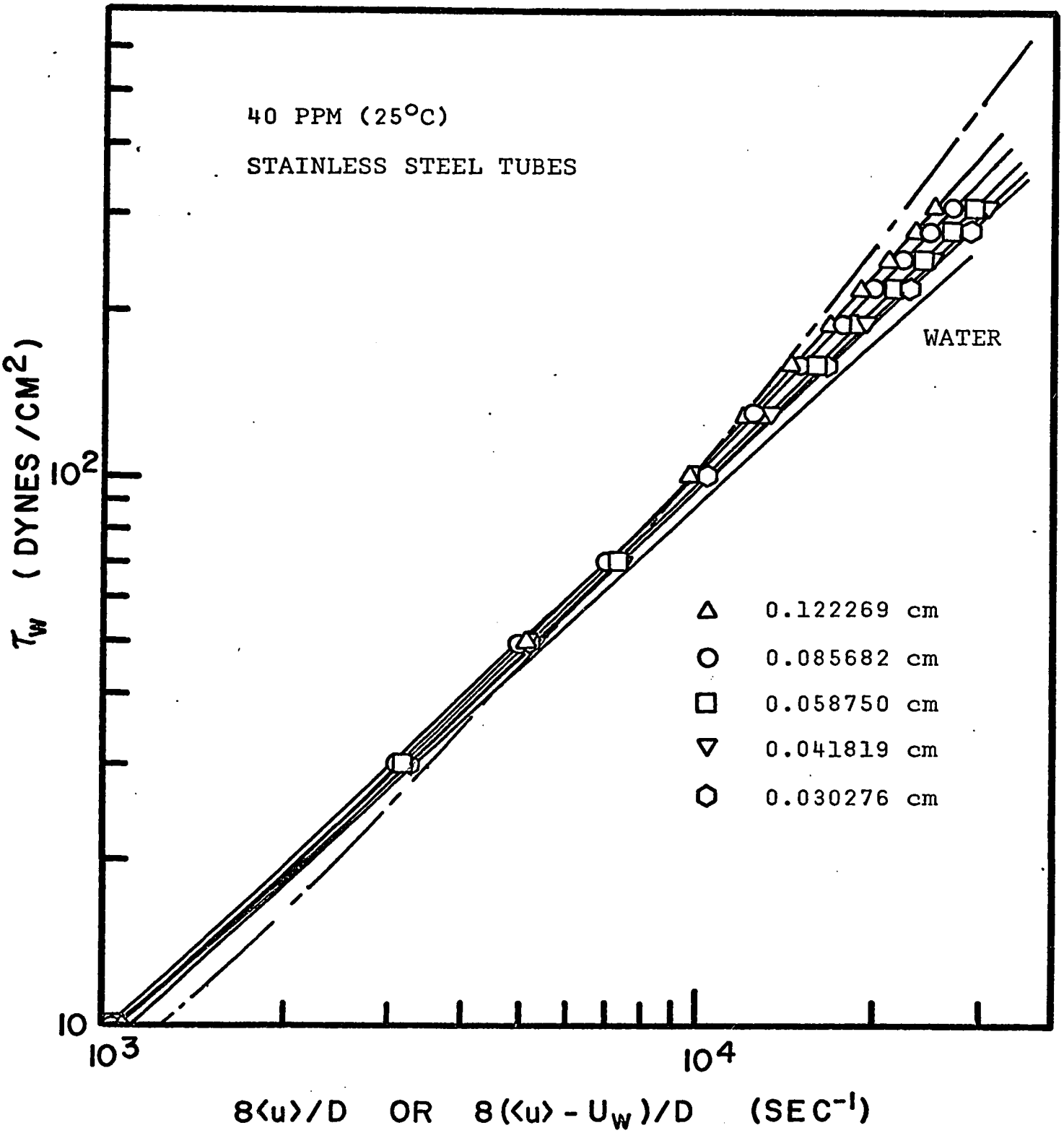

Fig. 7. Shear stress vs $\frac{8\langle u\rangle}{D}$ or $\frac{8(\langle u\rangle - U_w)}{D}$ for 40 ppm polyox solution at 25°C (Stainless Steel tubes)

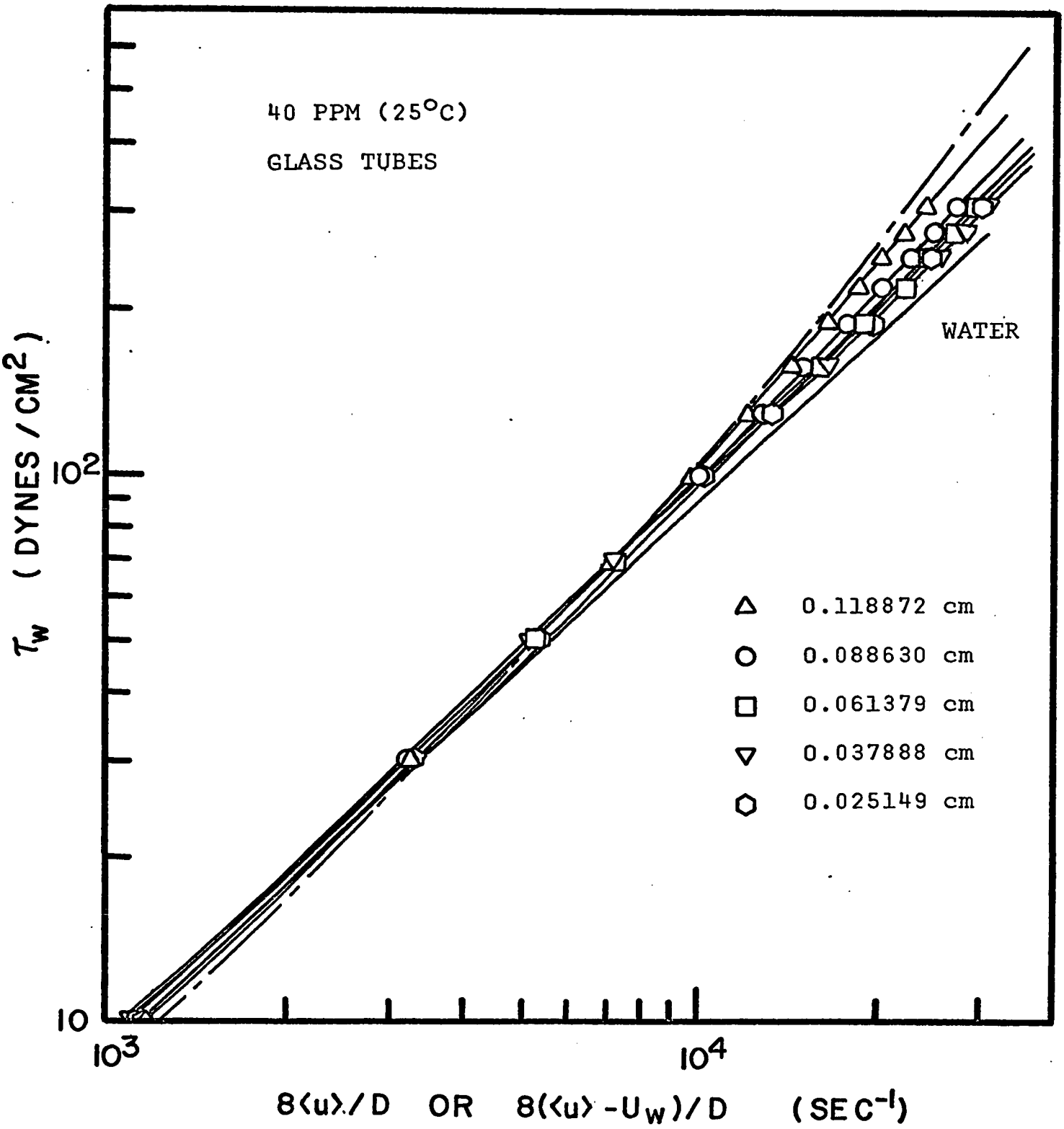

Fig. 8. Shear stress vs $\frac{8\langle u\rangle}{D}$ or $\frac{8(\langle u\rangle - U_w)}{D}$ for 40 ppm polyox solutions at 25°C (Glass tubes)

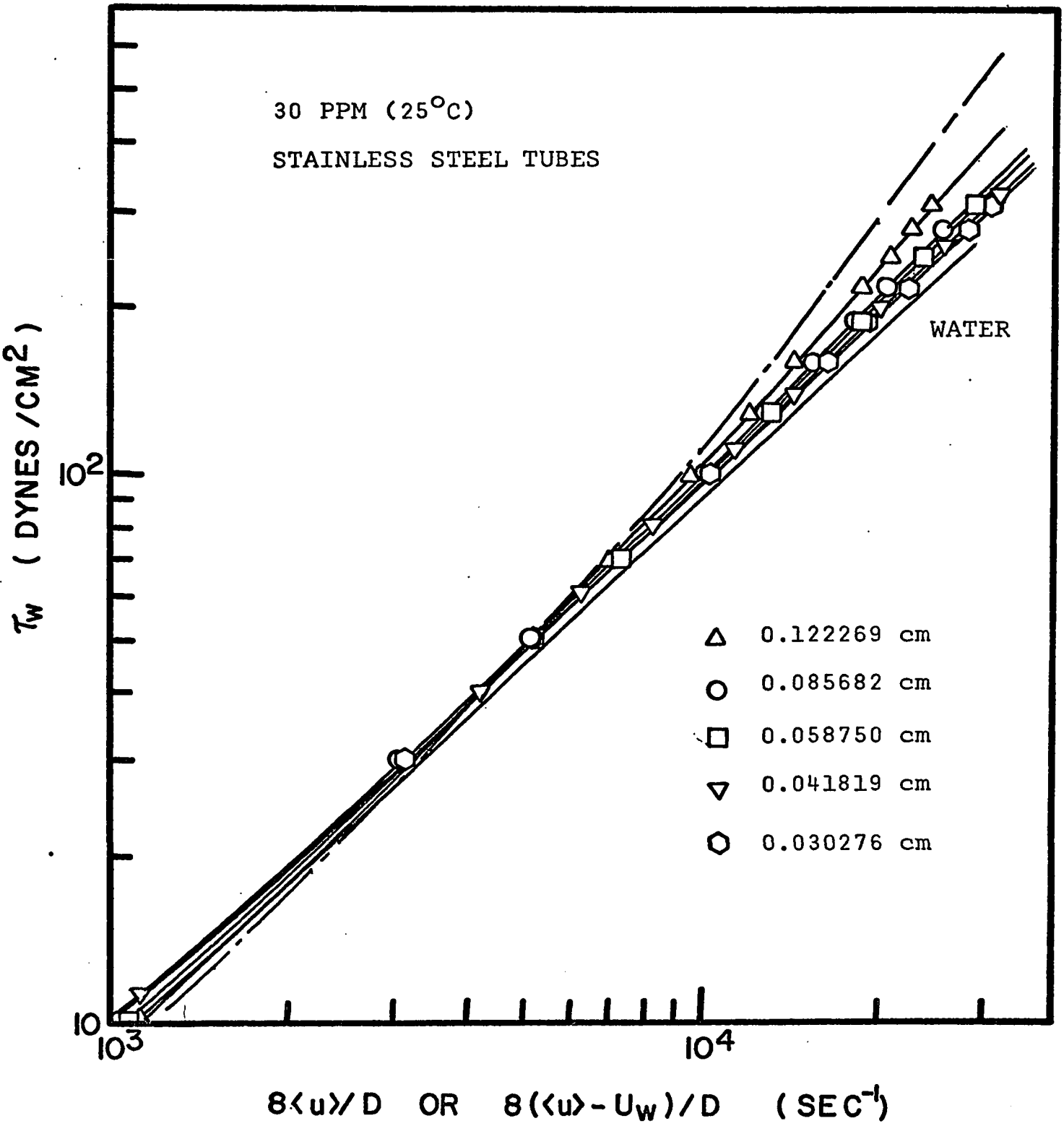

Fig. 9. Shear stress vs $\frac{8\langle u\rangle}{D}$ or $\frac{8(\langle u\rangle - U_w)}{D}$ for 30 ppm polyox solution at 25°C (Stainless steel tubes)

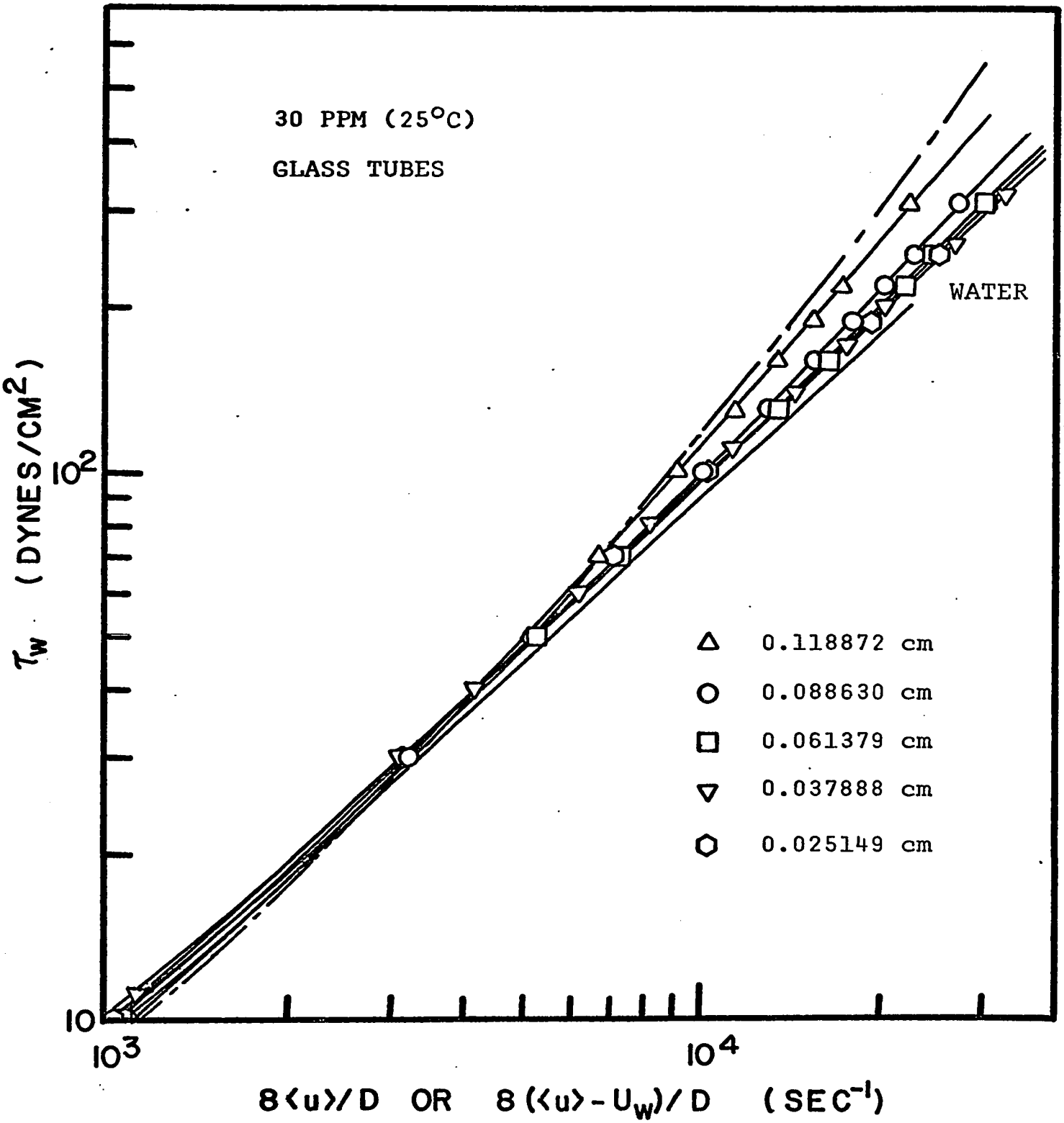

Fig. 10. Shear stress vs $\frac{8\langle u\rangle}{D}$ or $\frac{8(\langle u\rangle - U_w)}{D}$ for 30 ppm. polyox solution at 25°C (Glass tubes)

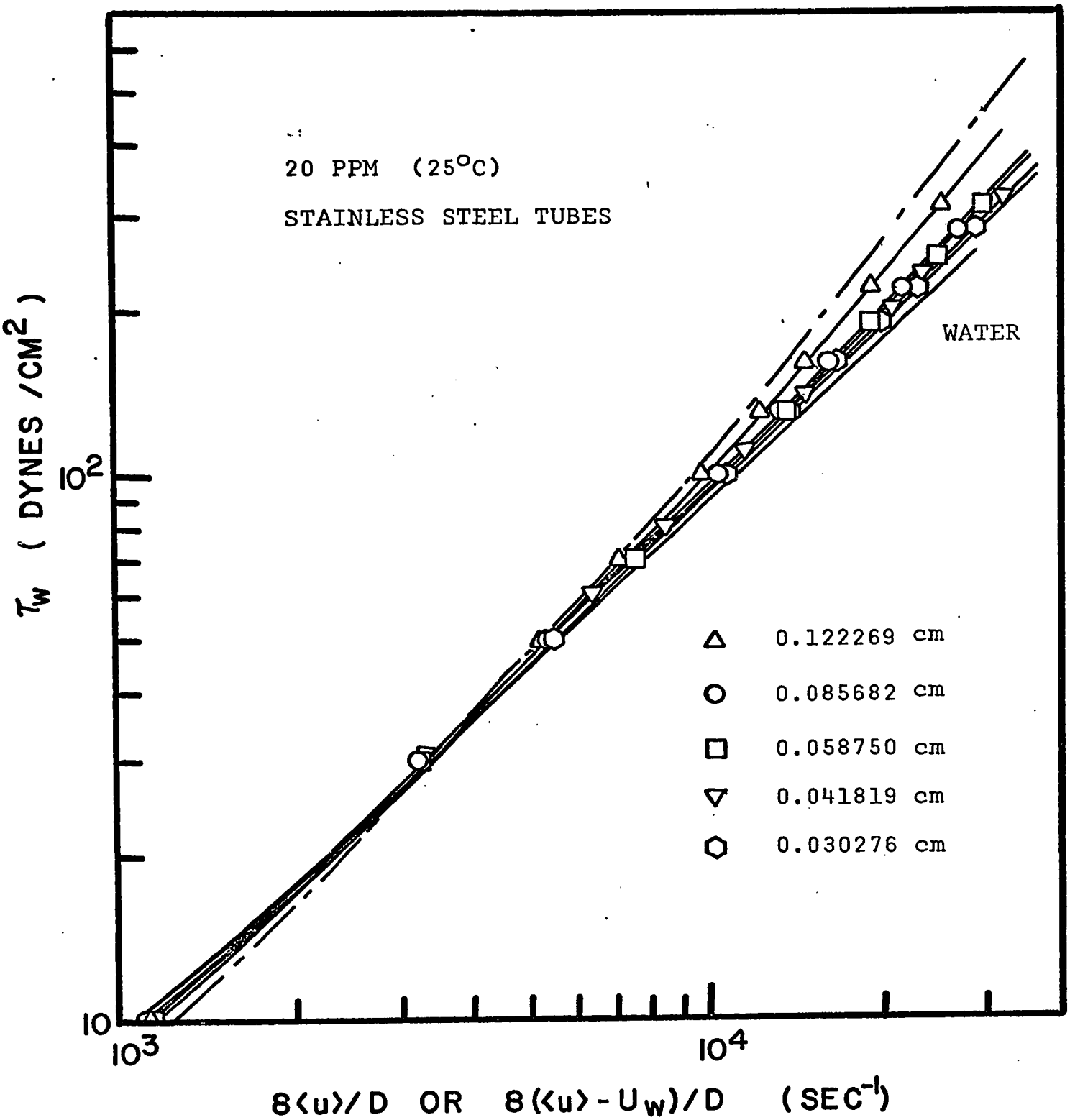

Fig. 11. Shear stress vs $\frac{8\langle u\rangle}{D}$ or $\frac{8(\langle u\rangle - U_w)}{D}$ for 20 ppm polyox solution at 25°C (Stainless Steel tubes)

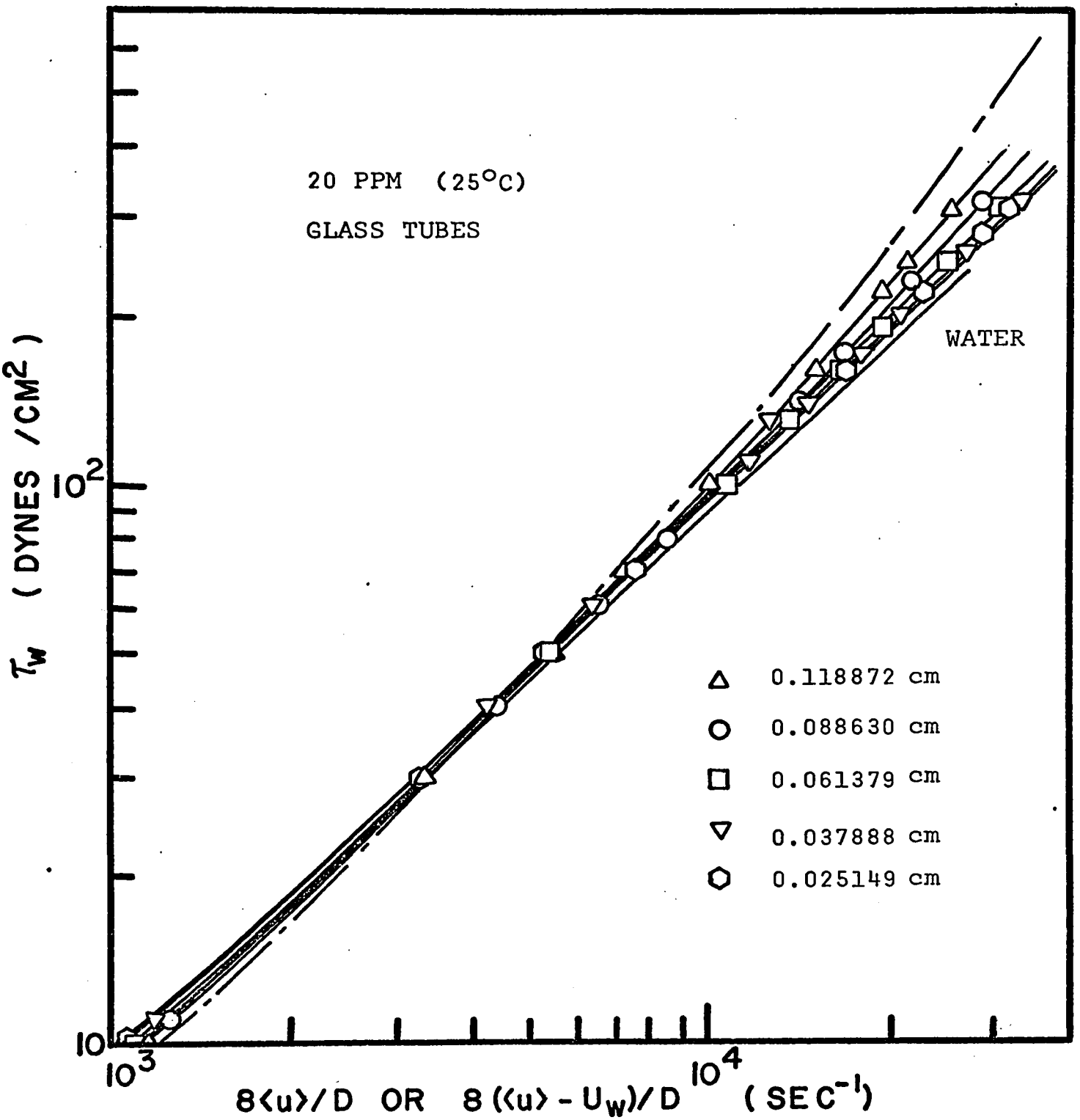

Fig. 12. Shear stress vs. $\frac{8\langle u\rangle}{D}$ or $\frac{8(\langle u\rangle - U_w)}{D}$ for 20 ppm polyox solutions at 25°C. (Glass Tubes)

TABLE 1

1a

Solution: 40 ppm. (by wt.) polyox

Calculations of $\frac{8\ U_w}{D}$ and $\frac{8(\langle u\rangle - U_w)}{D}$ for stainless steel tubes

τ_w dynes/cm^2	1/D cm^{-1}	$\frac{8\langle u\rangle}{D}$ sec^{-1}	$\frac{\partial \frac{8\langle u\rangle}{D}}{\partial\ 1/D}$	$\int \frac{\partial \frac{8\langle u\rangle}{D}}{\partial(1/D)} d(1/D)$	$\frac{8.U_w}{D}$ sec^{-1}	$\frac{8(\langle u\rangle - U_w)}{\text{sec}^{-1}D}$ exp.
	8.1787	24865.6	634.150	2290.00	2290.00	22575.60
	11.6711	26964.8	551.282	2100.00	4390.00	22574.80
310	17.0504	29164.0	350.000	2390.00	6780.00	22388.00
	23.9126	31000.6	153.409	1680.00	8460.00	22540.60
	33.0294	31673.9	27.472	824.53	9284.53	22389.37
	8.1787	20947.8	433.735	1560.00	1560.00	19387.80
	11.6711	22380.4	398.437	1460.00	3020.00	19360.40
250	17.0504	24070.5	235.290	1700.00	4720.00	19350.50
	23.9126	25220.1	85.526	980.00	5700.00	19520.10
	33.0294	25694.4	43.480	588.00	6288.00	19406.40

.....contd/..

τ_w	1/D	$\frac{8\langle u\rangle}{D}$	$\frac{\partial \frac{8\langle u\rangle}{D}}{\partial\, 1/D}$	$\int \frac{\partial \frac{8\langle u\rangle}{D}}{\partial(1/D)} d(1/D)$	$\frac{8.U_w}{D}$	$\frac{8(\langle u\rangle - U_w)}{D_{exp.}}$
190	8.1787	16724.9	213.00	490.00	490.00	16234.90
	11.6711	17548.9	326.09	970.00	1460.00	16088.90
	17.0504	18749.4	120.69	1170.00	2630.00	16119.40
	23.9126	19340.3	56.18	540.00	3170.00	16170.30
	33.0294	19644.9	19.61	345.47	3515.47	16129.43
130	8.1787	12111.9	24.39	10.00	10.00	12101.90
	11.6711	12425.4	148.94	330.00	340.00	12085.40
	17.0504	13172.4	79.79	650.00	990.00	12182.40
	23.9126	13355.4	18.46	260.00	1250.00	12105.40
	33.0294	13523.7	18.46	168.29	1418.29	12105.41

.....contd/...

τ_w	1/D	$\frac{8\langle u\rangle}{D}$	$\frac{\partial \frac{8\langle u\rangle}{D}}{\partial\, 1/D}$	$\int \frac{\partial \frac{8\langle u\rangle}{D}}{\partial\, 1/D} d(1/D)$	$\frac{8.\ U_w}{D}$	$\frac{8(\langle u\rangle - U_w)}{D}$ exp.
	8.1787	9620.52	21.127	20.00	20.00	9600.52
	11.6711	9735.92	53.190	150.00	170.00	9565.92
100	17.0504	10275.60	41.096	270.00	440.00	9835.60
	23.9126	10321.60	12.450	160.00	600.00	9721.60
	33.0294	10435.10	12.450	113.50	713.50	9721.60
	8.1787	6975.63	-24.193	-60.00	-60.00	7035.53
	11.6711	6949.19	-12.500	-80.00	-140.00	7089.19
70	17.0504	7298.85	25.424	50.00	-90.00	7388.85
	23.9126	7260.06	1.780	130.00	40.00	7240.06
	33.0294	7327.29	1.780	16.22	56.22	7271.07

.....CONTD/..

τ_w	1/D	$\frac{8<u>}{D}$	$\frac{\partial \frac{8<u>}{D}}{\partial\, 1/D}$	$\int_{\partial} \frac{\partial\, \frac{8<u>}{D}}{1/D}\, d(1/D)$	$\frac{8.U_w}{D}$	$\frac{8(<u>- U_w)}{D}$ exp.
	8.1787	5111.63	-37.34	-140.00	-140.00	5251.63
	11.6711	5031.72	-4.54	-70.00	-210.00	5241.72
50	17.0504	5266.29	9.35	25.00	-185.00	5451.29
	23.9126	5202.10	1.35	20.00	-165.00	5367.10
	33.0294	5244.72	1.35	12.30	-142.70	5387.42
	8.1787	3152.81	-37.31	-100.00	-100.00	3252.81
	11.6711	3062.20	-18.52	-100.00	-200.00	3262.20
30	17.0504	3192.92	-2.49	-50.00	-250.00	3442.92
	23.9126	3133.34	-2.49	-17.09	-267.09	3400.43
	33.0294	3153.14	-2.49	-22.70	-289.79	3442.93

TABLE 1b

Solution: 40 ppm (by wt.) Polyox

Calculation of $\frac{8\,U_w}{D}$ $\dot{\varepsilon}$ $\frac{8(\langle u\rangle - U_w)}{D}$ for Glass tubes

τ_w dynes/cm^2	1/D cm^{-1}	$\frac{8\langle u\rangle}{D}$ sec^{-1}	$\partial \frac{8\langle u\rangle}{D} / \partial\, 1/D$	$\int \partial \frac{8\langle u\rangle}{D} / \partial\, 1/D \; d(1/D)$	$\frac{8\,U_w}{D}$ sec^{-1}	$\frac{8(\langle u\rangle - U_w)}{D}$ sec^{-1}
310	8.4124	24279.2	689.66	1520.0	1520.0	22759.2
	11.2829	27421.6	944.44	3110.0	4630.0	22791.6
	16.2922	29886.6	367.19	2700.0	7330.0	22556.6
	26.3933	31271.1	0.00	1090.0	8420.0	22851.1
	39.7626	30056.6	-149.12	-995.8	7424.2	22611.4
250	8.4124	20608.5	513.89	1130.0	1130.0	19478.5
	11.2829	22854.6	632.35	1750.0	2880.0	19974.6
	16.2922	24542.3	234.37	2260.0	5140.0	19402.8
	26.3933	35442.8	-7.69	600.0	5740.0	19702.8
	39.7626	24783.1	-81.39	-595.4	5144.6	19638.5

.....contd/..

τ_w dynes/cm^2	1/D cm^{-1}	$\frac{8\langle u\rangle}{D}$ sec^{-1}	$\partial \frac{8\langle u\rangle}{D} / \partial \frac{1}{D}$	$\int \frac{\partial \frac{8\langle u\rangle}{D}}{\partial \frac{1}{D}} d(1/D)$	$\frac{8 U_w}{D}$ sec^{-1}	$\frac{8(\langle u\rangle - U_w)}{D}$ sec^{-1}
190	8.4124	16612.2	325.00	690.0	690.0	15922.2
	11.2829	18009.3	388.89	1080.0	1770.0	16239.3
	16.2922	19011.5	144.93	1400.0	3170.0	15841.5
	26.3933	19513.0	-3.84	300.0	3470.0	16043.0
	39.7626	19301.5	-16.48	-135.8	3334.2	15967.3
130	8.4124	12185.0	95.24	140.0	140.0	12045.0
	11.2829	12827.4	191.49	430.0	570.0	12257.4
	16.2922	13273.0	55.56	680.0	1250.0	12023.0
	26.3933	13476.0	6.13	129.2	1379.2	12096.8
	39.7626	13557.5	6.13	81.9	1461.1	12096.4
100	8.4124	9758.40	66.18	120.00	120.00	9638.40
	11.2829	10085.90	81.63	250.00	370.00	9715.90
	16.2922	10318.40	21.00	280.00	650.00	9668.40
	26.3933	10415.60	11.96	128.40	778.40	9737.20
	39.7626	10575.50	11.96	159.90	938.30	9636.20

.....contd/...

τ_w dynes/ cm^2	$1/D$ cm^{-1}	$\frac{8\langle u\rangle}{D}$ sec^{-1}	$\partial \frac{8\langle u\rangle}{D} / \partial \frac{1}{D}$	$\int \frac{\partial \frac{8\langle u\rangle}{D}}{\partial \frac{1}{D}} d(1/D)$	$\frac{8\,U_w}{D}$ sec^{-1}	$\frac{8(\langle u\rangle - U_w)}{D}$ sec^{-1}
70	8.4124	7146.99	23.26	30.00	30.00	7116.99
	11.2829	7227.22	31.82	90.00	120.00	7107.22
	16.2922	7302.11	12.50	110.00	330.00	6972.11
	26.3933	7326.13	8.90	81.10	413.63	6912.50
	39.7626	7511.07	8.90	119.00	532.63	6978.44
50	8.4124	5279.68	-10.93	-20.00	-20.00	5299.68
	11.2829	5248.32	-10.93	-30.00	-50.00	5298.32
	16.2922	5254.81	0.00	-20.00	-70.00	5324.81
	26.3933	5249.89	0.00	0.00	-70.00	5319.89
	39.7626	5419.12	46.88	90.00	20.00	5399.12
30	8.4124	3287.85	-24.69	-50.00	-50.00	3337.85
	11.2829	3204.14	-17.52	-70.00	-120.00	3324.14
	16.2922	3176.99	-10.34	-60.00	-180.00	3356.99
	26.3933	3160.32	9.34	0.84	-179.16	3339.48
	39.7626	3285.20	9.34	124.90	-54.30	3339.50

TABLE 1c

Solution: 30 ppm (by wt.) Polyox

Calculation of $\frac{8\ U_w}{D}$ and $\frac{8(\langle u\rangle - U_w)}{D}$ for Stainless Steel tubes

τ_w dynes/cm^2	1/D cm^{-1}	$\frac{8\langle u\rangle}{D}$ sec^{-1}	$\partial \frac{8\langle u\rangle}{D} / \partial \frac{1}{D}$	$\int \frac{\partial \frac{8\langle u\rangle}{D}}{\partial \frac{1}{D}} d(1/d)$	$\frac{8\ U_w}{D}$ sec^{-1}	$\frac{8(\langle u\rangle - U_w)}{D}$ sec^{-1}
310	8.1787	24757.9	1863.60	3410.0	3410.0	21347.9
	11.6711	28410.7	500.00	4350.0	7760.0	20750.7
	17.0504	29163.5	240.00	1630.0	9390.0	19773.5
	23.9126	31138.2	93.33	950.0	10340.0	20798.2
	33.0294	31483.1	-11.50	329.4	10669.4	20813.7
250	8.1787	20896.4	1068.20	1750.0	1750.0	19146.4
	11.6711	23474.9	375.00	2590.0	4340.0	19134.9
	17.0504	24106.0	150.90	1440.0	5780.0	18326.0
	23.9126	25366.0	66.70	810.0	6590.0	18776.0
	33.0294	25556.3	-12.10	370.0	6960.0	18596.3

.....contd/...

τ_w dynes/cm^2	1/D cm^{-1}	$\frac{8\langle u\rangle}{D}$ sec^{-1}	$\partial \frac{8\langle u\rangle}{D} / \partial \frac{1}{D}$	$\int \frac{\partial \frac{8\langle u\rangle}{D}}{\partial \frac{1}{D}} d(1/D)$	$\frac{8U_w}{D}$ sec^{-1}	$\frac{8(\langle u\rangle - U_w)}{D}$ sec^{-1}
190	8.1787	16723.5	732.10	1100.0	1100.0	15623.5
	11.6711	18311.5	259.30	1620.0	2720.0	15591.5
	17.0504	18812.2	111.10	970.0	3690.0	15122.2
	23.9126	19479.6	26.30	510.0	4200.0	15279.6
	33.0294	19553.3	6.20	148.5	4348.5	15204.8
130	8.1787	12148.6	267.85	910.0	910.0	11238.6
	11.6711	12886.0	137.10	780.0	1690.0	11196.0
	17.0504	13245.1	55.65	435.0	2125.0	11120.1
	23.9126	13471.9	-0.22	195.0	2320.0	11151.9
	33.0294	13469.9	-0.22	-2.0	2318.0	11151.9
100	8.1787	9668.66	137.68	525.0	525.0	9143.66
	11.6711	10061.60	81.81	475.0	1000.0	9061.60
	17.0504	10345.00	30.43	285.0	1285.0	9060.00
	23.9126	10419.70	-2.42	75.0	1360.0	9059.70
	33.0294	10397.60	-2.42	-22.1	1337.9	9059.70

.....contd/....

τ_w dynes/cm^2	1/D cm^{-1}	$\frac{8\langle u\rangle}{D}$ sec^{-1}	$\frac{\partial \frac{8\langle u\rangle}{D}}{\partial\, 1/D}$	$\int \frac{\partial \frac{8\langle u\rangle}{D}}{\partial\, 1/D} d(1/D)$	$\frac{8\,U_w}{D}$ sec^{-1}	$\frac{8(\langle u\rangle - U_w)}{D}$ sec^{-1}
70	8.1787	7027.16	26.67	70.0	70.0	6957.16
	11.6711	7153.96	42.73	100.0	170.0	6983.96
	17.0504	7357.75	15.87	190.0	360.0	7341.88
	23.9126	7334.94	-3.43	25.0	385.0	6949.94
	33.0294	7303.62	-3.43	-31.3	353.7	6949.92
50	8.1787	5159.02	0.00	0.0	0.0	5159.02
	11.6711	5165.65	0.00	0.0	0.0	5165.65
	17.0504	5313.89	16.30	30.0	30.0	5283.89
	23.9126	5258.73	-3.22	24.6	54.6	5204.13
	33.0294	5229.38	-3.22	-29.4	25.3	5204.08
30	8.1787	3189.04	-39.06	-100.0	-100.0	3289.04
	11.6711	3134.22	0.00	-70.0	-170.0	3304.22
	17.0504	3225.05	26.60	60.0	-110.0	3335.05
	23.9126	3167.30	-2.46	60.0	-50.0	3217.30
	33.0294	3144.85	-2.46	-27.5	-77.5	3222.35

TABLE 1d

Solution: 30 ppm. (by wt.) Polyox

Calculation of $\frac{8\ U_w}{D}$ and $\frac{8(\langle u\rangle - U_w)}{D}$ for Glass tubes

τ_w dynes/cm^2	1/D cm^{-1}	$\frac{8\langle u\rangle}{D}$ sec^{-1}	$\frac{\partial \frac{8\langle u\rangle}{D}}{\partial\ 1/D}$	$\int \frac{\partial \frac{8\langle u\rangle}{D}}{\partial\ 1/D}\, d(1/D)$	$\frac{8\ U_w}{D}$ sec^{-1}	$\frac{8(\langle u\rangle - U_w)}{D}$ sec^{-1}
310	8.4124	22518.5	1406.25	1380.0	1380.0	21138.5
	11.2829	27500.0	961.54	6080.0	7460.0	20040.0
	16.2922	30203.4	355.56	3030.0	10490.0	19713.4
	26.3933	31969.5	36.37	1890.0	12380.0	19589.5
	39.7626	31004.0	-313.73	-1842.2	10537.8	20466.2
250	8.4124	19158.3	1300.00	950.0	950.0	18208.3
	11.2829	22906.0	860.00	4210.0	5160.0	17746.0
	16.2922	24790.7	230.00	2380.0	7540.0	17250.7
	26.3933	25787.7	15.00	870.0	8410.0	17377.7
	39.7626	25190.2	108.40	-635.0	7775.0	17415.2

....contd/...

τ_w dynes/ cm^2	1/D cm^{-1}	$\frac{8\langle u\rangle}{D}$ sec^{-1}	$\frac{\partial \frac{8\langle u\rangle}{D}}{\partial 1/D}$	$\int \frac{\partial \frac{8\langle u\rangle}{D}}{\partial 1/D} d(1/D)$	$\frac{8\,U_w}{D}$ sec^{-1}	$\frac{8(\langle u\rangle - U_w)}{D}$ sec^{-1}
190	8.4124	15489.9	812.50	740.0	740.0	14749.9
	11.2829	18036.7	546.50	2550.0	3290.0	14746.7
	16.2922	19193.5	109.09	1260.0	4550.0	14643.5
	26.3933	19601.2	-15.50	400.0	4950.0	14651.2
	39.7626	19290.0	-23.21	-61.1	4888.9	14402.0
130	8.4124	11408.7	429.80	330.0	330.0	11078.7
	11.2829	12835.5	368.85	1440.0	1770.0	11065.5
	16.2922	13392.4	18.52	640.0	2410.0	10982.4
	26.3933	13412.3	-8.24	-62.6	2347.4	11064.9
	39.7626	13302.2	-8.24	-110.1	2237.3	11064.9
100	8.4124	9161.60	310.60	260.00	260.00	8901.60
	11.2829	10087.10	211.77	1020.00	1280.00	8807.10
	16.2922	10407.90	13.70	390.00	1670.00	8737.90
	26.3933	10317.90	-9.60	-70.98	1599.00	8718.90
	39.7626	10273.10	-3.35	-86.50	1512.50	8760.60

.....contd....

τ_w dynes/cm^2	1/D cm^{-1}	$\frac{8\langle u\rangle}{D}$ sec^{-1}	$\frac{\partial \frac{8\langle u\rangle}{D}}{\partial 1/D}$	$\int \frac{\partial \frac{8\langle u\rangle}{D}}{\partial 1/D} d(1/D)$	$\frac{8 U_w}{D}$ sec^{-1}	$\frac{8(\langle u\rangle - U_w)}{D}$ sec^{-1}
190	8.4124	15489.9	812.50	740.0	740.0	14749.9
	11.2829	18036.7	546.50	2550.0	3290.0	14746.7
	16.2922	19193.5	109.09	1260.0	4550.0	14643.5
	26.3933	19601.2	-15.50	400.0	4950.0	14651.2
	39.7626	19290.0	-23.21	-61.1	4888.9	14402.0
130	8.4124	11408.7	429.80	330.0	330.0	11078.7
	11.2829	12835.5	368.85	1440.0	1770.0	11065.5
	16.2922	13392.4	18.52	640.0	2410.0	10982.4
	26.3933	13412.3	-8.24	-62.6	2347.4	11064.9
	39.7626	13302.2	-8.24	-110.1	2237.3	11064.9
100	8.4124	9161.60	310.60	260.00	260.00	8901.60
	11.2829	10087.10	211.77	1020.00	1280.00	8807.10
	16.2922	10407.90	13.70	390.00	1670.00	8737.90
	26.3933	10317.90	-9.60	-70.98	1599.00	8718.90
	39.7626	10273.10	-3.35	-86.50	1512.50	8760.60

.....contd....

τ_w dynes/cm^2	1/D cm^{-1}	$\frac{8\langle u\rangle}{D}$ sec^{-1}	$\frac{\partial \frac{8\langle u\rangle}{D}}{\partial \frac{1}{D}}$	$\int \frac{\partial \frac{8\langle u\rangle}{D}}{\partial \frac{1}{D}} d(1/D)$	$\frac{8U_w}{D}$ sec^{-1}	$\frac{8(\langle u\rangle - U_w)}{D}$ sec^{-1}
70	8.4124	6732.95	114.29	70.00	70.00	6662.95
	11.2829	7223.79	104.94	460.00	530.00	6693.79
	16.2922	7362.84	6.09	150.00	680.00	6682.84
	26.3933	7218.76	-14.27	-176.87	503.13	6715.63
	39.7626	7220.08	0.00	-95.34	407.79	6812.29
50	8.4124	4987.98	85.23	60.00	60.00	4927.98
	11.2829	5243.53	40.23	220.00	280.00	4963.53
	16.2922	5297.26	0.00	50.00	330.00	4967.26
	26.3933	5156.59	-13.93	-70.33	259.67	4896.92
	39.7626	5171.09	0.00	-93.09	166.58	5004.51
30	8.4124	3116.96	31.25	35.00	35.00	3081.96
	11.2829	3199.61	12.71	85.00	120.00	3079.61
	16.2922	3201.92	0.00	5.00	125.00	3076.92
	26.3933	3087.34	-11.34	-57.27	67.73	3019.61
	39.7626	3111.24	1.79	-75.80	-8.07	3119.31

TABLE 1e

Solution: 20 ppm. (by wt.) polyox

Calculation of $\frac{8.U_w}{D}$ and $\frac{8(\langle u\rangle - U_w)}{D}$ for Stainless Steel tubes

τ_w dynes/cm^2	1/D cm^{-1}	$\frac{8\langle u\rangle}{D}$ sec^{-1}	$\frac{\partial \frac{8\langle u\rangle}{D}}{\partial \frac{1}{D}}$	$\int \frac{\partial \frac{8\langle u\rangle}{D}}{\partial \frac{1}{D}} d(1/D)$	$\frac{8.U_w}{D}$ sec^{-1}	$\frac{8(\langle u\rangle - U_w)}{D}$ sec^{-1}
	8.1787	25531.1	833.300	2650.00	2650.00	22881.10
	11.6711	30052.3	710.526	2820.00	5470.00	24582.30
310	17.0504	30326.3	217.950	2440.00	7910.00	22416.30
	23.9126	31664.0	117.647	1050.00	8960.00	22704.00
	33.0294	32406.2	43.750	735.70	9695.70	22710.50
	8.1787	21503.0	65.280	1950.00	1950.00	19553.00
	11.6711	24716.4	494.737	2170.00	4120.00	20596.00
250	17.0504	25027.6	106.383	1290.00	5410.00	19617.60
	23.9126	25827.0	82.474	690.00	6100.00	19727.00
	33.0294	26386.6	33.784	529.95	6629.95	19756.65

....contd/...

τ_w dynes/ cm^2	1/D cm^{-1}	$\frac{8<u>}{D}$ sec^{-1}	$\frac{\partial \frac{8<u>}{D}}{\partial 1/D}$	$\int_{\partial} \frac{\partial \frac{8<u>}{D}}{\partial 1/D} d(1/D)$	$\frac{8.U_w}{D}$ sec^{-1}	$\frac{8(<u> - U_w)}{D}$ sec^{-1}
190	8.1787	17162.8	407.407	1140.00	1140.00	16022.80
	11.6711	19179.2	338.710	1400.00	2540.00	16639.20
	17.0504	19495,9	78.125	960.00	3500.00	15995.20
	23.9126	19860.2	50.000	390.00	3890.00	15970.20
	33.0294	20253.3	30.000	364.67	4254.67	15998.63
130	8.1787	12424.0	244.680	670.00	670.00	11754.00
	11.6711	13415.9	152.540	810.00	1480.00	11935.90
	17.0504	13697.7	37.500	440.00	1920.00	11777.70
	23.9126	13754.6	19.230	130.00	2050.00	11704.60
	33.0294	13999.3	19.230	175.32	2225.32	11773.98
100	8.1787	9865.79	169.49	450.00	450.00	9415.79
	11.6711	10440.70	117.65	560.00	1010.00	9430.70
	17.0504	10685.90	15.15	300.00	1310.00	9375.90
	23.9126	10646.90	8.33	20.00	1330.00	9316.90
	33.0294	10824.90	8.33	75.97	1405.97	9418.93

.....contd/...

τ_w dynes/cm^2	1/D cm^{-1}	$\frac{8\langle u\rangle}{D}$ sec^{-1}	$\frac{\partial \frac{8\langle u\rangle}{D}}{\partial 1/D}$	$\int \frac{\partial \frac{8\langle u\rangle}{D}}{\partial 1/D} d(1/D)$	$\frac{8 U_w}{D}$ sec^{-1}	$\frac{8(\langle u\rangle - U_w)}{D}$ sec^{-1}
70	8.1787	7151.28	45.45	120.00	120.00	7031.28
	11.6711	7396.85	58.82	200.00	320.00	7176.85
	17.0504	7590.69	0.00	160.00	480.00	7110.69
	23.9126	7500.35	0.00	0.00	480.00	7020.35
	33.0294	7617.57	0.00	0.00	480.00	7137.57
50	8.1787	5239.07	9.62	5.00	5.00	5234.07
	11.6711	5327.26	50.73	110.00	115.00	5212.26
	17.0504	5477.19	0.00	140.00	255.00	5222.19
	23.9126	5380.49	-1.04	-7.13	247.87	5132.62
	33.0294	5460.50	-1.04	-9.48	237.39	5223.17
30	8.1787	3230.55	0.00	0.00	0.00	3230.55
	11.6711	3223.57	0.00	0.00	0.00	3223.57
	17.0504	3320.81	10.75	60.00	60.00	3260.81
	23.9126	3242.40	0.00	0.00	60.00	3182.40
	33.0294	3288.10	0.00	0.00	60.00	3228.10

TABLE 1f

Solution: 20 ppm. (by wt.) polyox

Calculation of $\frac{8.U_w}{D}$ and $\frac{8(<u> - U_w)}{D}$ for Glass tubes

τ_w dynes/cm^2	1/D cm^{-1}	$\frac{8<u>}{D}$ sec^{-1}	$\frac{\partial \frac{8<u>}{D}}{\partial 1/D}$	$\int \frac{\partial \frac{8<u>}{D}}{\partial(1/D)} d(1/D)$	$\frac{8.U_w}{D}$ sec^{-1}	$\frac{8(<u> - U_w)}{D}$ sec^{-1}
310	8.4124	25632.0	833.300	3350.00	3350.00	22282.00
	11.2829	28187.4	757.143	2380.00	5730.00	22507.40
	16.2922	30568.7	305.550	2660.00	8390.00	22178.70
	26.3933	32183.7	55.556	1480.00	9870.00	22363.70
	39.7626	31839.2	-87.300	-438.90	9441.10	22398.10
250	8.4124	21663.4	796.875	2370.00	2370.00	19293.40
	11.2829	23574.6	481.481	1820.00	4190.00	19384.60
	16.2922	25162.1	216.216	1630.00	5820.00	19342.10
	26.3933	26137.1	22.220	960.00	6780.00	19357.10
	39.7626	25954.2	-46.153	-247.34	6532.66	19421.54

.....contd/...

τ_w	1/D	$\frac{8\langle u\rangle}{D}$	$\frac{\partial \frac{8\langle u\rangle}{D}}{\partial (1/D)}$	$\int \frac{\partial \frac{8u}{D}}{\partial (1/D)} d(1/D)$	$\frac{8.U_w}{D}$	$\frac{8(\langle u\rangle - U_w)}{D}$
	8.4124	17366.8	513.51	1790	1790	15576.8
	11.2829	18654.4	307.70	1180	2970	15684.4
190	16.2922	19543.1	90.36	910	3880	15663.1
	26.3933	20006.6	0.00	265	4145	15861.6
	39.7626	19945.2	-3.74	-25	4120	15825.2
	8.4124	15066.9	385.42	1240	1240	13826.9
	11.2829	16054.4	223.40	930	2170	13884.4
160	16.2922	16645.9	71.42	660	2830	13815.9
	26.3933	16909.0	0.00	160	2990	13919.0
	39.7626	16891.7	-1.50	-10	2980	13911.7

.....contd....

τ_w	1/D	$\frac{8\langle u\rangle}{D}$	$\frac{\partial \frac{8\langle u\rangle}{D}}{\partial 1/D}$	$\int \frac{\partial \frac{8\langle u\rangle}{D}}{\partial (1/D)} d(1/D)$	$\frac{8.U_w}{D}$	$\frac{8(\langle u\rangle - U_w)}{D}$
130	8.4124	12644.5	330.00	870.0	870.0	11774.5
	11.2829	13355.7	125.00	620.0	1490.0	11865.7
	16.2922	13685.1	35.21	360.0	1850.0	11835.1
	26.3933	13789.1	0.00	60.0	1910.0	11879.1
	39.7626	13804.1	0.00	0.0	1910.0	11894.1
100	8.4124	10077.9	206.52	640.0	640.0	9437.9
	11.2829	10533.8	93.75	460.0	1100.0	9433.8
	16.2922	10656.2	24.43	150.0	1250.0	9406.2
	26.3933	10646.0	-1.00	0.0	1250.0	9596.0
	39.7626	10681.2	2.63	35.2	1285.2	9396.0

.....contd/...

τ_w	1/D	$\frac{8<u>}{D}$	$\frac{\partial \frac{8<u>}{D}}{\partial\ 1/D}$	$\int \frac{\partial \frac{8<u>}{D}}{\partial(1/D)} d(1/D)$	$8.U_w$	$\frac{8(<u> - U_w)}{D}$
70	8.4124	7337.42	140.00	390.00	390.00	6947.42
	11.2829	7574.89	24.00	295.00	585.00	6989.89
	16.2922	7554.34	-4.11	-10.00	575.00	6979.34
	26.3933	7479.96	-8.12	-61.77	513.23	6966.73
	39.7626	7521.68	3.16	-29.01	484.22	7037.46
50	8.4124	5394.34	35.20	80.00	80.00	5314.34
	11.2829	5515.40	12.98	70.00	150.00	5365.40
	16.2922	5443.06	-14.37	-40.00	110.00	5333.06
	26.3933	5356.07	-8.61	-116.10	-6.10	5362.17
	39.7626	5394.36	2.86	-31.95	-38.05	5432.41
30	8.4124	3339.98	10.84	5.00	5.00	3334.98
	11.2829	3377.10	10.84	25.00	30.00	3347.10
	16.2922	3295.05	-16.38	-50.00	-20.00	3315.05
	26.3933	3222.04	-7.23	-119.23	-139.23	3361.27
	39.7626	3249.84	2.08	-37.58	-176.81	3426.65

A plot of frictional pressure drop, ΔP vs. length of the capillary tube L is found to be linear as shown in fig. 13(a) and 13(b).

Figs. 14 and 15 show the plot of $\frac{8\langle u\rangle}{D}$ vs. 1/D for stainless steel and glass tubes respectively for 40 ppm. polyox solution with shear stress as a parameter. The slopes of the tangents to the curve were determined in the range of 1/D where the experimental data was available. This was necessary because the nature of the extrapolated curve was not reliable. The values of the slope of the tangents to these curves for a given value of 1/D and shear stress are listed in the Table 1.

Figs. 16(a) and 16(b) show the plots of the slope $\frac{\partial \frac{8\langle u\rangle}{D}}{\partial \frac{1}{D}}$ vs. 1/D for stainless steel and glass tubes respectively for 40 ppm. polyox solution with shear stress as a parameter. At a given shear stress, the area under the curve was determined from 1/D = 0 to the value of 1/D corresponding to the particular tube, with the help of planimeter. This gives the value of $\frac{8\ U_w}{D}$ for that particular tube at a given shear stress. This procedure was repeated for all the tubes for various values of shear stress. These values are tabulated in Table 1. Knowing $\frac{8\ U_w}{D}$ the experimental points were corrected to give the true curve as shown by dotted lines in figs. 6 to 12. The values used to determine the final curve are given in table 2. Critical shear stress for a tube is the point of intersection of this final curve [τ_w vs. $\frac{8(\langle u\rangle - U_w)}{D}$] with the flow curve

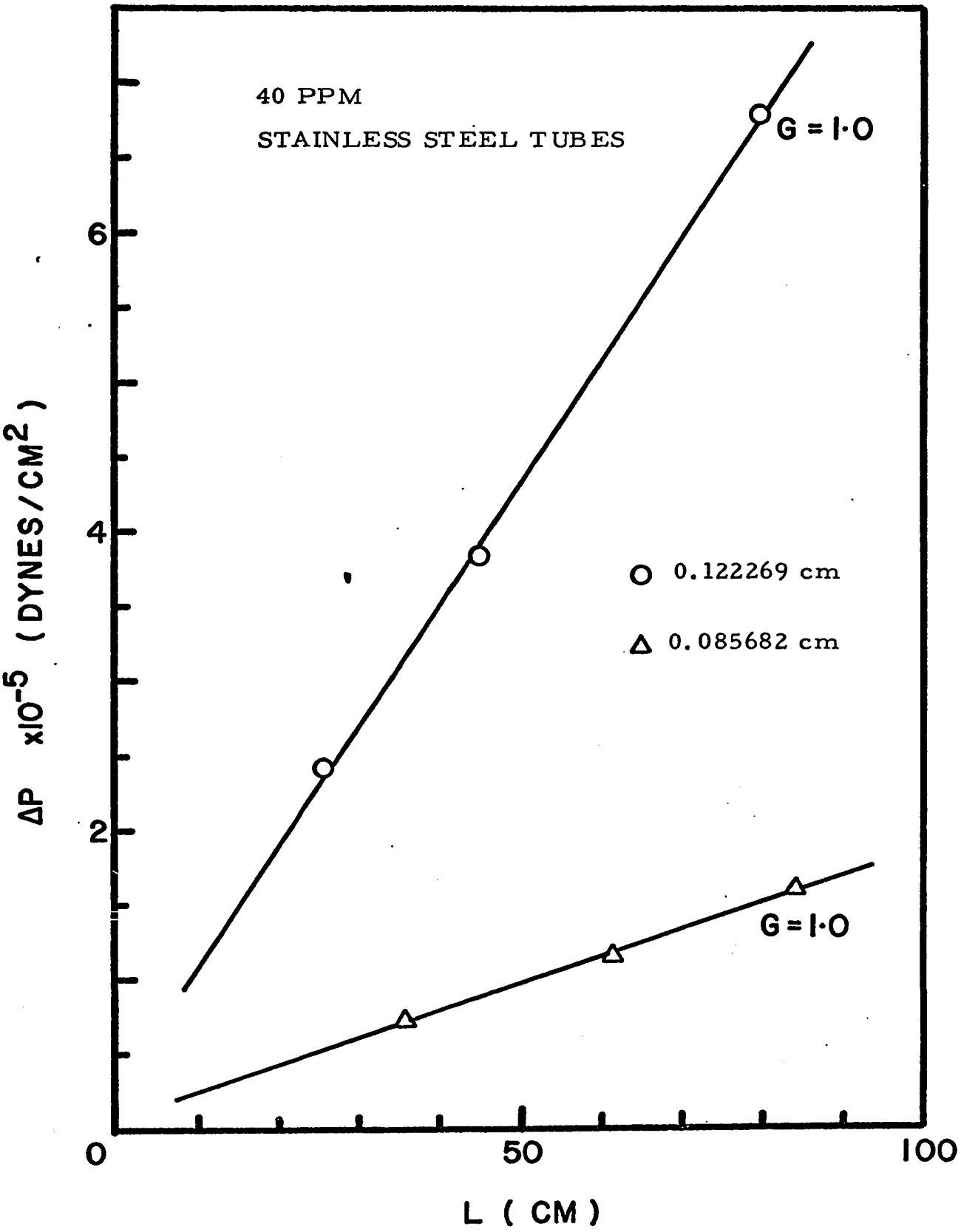

Fig. 13(a). Pressure drop vs length of the capillary tube for 40 ppm polyox solution (1 and 2 stainless steel tubes)

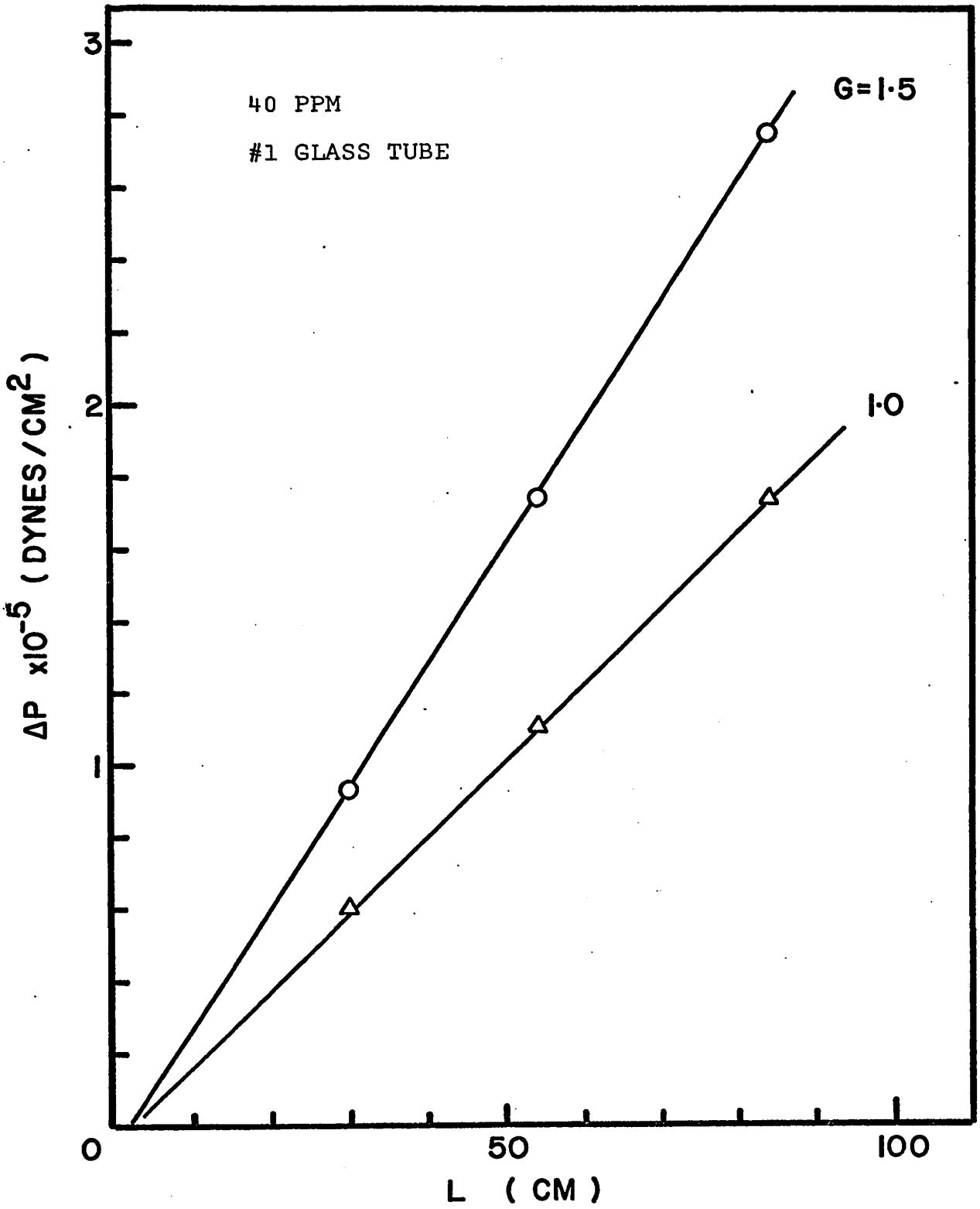

Fig. 13(b). Pressure drop vs length of the capillary tube for 40 ppm polyox solution (glass tubes)

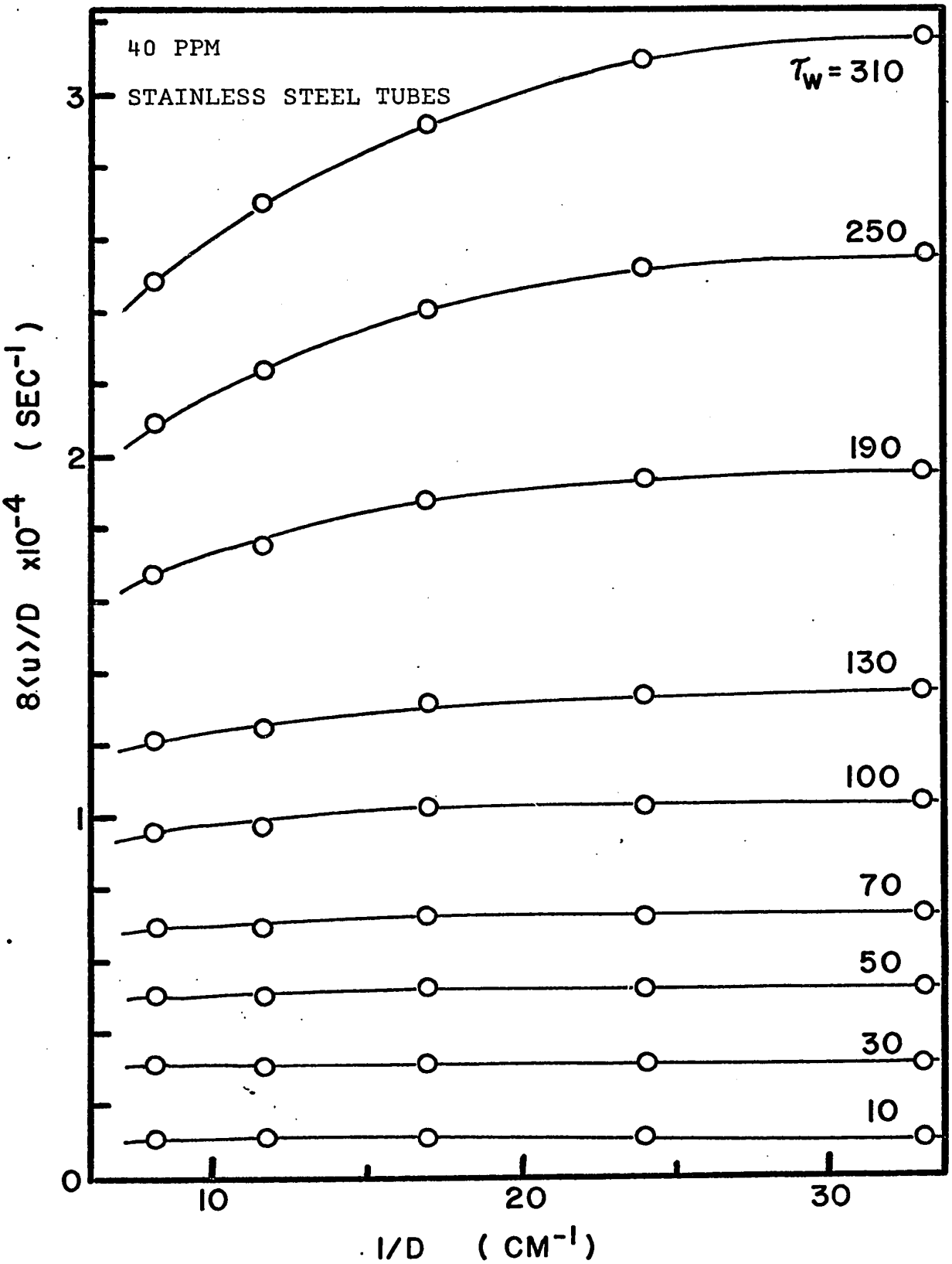

Fig. 14. $\frac{8\langle u\rangle}{D}$ vs 1/D for 40 ppm. polyox solution in case of stainless steel tubes.

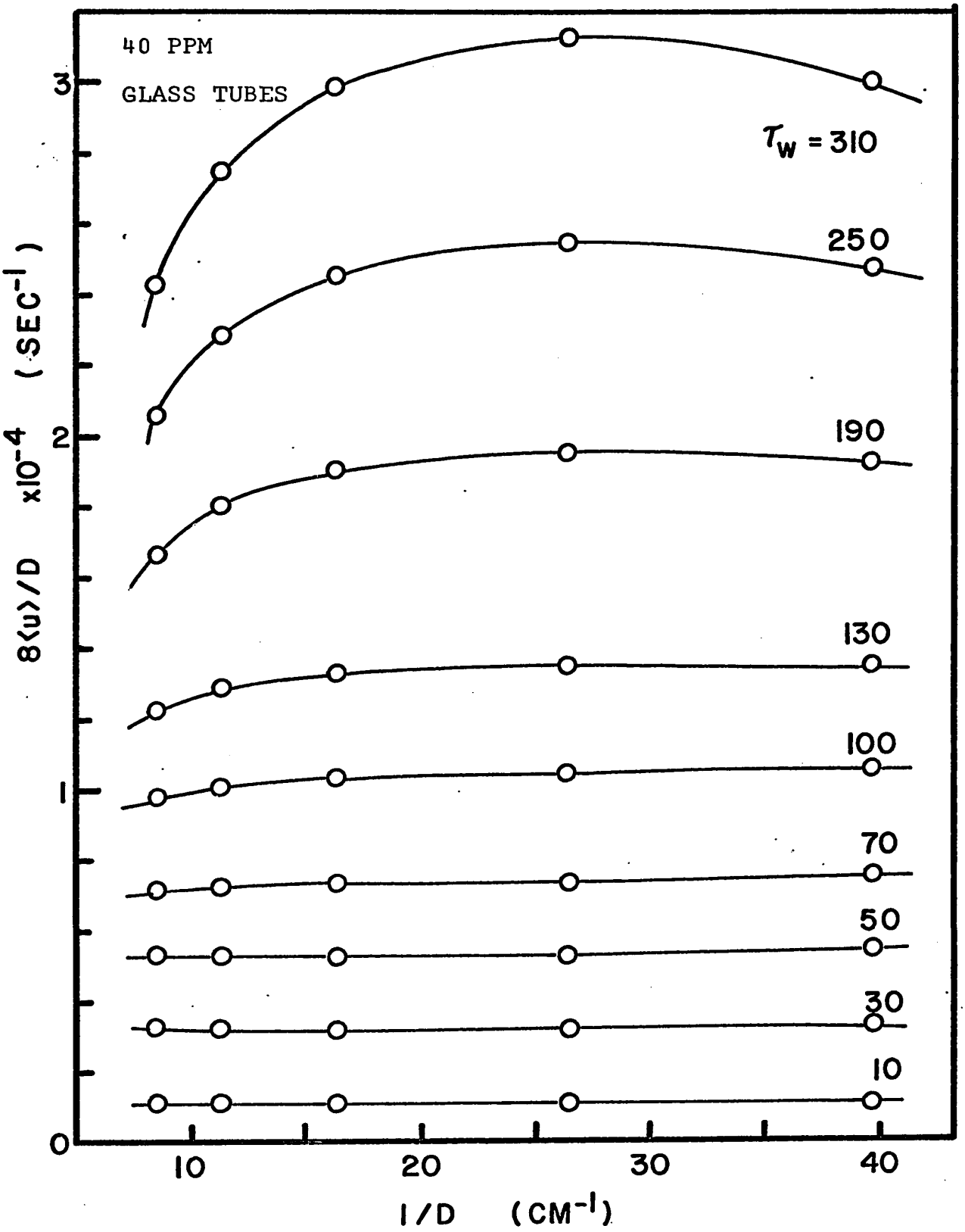

Fig. 15. $\frac{8\langle u\rangle}{D}$ vs. 1/D for 40 ppm polyox solution in case of glass tubes.

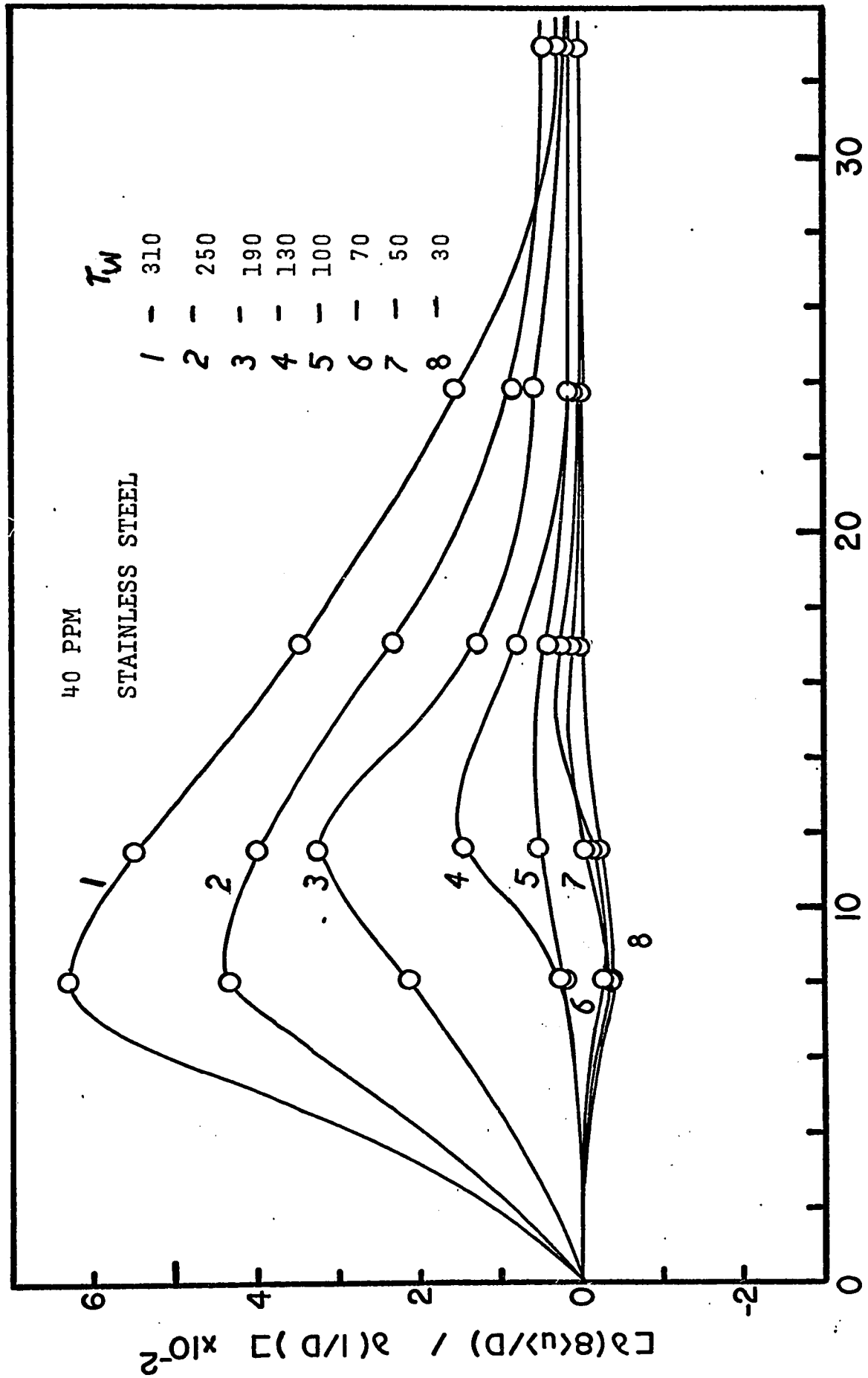

Fig. 16(a). $\frac{\partial(\frac{8\langle u\rangle}{D})}{\partial\, 1/D}$ vs 1/D for 40 ppm polyox solution with shear stress as a parameter.

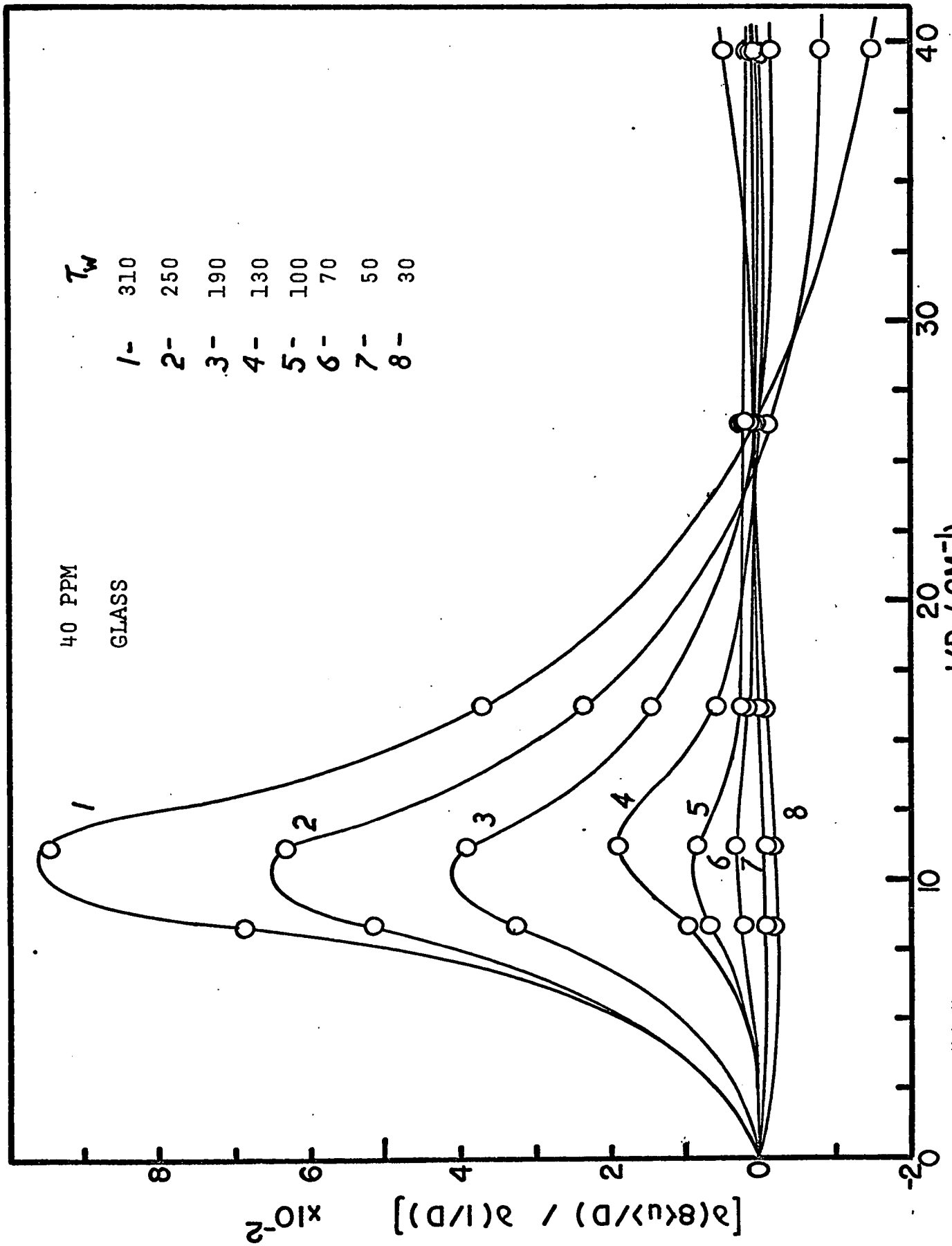

Fig. 16(b). $\frac{\partial(\frac{8\langle u\rangle}{D})}{\partial\ 1/D}$ vs 1/D for 40 ppm polyox solution with shear stress as a parameter.

TABLE 2

Values of $\frac{8(\langle u \rangle - U_w)}{D}$ at a given shear stress for 40 ppm. polyox solution.[2a]

Stainless Steel			Glass		
$\frac{8(\langle u \rangle - U_w)}{D}$ sec^{-1}	τ_w dynes/cm^2	τ_w cal. dynes/cm^2	$\frac{8(\langle u \rangle - U_w)}{D}$ sec^{-1}	τ_w dynes/cm^2	τ_w cal. dynes/cm^2
22389.4	310	308.008	22611.4	310	307.771
19406.4	250	250.558	19638.5	250	252.441
16129.4	190	193.261	15967.3	190	190.324
12105.4	130	131.233	12096.4	130	132.262
9721.6	100	98.819	9636.2	100	99.325
7271.1	70	68.857	6978.4	70	67.208
5387.4	50	48.142	5399.1	50	49.827
3442.9	30	28.867	3339.5	30	29.068

Coefficients of the equation 3.C.10 for 40 ppm. polyox solution

Concentration	Tube material	$\alpha \times 10^3$	$\beta \times 10^7$
40 ppm.	Stainless	7.40828	2.83559
	Glass	7.85394	2.54628

TABLE 2b

Values of $\frac{8(\langle u \rangle - U_w)}{D}$ at a given shear stress for 30 ppm. polyox solution

Stainless Steel			Glass		
$\frac{8(\langle u \rangle - U_w)}{D}$ sec^{-1}	τ_w dynes/cm^2	$\tau_{w\,cal.}$ dynes/cm^2	$\frac{8\langle u \rangle - U_w}{D}$ sec^{-1}	τ_w dynes/cm^2	$\tau_{w\,cal.}$ dynes/cm^2
20813.7	310	303.158	20466.2	310	311.758
18596.3	250	257.521	17415.1	250	247.047
15204.8	190	193.872	14402.0	190	189.412
11151.9	130	127.572	11064.9	130	132.852
9059.7	100	97.506	8706.5	100	98.256
6949.9	70	70.056	6812.3	70	71.850
5204.1	50	49.518	5004.5	50	49.679
3222.3	30	28.595	3119.3	30	28.947

Coefficients of the equation 3.C.10 for 30 ppm. polyox solution.

Concentration	Tube material	$\alpha \times 10^3$	$\beta \times 10^7$
30 ppm.	Stainless	7.83155	3.23530
	Glass	8.20940	3.43176

TABLE 2c

Value of $\frac{8(\langle u \rangle - U_w)}{D}$ at a given shear stress for 20 ppm. polyox solution

$\frac{8(\langle u \rangle - U_w)}{D}$ sec^{-1}	Stainless Steel τ_w dynes/cm^2	τ_w cal. dynes/cm^2	$\frac{8\langle u \rangle - U_w}{D}$ sec^{-1}	Glass τ_w dynes/cm^2	τ_w cal dynes/cm^2
22710.5	310	307.095	22398.1	310	308.224
19756.6	250	253.584	19421.5	250	252.103
15998.6	190	191.369	15825.2	190	190.495
11774.0	130	129.271	13911.7	160	160.480
9418.9	100	98.256	11894.1	130	130.913
7137.6	70	70.649	9396.0	100	97.648
5223.2	50	49.392	7037.5	70	68.727
3228.1	30	29.028	5432.4	50	50.802
			3426.6	30	30.107

Coefficients of the equation 3.C.10 for 20 ppm. polyox solution

Concentration	Tube material	$\alpha \times 10^3$	$\beta \times 10^7$
20 ppm.	Stainless Steel	8.24185	2.32508
	Glass	7.88744	2.62244

of that particular tube. Flow curve for water was also plotted in the figs. 6 to 12 as shown. α and β the coefficients of the equation 3.C.10 are also listed in Table 2.

For the purpose of comparison, the final curves for glass and stainless steel tubes were plotted on the same graph paper at a given concentration. The final curves match fairly well for all the three concentration as shown in figs. 17, 18 and 19.

No definite trend was observed when final curves, τ_w vs. $\frac{8(\langle u \rangle - U_w)}{D}$, were plotted together with concentration as a parameter. Figs. 20 and 21 show these plots for stainless steel and glass tubes respectively.

Knowing $\frac{8\ U_w}{D}$ at a given shear stress, the values of U_w were determined for all the tubes at different concentrations. The calculated values of effective slip velocity are given in Table 3. Variation of U_w with τ_w, the shear stress for stainless steel and glass tubes respectively is shown in fig. 22 and 23 for 40 ppm. polyox solution. There is no definite pattern of how U_w varies with τ_w for different tubes.

Non-Newtonian viscosity η_w was determined using both glass and stainless steel tubes for a given concentration with the help of equation 3.D.11. Table 3 gives the results for all the three concentrations.

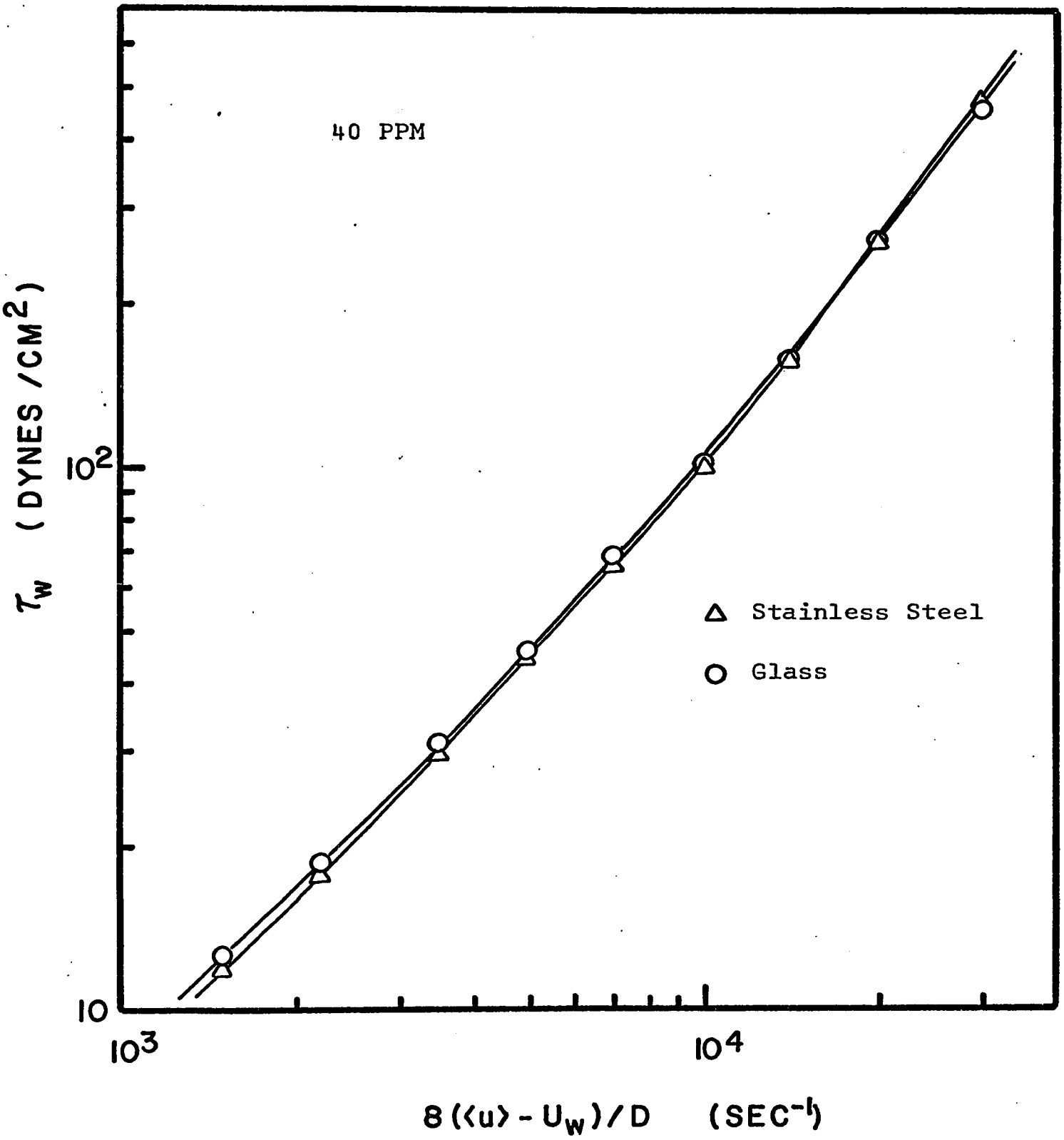

Fig. 17. Shear stress vs $\frac{8(\langle u\rangle - U_w)}{D}$ for 40 ppm polyox solution in case of stainless steel and glass tubes.

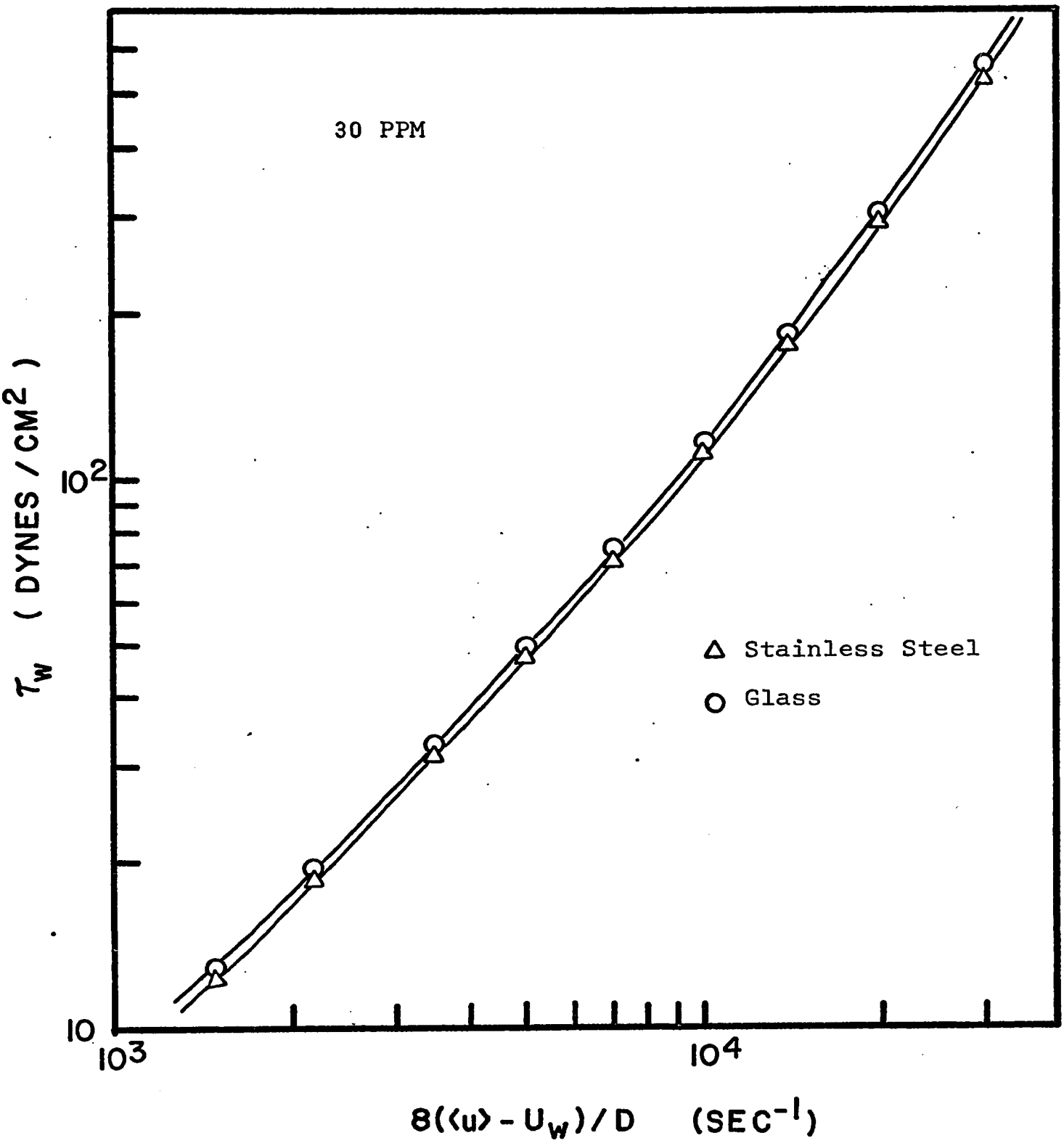

Fig. 18. Shear stress vs $\frac{8(\langle u \rangle - U_w)}{D}$ for 30 ppm polyox solution in case of stainless steel and glass tubes.

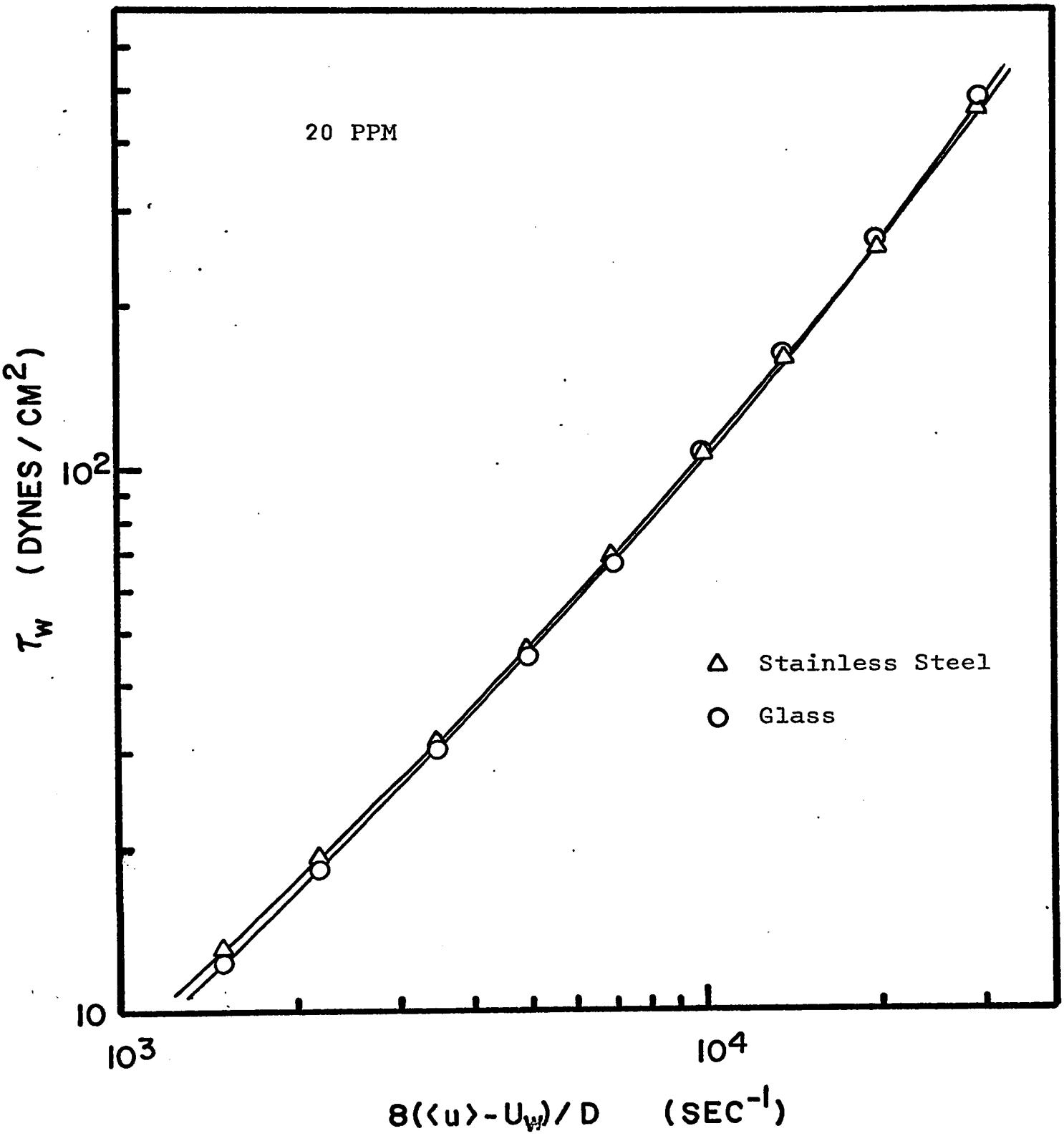

Fig. 19. Shear stress vs $\frac{8(\langle u \rangle - U_w)}{D}$ for 20 ppm polyox solution in case of stainless steel and glass tubes.

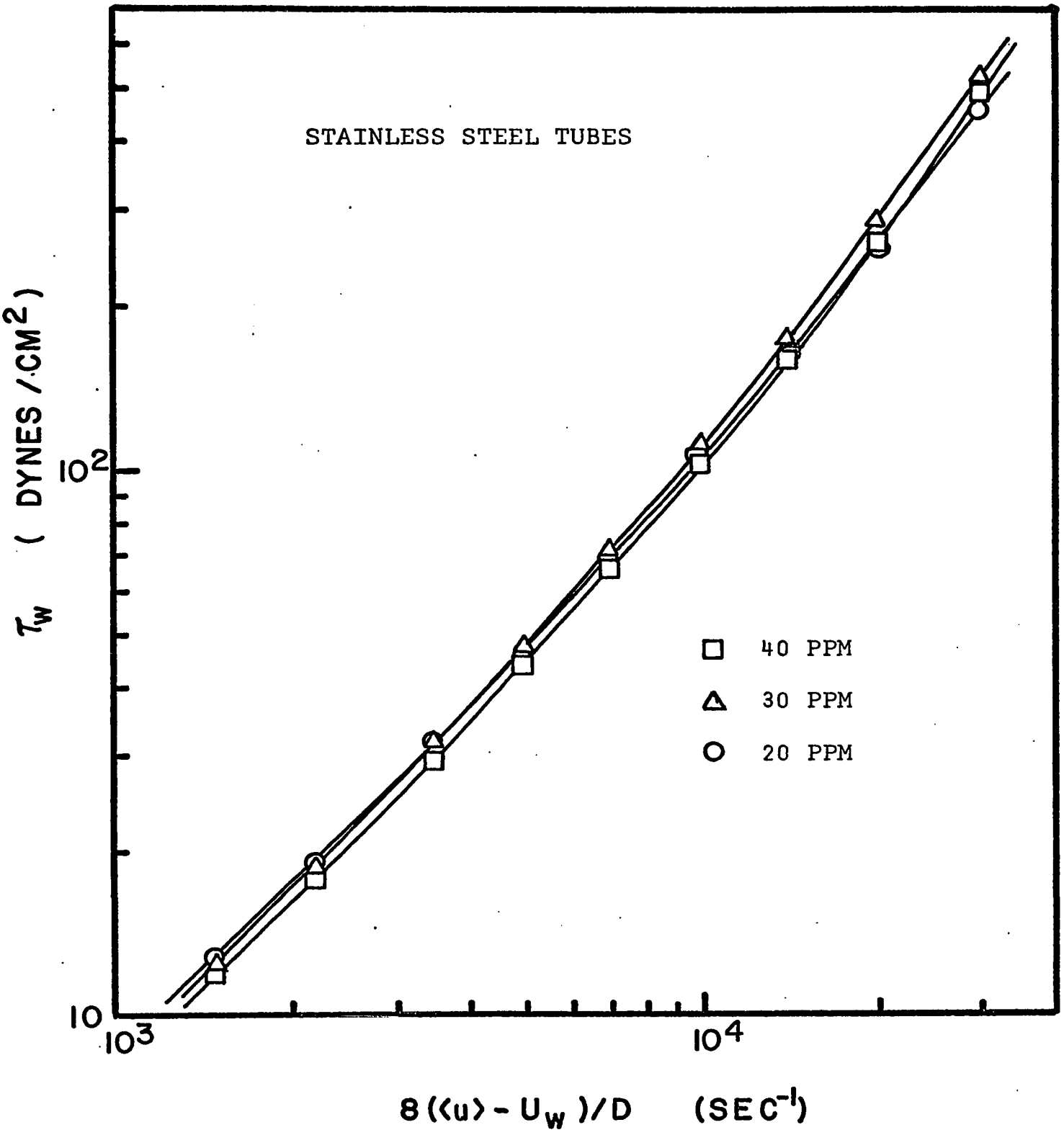

Fig. 20. Shear stress vs $\frac{8(\langle u \rangle - U_w)}{D}$ for stainless steel tubes with concentration as a parameter.

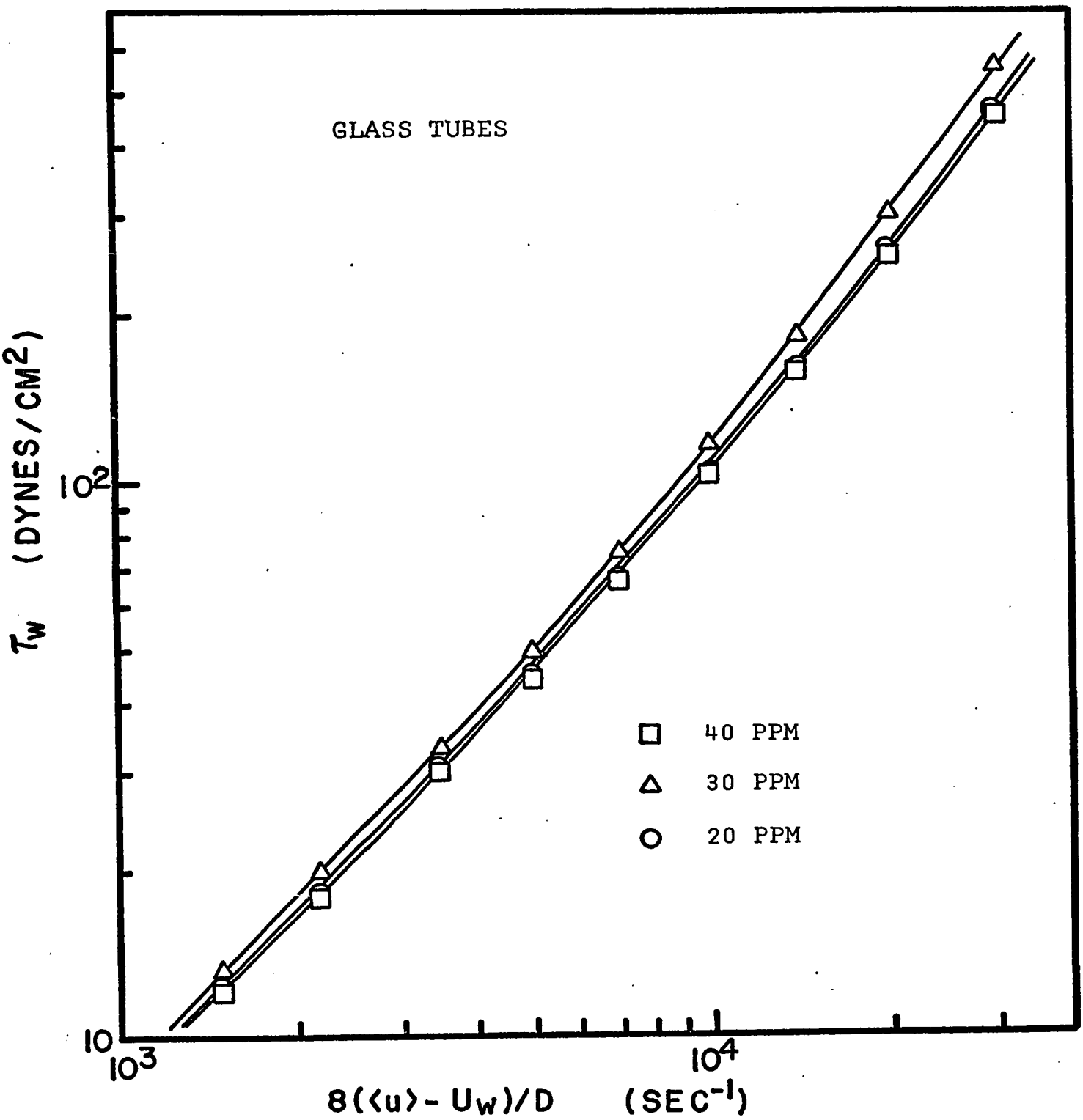

Fig. 21. Shear stress vs. $\frac{8(\langle u \rangle - U_w)}{D}$ for glass tubes with concentration as a parameter.

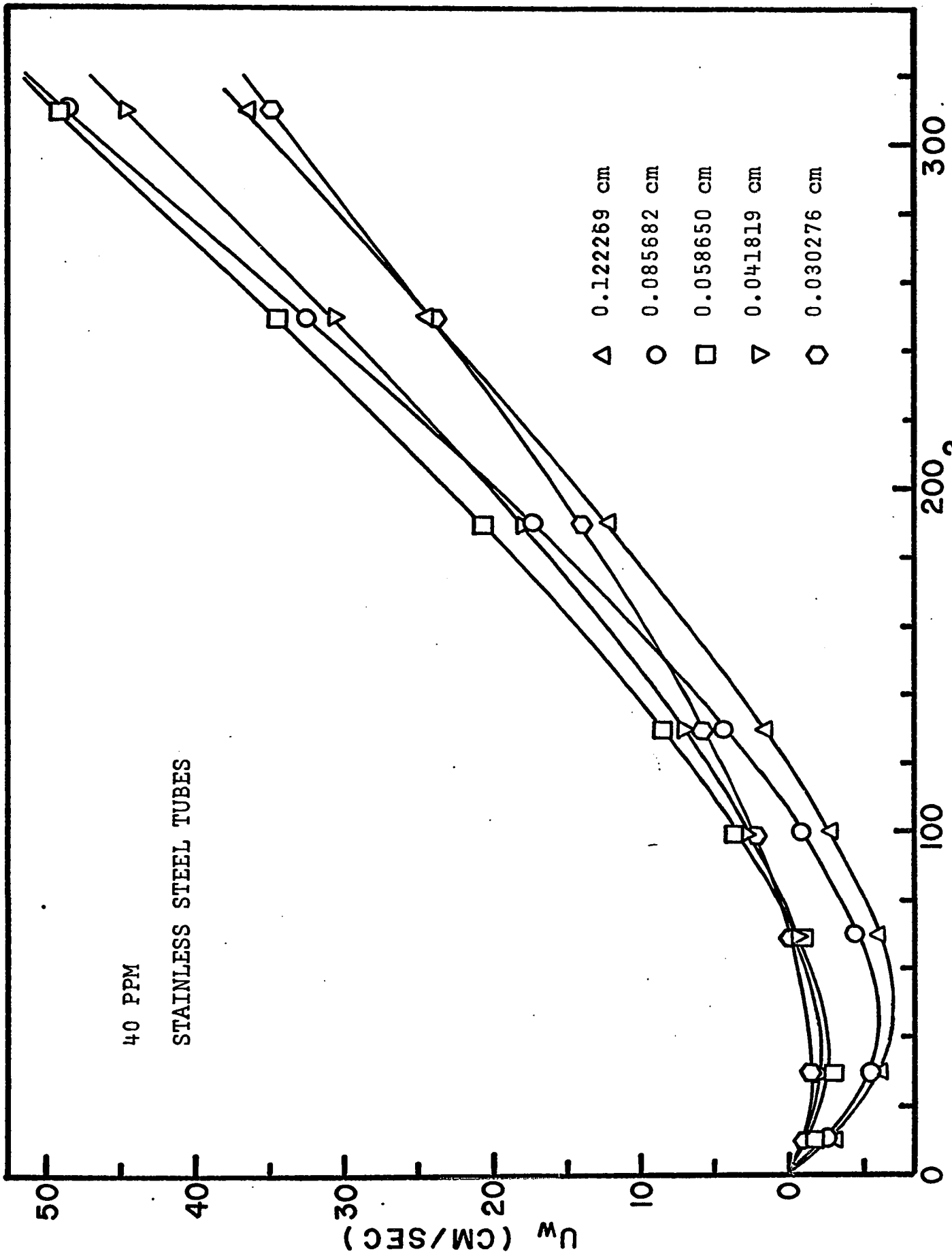

Fig. 22. Effective velocity at the wall vs shear stress for 40 ppm polyox solution.

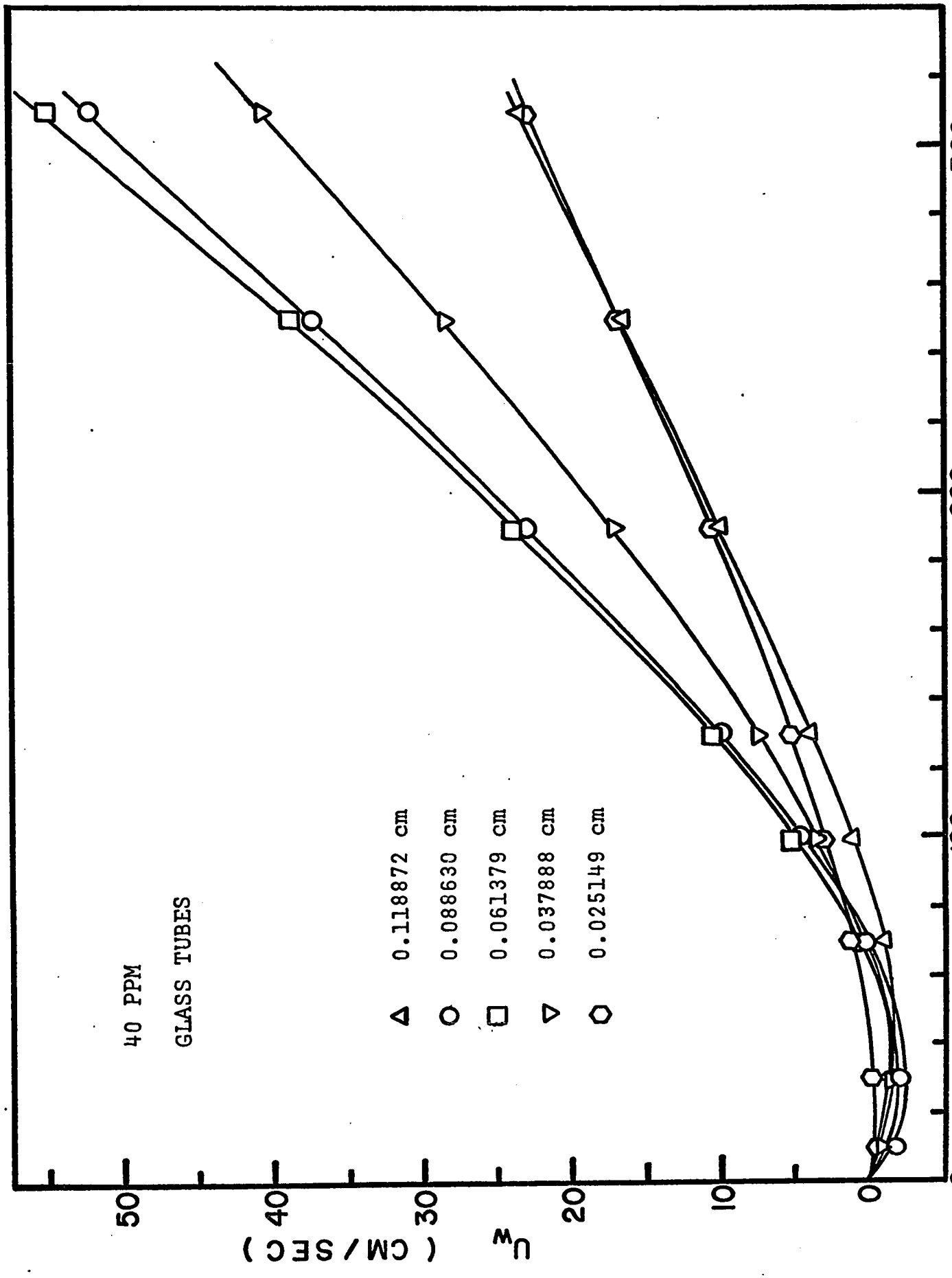

Fig. 23. Effective velocity at the wall vs shear stress for 40 ppm polyox solution.

TABLE 3

3a

Values of U_w and δ for different tubes at a given shear stress for 40 ppm. polyox solution.

Capillary	Stainless Steel			Glass		
	τ_w dynes/cm^2	U_w cm/sec.	$\delta \times 10^4$ cm.	τ_w dynes/cm^2	U_w cm/sec.	$\delta \times 10^4$ cm.
1	310	36.3346	25.9956	310	23.0753	16.9007
	250	24.0216	23.9158	250	16.4483	16.7270
	190	12.1212	18.8731	190	9.8853	15.6257
	130	1.4216	4.3779	130	3.7218	11.4075
	100	-2.9390	3.1647	100	1.0304	5.2366
	70	-6.0269	8.5638	70	-1.1128	1.6049
	30	-6.2770	18.0997	30	-2.2142	6.5927
	10	-3.1112	24.4573	10	-1.2200	10.0550
2	310	48.4329	34.6513	310	52.0193	38.0998
	250	32.4746	32.3316	250	37.1485	37.7781
	190	17.4536	27.1759	190	22.8482	36.1161
	130	4.3650	13.4419	130	9.8977	30.3185
	100	-0.8527	0.9182	100	4.3982	22.3510
	70	-4.5574	6.4758	70	0.0595	0.6618
	30	-5.4120	15.6055	30	-2.5784	7.6772
	10	-2.7016	21.2381	10	-1.5178	12.5086

.....contd/..

Capillary	Stainless Steel			Glass		
	τ_w dynes/cm^2	U_w cm/sec.	$\delta \times 10^4$ cm.	τ_w dynes/cm^2	U_w cm/sec.	$\delta \times 10^4$ cm.
3	310	48.9704	35.0359	310	54.9371	40.2369
	250	34.4157	34.2642	250	38.6746	39.3300
	190	20.6571	32.1624	190	23.5116	37.1648
	130	8.4565	26.0413	130	10.2684	31.4733
	100	3.3941	17.8372	100	4.8290	24.5402
	70	-0.5217	7.4132	70	0.6150	6.8430
	30	-2.7173	7.8354	30	-1.9937	5.9362
	10	-1.5446	12.1429	10	-1.2076	9.9525
4	310	44.4979	31.8360	310	40.4688	29.6400
	250	30.5508	30.4162	250	28.1387	28.6155
	190	17.8168	27.7414	190	16.8890	26.6964
	130	6.9855	21.5114	130	7.3000	22.3748
	100	2.6617	13.9881	100	3.4413	17.4880
	70	-0.5749	8.1683	70	0.4938	5.4944
	30	-2.2587	6.5131	30	-1.3096	3.8995
	10	-1.2520	9.8422	10	-0.7940	6.5437

.....contd/...

Capillary	Stainless Steel			Glass		
	τ_w dynes/cm^2	U_w cm/sec.	$\delta \times 10^4$ cm.	τ_w dynes/cm^2	U_w cm/sec.	$\delta \times 10^4$ cm.
5.	310	34.7633	24.8714	310	22.9789	16.8301
	250	23.9124	23.8072	250	16.6040	16.8853
	190	14.0532	21.8814	190	10.5453	16.6690
	130	5.6949	17.5371	130	5.1035	15.6424
	100	2.3563	12.3831	100	2.7869	14.1627
	70	-0.1625	0.2308	70	0.9092	10.1170
	30	-1.5523	4.4762	30	-0.4767	1.4193
	10	-0.8826	6.9384	10	-0.3709	3.0564

Values of η_w at a given shear stress for 40 ppm. solution

τ_w	Stainless Steel	Glass
dynes/cm^2	$\eta_w \times 10^3$ ($\frac{gm.}{cm.sec}$)	$\eta_w \times 10^3$ ($\frac{gm.}{cm.sec}$)
310	14.9686	14.7382
250	13.9436	13.7815
190	12.8054	12.7230
130	11.5055	11.5211
100	10.7682	10.8440
70	9.9465	10.0953
30	8.6505	8.9325
10	7.8612	8.2416

TABLE 3b

Values of U_w and δ for different tubes at a given shear stress for 30 ppm. polyox solution.

Capillary.	Stainless Steel			Glass		
	τ_w dynes/cm^2	U_w cm/sec.	$\delta \times 10^4$ cm.	τ_w dynes/cm^2	U_w cm/sec.	$\delta \times 10^4$ cm.
1	310	55.3962	36.3644	310	31.6705	19.9106
	250	40.9762	36.8283	250	23.7325	20.2527
	190	26.5731	36.3448	190	15.6836	20.0759
	130	12.7762	32.6193	130	7.8001	18.0946
	100	6.5351	26.6899	100	4.1431	14.9038
	70	1.2492	10.3776	70	0.9633	6.5850
	30	-2.6644	8.1433	30	1.5419	4.9178
	10	-1.7977	1.4956	10	-1.0961	9.5406
2	310	77.9429	51.1649	310	78.7564	49.5231
	250	56.3306	50.6284	250	59.1712	50.5088
	190	35.6297	48.7318	190	39.8689	51.0537
	130	16.8512	43.0233	130	21.5890	50.1130
	100	8.7878	35.8900	100	13.3109	47.9251
	70	2.2327	18.5478	70	6.1304	41.9662
	30	-2.4539	7.4990	30	-0.2493	0.7948
	10	-1.7021	14.1612	10	-0.8498	7.3930

.....contd/....

Capillary.	Stainless Steel			Glass		
	τ_w dynes/cm^2	U_w cm/sec.	$\delta \times 10^4$ cm.	τ_w dynes/cm^2	U_w cm/sec	$\delta \times 10^4$ cm.
3	310	58.8709	38.6453	310	75.3146	47.3488
	250	43.1861	38.8145	250	55.4679	47.3348
	190	28.0591	38.3773	190	36.5147	46.7407
	130	14.1669	36.1700	130	19.2468	44.6489
	100	8.0928	33.0516	100	11.7006	42.0904
	70	3.0224	25.1086	70	5.3296	36.4329
	30	-1.0147	3.1013	30	-0.1442	00.4600
	10	-0.9392	7.8137	10	-0.6631	5.7715
4	310	52.2992	34.3313	310	54.8437	34.4479
	250	37.3795	33.5957	250	38.9503	33.2391
	190	23.4961	32.1363	190	24.4813	31.3374
	130	11.2861	28.8149	130	11.9755	27.7809
	100	6.1635	25.1724	100	6.7856	24.4100
	70	2.0344	16.9009	70	2.6079	17.8273
	30	-1.0242	3.1302	30	-0.6206	1.9793
	10	-0.8156	6.7854	10	-0.6578	5.7261

.....contd.....

Capillary	Stainless Steel			Glass		
	τ_w dynes/cm^2	U_w cm/sec	$\delta \times 10^4$ cm.	τ_w dynes/cm^2	U_w cm/sec.	$\delta \times 10^4$ cm.
	310	39.1675	25.7112	310	33.3765	20.9831
	250	27.7819	24.9697	250	23.9835	20.4669
	190	17.2894	23.6473	190	15.2668	19.5423
	130	8.1650	20.8464	130	7.6034	17.6383
5	100	4.3763	17.8732	100	4.3708	15.7231
	70	1.3565	11.2691	70	1.7355	11.8638
	30	-0.8267	2.5267	30	-0.3444	10.9852
	10	-0.6252	5.2016	10	-0.3830	3.3339

Values of η_w at a given shear stress for 30 ppm. polyox solution

τ_w	Stainless Steel	Glass
Dynes/cm^2	$\eta_w \times 10^3$ ($\frac{gm.}{cm.sec}$)	$\eta_w \times 10^3$ ($\frac{gm.}{cm.sec}$)
310	15.9354	16.5061
250	14.8392	15.3795
190	13.6215	14.1287
130	12.2301	12.7008
100	11.4405	11.8912
70	10.5599	10.9894
30	9.1689	9.5684
10	8.3199	8.7044

TABLE 3c

Values of U_w and δ for different tubes at a given shear stress for 20 ppm. polyox solution

Capillary	Stainless steel			Glass		
	τ_w dynes/cm^2	U_w cm/sec.	$\delta \times 10^4$ cm.	τ_w dynes/cm^2	U_w cm/sec.	$\delta \times 10^4$ cm.
1	310	40.7529	30.3387	310	46.6591	33.6146
	250	29.8416	30.7486	250	34.9951	34.9169
	190	19.1289	30.4133	190	23.3183	36.0170
	130	9.1229	27.5540	130	12.0741	35.8732
	100	4.7240	23.0302	100	6.9380	33.8932
	70	1.0985	10.9216	70	2.5036	26.2683
	30	-1.4837	4.5488	30	-1.1408	3.4179
	10	-0.9961	8.5478	10	-0.9877	8.1801
2	310	76.9814	57.3091	310	63.1375	45.4768
	250	55.3283	57.0101	250	47.3016	47.1831
	190	35.0021	55.6503	190	31.6830	48.9180
	130	17.0171	51.3971	130	16.9091	50.2058
	100	9.4662	46.1491	100	10.2484	50.0165
	70	3.3990	33.7941	70	4.5183	47.3248
	30	-1.1147	3.4173	30	-0.4272	1.2804
	10	-0.9709	8.3316	10	-0.7561	6.2637

.....contd/...

Capillary	Stainless steel			Glass		
	τ_w dynes/cm^2	U_w cm/sec.	δ x 10^4 cm.	τ_w dynes/cm^2	U_w cm./sec.	δ x 10^4 cm.
3	310	54.7083	40.7245	310	61.9947	44.6537
	250	40.1546	41.3752	250	44.9388	44.8263
	190	26.2806	41.7839	190	28.7603	44.4055
	130	13.7149	41.4234	130	14.2379	42.2745
	100	8.2782	40.3576	100	8.0371	39.2245
	70	3.7479	37.2628	70	2.9705	31.1128
	30	-0.0502	0.1538	30	-0.9252	2.7729
	10	-0.4071	3.4932	10	-0.8452	7.0021
4	310	45.9986	34.2439	310	45.9165	33.0729
	250	32.8108	33.8081	250	32.3569	32.2759
	190	20.6422	32.8194	190	19.9484	30.8000
	130	10.0755	30.4315	130	9.2815	27.5583
	100	5.6976	27.7766	100	4.9159	23.9915
	70	2.2007	21.8797	70	1.4800	15.5020
	30	-0.4453	1.3651	30	-0.9183	2.7521
	10	-0.4654	3.9942	10	-0.6749	5.5914

.....contd/....

Capillary	Stainless Steel			Glass		
	τ_w dynes/cm^2	U_w cm/sec	$\delta \times 10^4$ cm.	τ_w dynes/cm^2	U_w cm/sec.	$\delta \times 10^4$ cm.
	310	36.1096	26.8819	310	29.3953	21.1729
	250	25.8716	26.6580	250	20.9025	20.8502
	190	16.4329	26.1267	190	13.0482	20.1462
5	130	8.2213	24.8310	130	6.2079	18.4323
	100	4.7994	23.3978	100	3.3714	16.4536
	70	2.0367	20.2491	70	1.1146	11.6744
	30	-0.1501	0.0460	30	-0.5217	1.5635
	10	-0.2826	2.4251	10	-0.4116	3.4101

Values of η_w at a given shear stress for 20 ppm. solution

τ_w	Stainless Steel	Glass
dynes/cm^2	$\eta_w \times 10^3$ ($\frac{gm.}{cm.sec.}$)	$\eta_w \times 10^3$ ($\frac{gm.}{cm.sec.}$)
310	14.5851	14.9011
250	13.6847	13.9287
190	12.6918	12.8524
130	11.5706	11.6297
100	10.943	10.9404
70	10.2537	10.1776
30	9.1973	8.9912
10	8.5816	8.2846

The curves of η_w vs. τ_w for 40 ppm polyox solution obtained with stainless steel and glass tubes match very closely as shown in fig. 24. Non-Newtonian viscosity is found to increase with shear stress.

Depending on whether separation phenomenon or the polymer adsorption takes place, the values of δ were calculated with equation 3.E.1 or 3.E.2.

Figs. 25 and 26 show the variation of δ with the shear stress for stainless steel and glass tubes respectively for 40 ppm polyox solution. Table 3 gives the results for all the tubes at all the three concentrations.

A comparison of δ with shear stress for glass and stainless steel tubes of approximately the same diameter is made as shown in fig. 27. Tubes 1 & 5 were compared. Anomalous layer thickness for steel tubes is found to be more than that for glass tubes both in separation and adsorption region however the difference is not of a very high order.

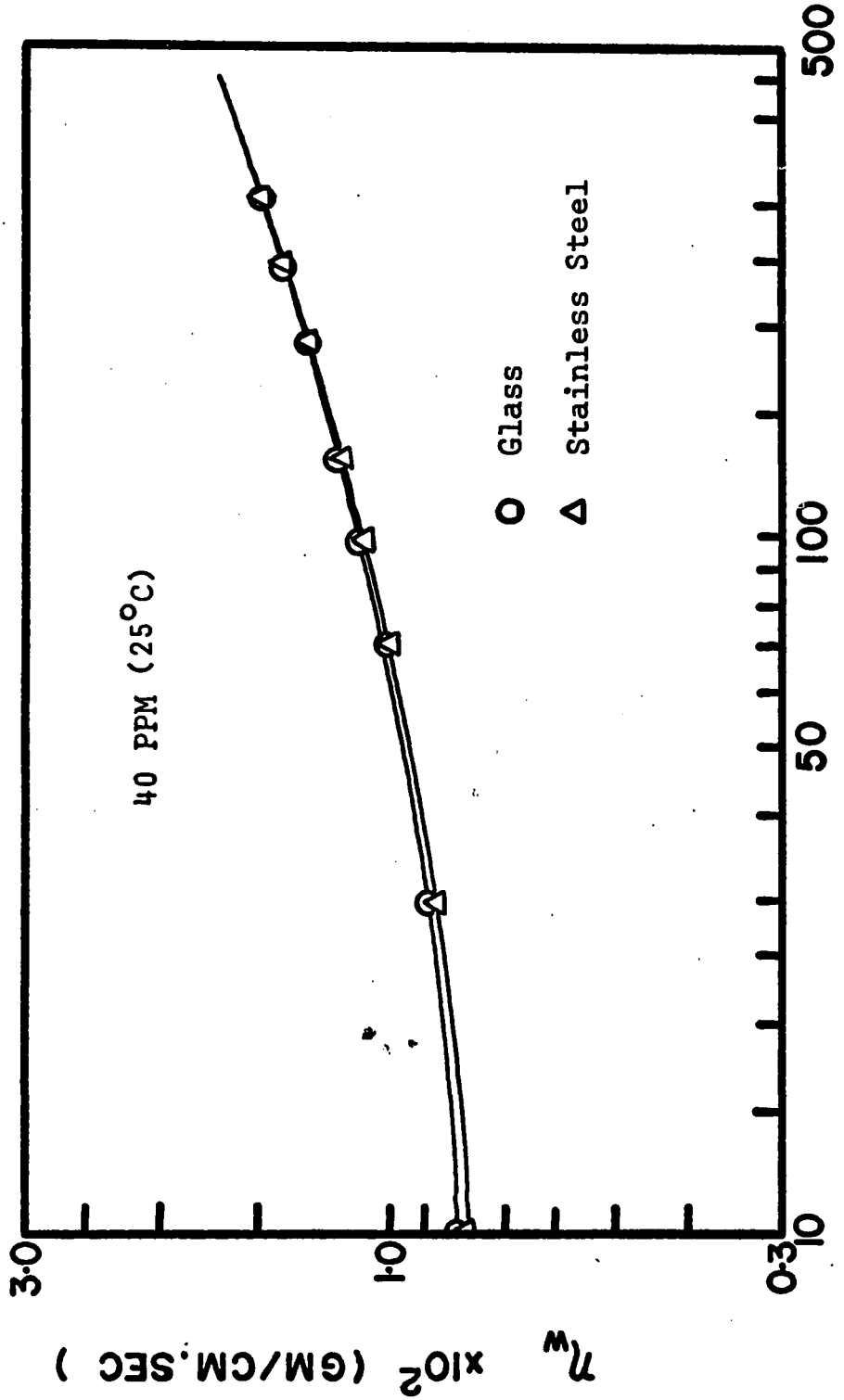

Fig. 24. Non-Newtonian viscosity vs shear stress in case of 40 ppm polyox solution at 25°C.

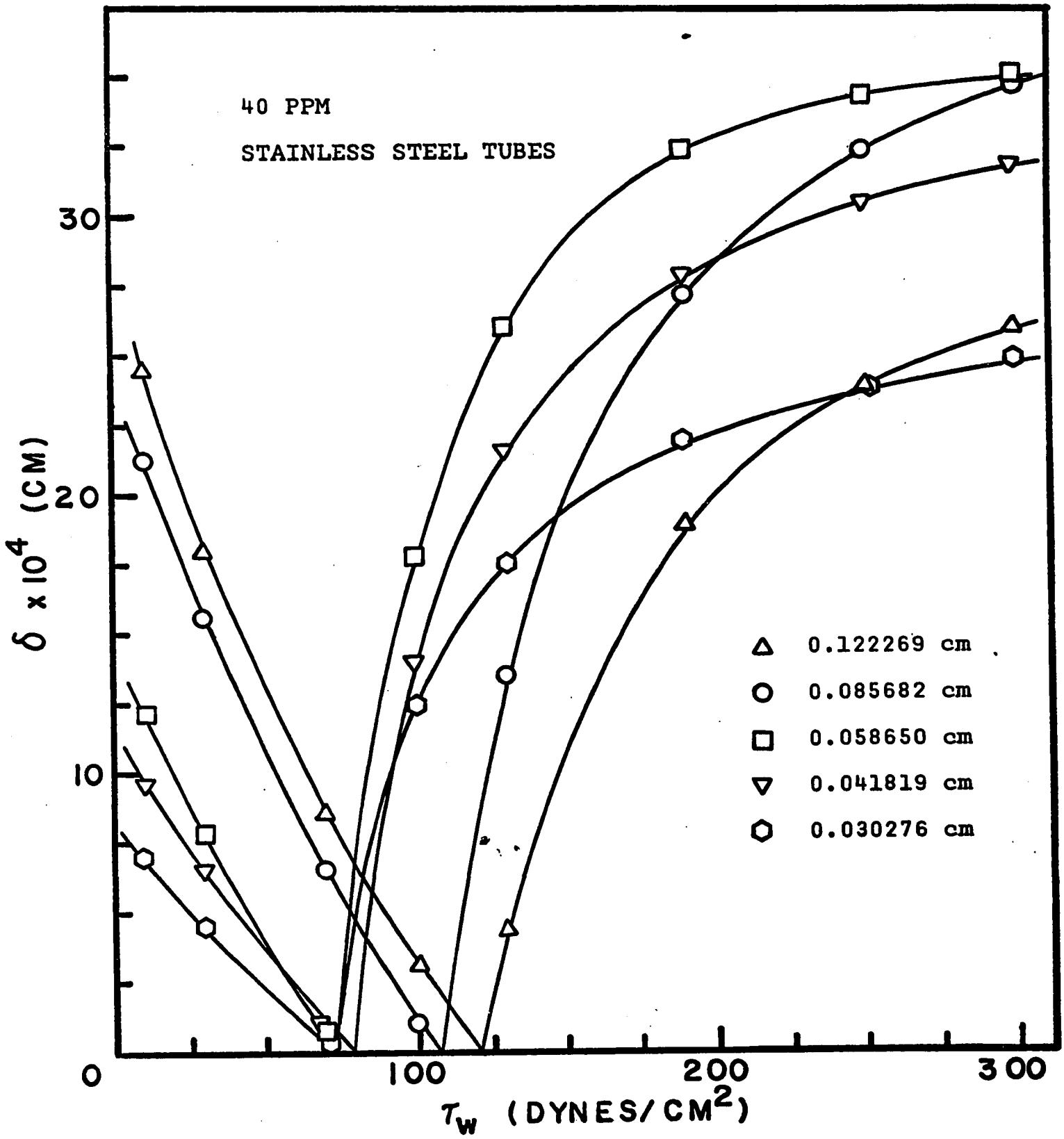

Fig. 25. Anomalous layer thickness vs shear stress for stainless steel tubes in case of 40 ppm polyox solution.

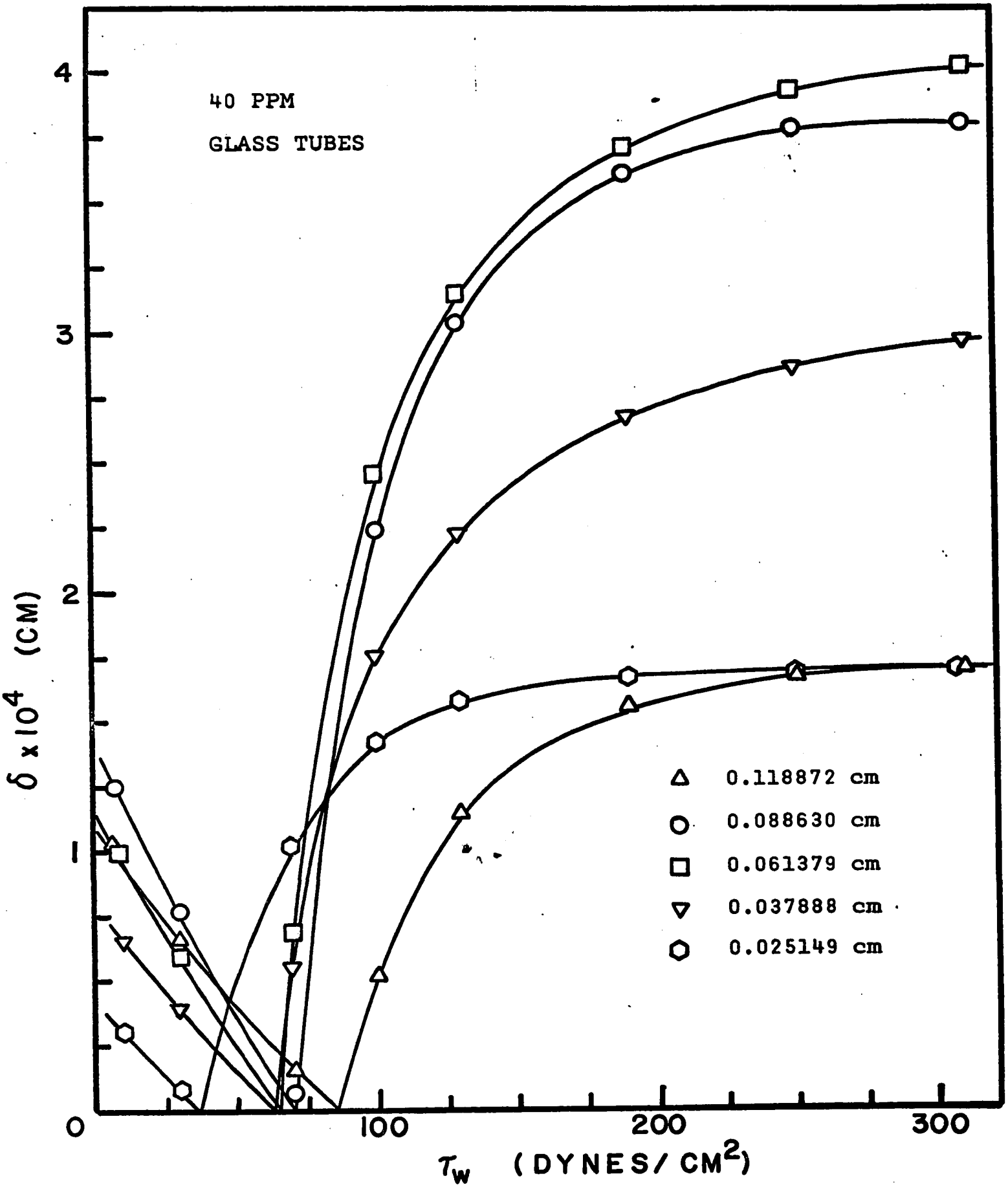

Fig. 26. Anomalous layer thickness vs shear stress for Glass tubes in case of 40 ppm polyox solution

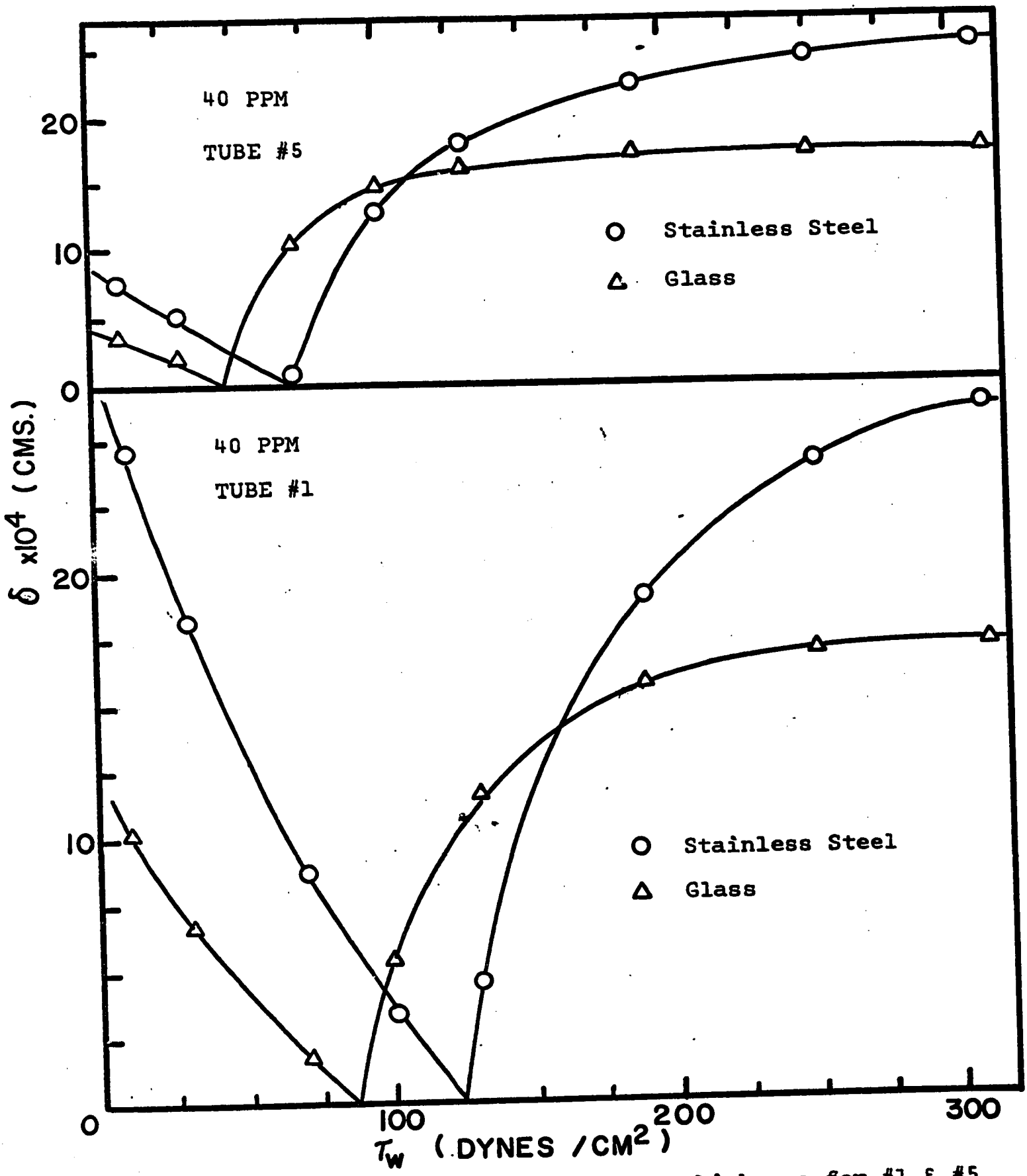

Fig. 27. Comparison of Anomalous layer thickness for #1 & #5 glass and stainless steel tubes for 40 ppm polyox solution.

CHAPTER VI

DISCUSSION

The data obtained in the present work was treated in an entirely new fashion, with the help of mathematical equations, which represented the data with a very good accuracy.

In the above process of calculation of $\frac{8\langle u\rangle}{D}$ for a given τ_w for a particular tube using equation 3.B.19, the entrance losses, which are accounted by an extra length of capillary tube or by an additional pressure drop to overcome the abrupt changes in the velocity profile, when the polymer solution enters the tube from the reservoir, are taken care of. The variable n is always supposed to be positive (11, 43, 53) because τ_w' in the equation 3.A.4 is positive. For stainless steel tubes the values of n were found to be positive but surprisingly for glass tubes, in some cases, n was even found to be negative. An unknown phenomenon appears to be taking place in the case of the glass tubes.

Separation in the τ_w vs. $\frac{8\langle u\rangle}{D}$ curve for different tubes in the figs. 6 to 12 was attributed to the anomalous surface effects at the tube wall. The possibility that the separation is due to time dependency of fluids was rejected because a plot of ΔP vs. L was found to be linear with points falling on the line as shown in fig. 13(a) & 13(b). The curves also had a tendency to intersect each other

suggesting presence of critical shear stress which marks the transition from a positive slip velocity to a negative effective velocity at the wall. To find the final curve, evaluation of the velocity at the wall was necessary for all the tubes.

In the present work data was taken for $1/D \gtrsim 8$ and hence the nature of $\frac{8\langle u\rangle}{D}$ vs. $1/D$ and $\frac{\partial \frac{8\langle u\rangle}{D}}{\partial\, 1/D}$ vs. $1/D$ curves was not known for $1/D \lesssim 8$. To evaluate the surface effects it was necessary to extrapolate $\frac{\partial \frac{8\langle u\rangle}{D}}{\partial\, 1/D}$ vs. $1/D$ curve to $1/D = o$, for all the shear stresses and hence the values of area under the curve i.e. $\frac{8\ U_w}{D}$ at a given shear stress for all the tubes had some uncertainty. This uncertainty was maximum for the largest diameter tube and least for the smallest dia tube because the extrapolated area is largest percentage of the total area to be considered for the largest diameter tube and least percentage of the total area to be considered for the smallest diameter tube as can be seen from the fig. 16(a) and 16(b). Due to this uncertainty in the value of $\frac{8\ U_w}{D}$ slight deviation was found in the calculated values of $\frac{8(\langle u\rangle - U_w)}{D}$ at a given shear stress for different tubes. The final curve [τ_w vs. $\frac{8(\langle u\rangle - U_w)}{D}$] was decided on the basis of the values of $\frac{8(\langle u\rangle - U_w)}{D}$ obtained for the smallest diameter tube because the uncertainty was minimum for the smallest tube. Dotted line on the figs. 6 to 12 indicates the final curve for each set. It was noted

that at low shear stresses the flow curve of solutions was very close to the flow curve for water but as the shear stress increases the flow curve for solutions moves upward consequently for a given shear stress the flow is comparitively slower for solutions than that for water. This behaviour of dilute polymer solutions could possibly be due to dilatency. Forame, Hansen & Little (54) have tried to explain this behaviour of drag reducing polymer solutions on the basis of early turbulence. In such a case, the analysis which is valid for laminar flow would not be applicable over the entire range over which experimental data was collected. This could offer an explanation for the shift of the final curves to the left in the figures 6 to 12. However, it should be noted that no direct experimental evidence of early turbulence has yet been reported.

Figs. 17, 18 and 19 show that for a given concentration the final curve obtained with stainless steel and glass tubes match fairly well. This is because the final curve is a function of the property of the main stream fluid and is independent of the tube material. The independence of the non-Newtonian viscosity for a given solution of tube material is indicated by fig. 24 for 40 ppm polyox solution.

Increase in viscosity with shear stress could be because of dilatent behaviour of the fluid. However, increasing viscosity at high shear stress could also be

expected if the data falls in turbulent region due to early turbulence. The calculated values of non-Newtonian viscosity at high shear stress in that case will not be correct, because the analysis is valid only for laminar flow.

Since the final curves obtained with glass and stainless steel have no relation with the polymer concentration as shown by figs. 20 and 21, it shows that the flow behaviour of dilute polyox solution is quite complicated. Normally one would expect the flow curve of the most dilute solution to be closest to the flow curve of water and as the concentration increases the separation from water line would increase. However this is not found to be true for drag reducing polymers.

The variation of U_w with shear stress is independent of tube diameter for a given concentration of polyox solution for both glass and stainless steel tubes as shown in fig. 22 & 23. However the most important thing to note is that even with polyox which is a very effective drag reducing agent, both negative and positive effective velocities are obtained at the tube wall within the anomalous sublayer.

Drag reduction in turbulent flow of viscoelastic polymer solutions is a purely viscous flow property that is attributed to anomalous behaviour observed in the vicinity of the tube wall (26). Combined effects of the anomalous behaviour observed under laminar flow conditions in the

anomalous layer (i.e. polymer adsorption on the tube wall or "separation phenomenon"), and in the laminar sublayer of increased thickness (thickness greater than that applicable to the purely viscous fluids) cause drag reduction.

Adsorption of the polymer molecules on the surface causes a negative effective velocity at the wall however this also increases the thickness of the laminar sublayer near the wall. It is postulated that inspite of the negative effective velocity at the wall drag reduction in turbulent flow of polyox solution is obtained mainly due to increased laminar sublayer thickness. Results indicating increased laminar and transition region have been reported (55).

The variation of anomalous layer thickness δ, with shear stress for a given concentration is indicated by figs. 25 & 26 for stainless steel and glass tubes respectively. At low shear stress in adsorption region δ increases with the tube diameter however for a given tube the anomalous layer thickness reduces with increasing shear stress. At the critical shear stress δ is zero. At shear stress larger than critical shear stress (i.e. in separation region) increases with shear stress however no definite trend is found for the variation of δ with tube diameter in this region. This could be because the data in the high shear stress region shows the presence of 'early turbulence' where the results are doubtful as the analysis is restricted to laminar flow only.

Variation of δ with shear stress for glass and stainless steel tubes of approximately the same diameter is shown in fig. 27. Anomalous layer thickness for stainless steel tubes is found to be more than that for glass tubes both in 'adsorption' and 'separation' region. The exact reason for this behaviour could not be determined. Probably metallic nature of steel is the answer. Surface roughness could also be an important factor. Further investigations are needed to understand the phenomenon.

CHAPTER VII

CONCLUSION AND RECOMMENDATIONS

This work was conducted to determine the anomalous behaviour of drag reducing polyox solutions in laminar flow region. An attempt was made to use some aspects of this study to explain the phenomenon of turbulent drag reduction. Though nothing conclusive could be obtained, an attempt was also made to compare the effect of stainless steel and glass as tube wall material on the anomalous behaviour. The conclusions of this study can be summarized as follows:

1. No conclusion could be drawn about the mechanism underlying the phenomenon of turbulent drag reduction, however it was found that in the laminar flow regime, both positive and negative wall effects were observed with the drag reducing polyox solutions.

2. Greater wall effects are observed with tubes of small diameter as compared to tubes of larger because comparitively greater amount of fluid is under the influence of wall in small diameter tubes. Similar results have been reported by many other workers (25, 55, 9). For this reason the true rheological curve is closest to the curve for the largest diameter tube.

3. The wall effects are comparitively large at high shear stress with very dilute polyox solution than at low shear stress. Jastrzebski (11) reported greater discrepancies in the region of low shear stress than at high shear stress

for concentrated suspensions. Pasari (25) reported comparable discrepancies in the two regions with aqueous solutions of high molecular weight polymers.

4. Final curves obtained with glass and stainless steel tubes for a given concentration matched very closely. This is reflected in the non-Newtonian viscosity based on the data taken with stainless steel and glass tubes for a given concentration which was found to be very close for both case.

5. The anomalous layer thickness was found to be slightly greater for stainless steel tube than for glass tube, for a given tube diameter.

6. Some results were consistent with the possibility of early turbulence at the higher shear stresses.

The accuracy of this method of calculation can be improved by taking data with larger tubes. If nature of $\frac{8\langle u\rangle}{D}$ vs. 1/D curve is known for $1/D < 11$ final curves can be obtained with better accuracy.

In order to establish the influence of wall material on surface effect it is recommended that data be taken with tubes of several other wall materials.

CHAPTER VIII

REFERENCES

1. Toms, B.A., Proc. 1st. Int. Cong. Rheology, Holland (1948)
2. Toms, B.A., J. Colloid. Sci., 4, 511 (1949).
3. Buckingham, E., Proc. Am. Soc. Testing Materials 21, 1154 (1921).
4. Daly, J.W., Bugliarello, G., Ind. Eng. Chem., 51, 887 (1959).
5. Green, H., Proc. Am. Soc. Testing Materials 20-II, 477 (1920).
6. Mooney, M., J. Rheol. 2, 337 (1931).
7. Schofield, R.K., and Blair, G.W.S., J. Phy. Chem., 34, 248 (1930).
8. Schofield, R.K., and Blair, G.W.S., J. Phy. Chem., 35, 1212 (1931).
9. Oldroyd, J.W., J. Colloid Sci., 4, 333 (1949).
10. Maude, A.D., Whitemore, R.L., British J. of App. Phy. Vol.7, 98 (1956).
11. Jastrzebski, Z.D., I & E C Fundls, Vol. 6, No.3, 445 (1967).
12. Astarita, G., Marrucci, G., and Palumbo, G., I & E C Fundles, 3, 333 (1964).
13. Morrison, S.R., and Harper, J.C., I & E C fundamentals 4, 176 (1965).
14. Luce, J.E., and Robertson, A.A., J. Polymer Sci., 51, 317 (1961).
15. Koral, J., Ullman, R., and Eirich, F.R., J. Phys. chem., 62, 541 (1958).
16. Hobden, J.F., and Jellinek., H.H.G., J. Polymer Sci., 11, 365 (1953).
17. Frish, H.L., Hellman, M.Y., and Lundberg, J.L, J. Poly. Sci., 38, 441 (1959).
18. Yurzhenko, A.L., and Maleyev, L.L., J. Polymer Sci., 31, 301 (1958).

19. Sadowski, T.J., Ph. D. Thesis, Univ. of Wisconsin (1963).

20. Sadowski, T.J., and Bird, R.B., Trans. Soc. Rheol., 9, 243 (1965).

21. Kozicki, W., Hsu, C.J., and Tiu, C., Chem. Engg. Sci., 22, 487 (1967).

22. Ohrn, O.E., J. Polymer, Sci., 17, 137 (1955).

23. Kozicki, W., Pasari, S.N., Rao, A.R.K., Tiu, C., Chem. Eng. Sci., 25, 41 (1970).

24. Arunachalam., V.R., Fulford, G.D., Chem. Eng. Sci., Vol. 26, 1065 (1971).

25. Pasari, S.N., M.A.Sc. Thesis, Univ. of Ottawa, 1969.

26. Kozicki, W., Tiu, C., Chem. Eng. Sci., Vol. 23, 231 (1968).

27. Savins, J.G., Reprint of paper at Symp. on Non-Newtonian fluid Mechanics, 56th Annual A.I.Ch.E. Meeting, Houston, Texas (1963).

28. Lumley, J.G., in annual review of fluid mechanics, Vol. 1, (1969), Annual Rev. Inc., Palo Alto, California (1969).

29. Shin, H., Sc. D. Thesis, M.I.T., Cambridge, Mass. (1965).

30. Metzner, A.B., Park, M.G., J. Fluid Mech., 20, 291 (1964).

31. Hoyt, J.W., and Fabula, A.G., in fifth symposium on naval hydrodynamics, Bergen, Norway, P.947, U.S. Govt. Printing Office, Washington 1964.

32. Merrill, E.W., Smith, K.A., Shin, H., and Mickley, Trans. Soc. Rheol, 10, Pt. 1, 335 (1966).

33. Shin, H., Sc. D. Thesis, M.I.T. Cambridge, Mass. (1966).

34. Hershey, H.C., and Zakin, J.L., Ind. Eng. Chem. Fundls., 6, 381 (1967).

35. Flory, P.J., "Principles of polymer chemistry", Cornell Univ. Press, New York, 1953

36. Sylvester, N.D., Tyler, J.S., Ind. Eng. Chem. Prod. Res. Develop, Vol. 9, No.4 (1970).

37. Bailey, F.E., Jr., Powell, G.M., and Smith, K.L., I & E C Vol. 50, No.1, 1958.

38. Skelland, A.H.P., "Non-Newtonian Flow and Heat Transfer", John Wiley & Sons, N.Y., (1967).

39. Foust, A.S., et al., Principles of Unit operations, P 542, John Wiley & Sons, N.Y. (1960).

40. Bogue, D.C., Ind. Eng. Chem., 51, 874 (1959).

41. Weltmann, R.N., and Keller, T.A., N.A.C.A., Tech. Mem., 3889 (1957).

42. Metzner, A.B., Handbook of fluid dynamics edited by Streeter, V.L., Section 7, McGraw Hill Book Co., N.Y., (1961).

43. Bagley, E.B., J. Appl. Phys., 28, 624, (1957).

44. Eirich, F.R., "Rheology", Vol. 1, chapter by Oldroyd,J.G., "Non-Newtonian flow of liquids and solids", Academic, N.Y., 1956.

45. Mooney, M., J. of Rheol., Vol. 2, No.2, 210 (1931).

46. Kozicki, W., Chou, C.H., and Tiu, C., Chem. Eng. Sci, 21, 667, 1966.

47. Rabinowitsch, B., Z Phys. Chem., 1, A 145, (1929).

48. Metzner, A.B., and Reed, J.C., A.I. Ch. E. Journal, 1, 434 (1955).

49. Bowen, R.L., Chem. Engg., Aug. 21, 1961.

50. Severs, E.T., and Austin, J.M., I & E C, 46, 2369 (1954).

51. Toors, H.L., Trans. Soc. Rheol., 1, 177 (1957).

52. Arunachalam,V.R., Ph. D. Thesis, University of Waterloo, (1969).

53. Oliver, D.R., & MacSporan, W.C., Canadian Journal of Ch. Engrs., Vol. 48, June 1970.

54. Forame, P.C., Hansen, R.J., and Little, R.C., A.I.Ch.E. Journal, Vol. 18, No.1, pp. 213.

55. Arunachalam,V.R., Hummel, R.L., and Smith, J.W., University of Toronto.

56. Winding, C.C., Baumann, G.P., and Kranich, W.L., Chem. Eng. Prog., 43, 527 (1947).

CHAPTER IX

APPENDIX (a)

SUMMARY OF VISCOMETRIC RESULTS*

FOR POLYOX SOLUTIONS

* All the measurements were taken at 25°C.

TABLE I

Capillary tube specifications

Stainless Steel tubes

Capillary	Calibrated diameter D (in cms.)	$1/D_{-1}$ cms	Length, L (in cms)	L/D
1S1			84.364	689.987
IS2	0.122269	8.1787	61.513	503.096
1S3			35.943	293.967
2S1			79.479	927.605
2S2	0.085682	11.6711	45.291	528.594
2S3			25.337	295.710
3S	0.05865	17.0504	41.415	706.141
4S	0.041819	23.9126	41.432	990.756
5S	0.030276	33.0294	31.735	1048.189

Glass tubes

Capillary	Calibrated diameter D (in cms.)	$1/D_{-1}$ cms	Length, L (in cms)	L/D
1G1			84.389	709.912
1G2	0.118872	8.4124	54.304	456.826
1G3			30.008	252.439
2G1			84.059	948.426
2G2	0.088630	11.2829	55.914	630.870
2G3			28.894	326.007
3G	0.061379	16.2922	67.938	1106.859
4G	0.037888	26.3933	83.957	2215.899
5G	0.025149	39.7626	50.859	2022.289

TABLE II
IIa

Solution: 40 ppm (by wt.) polyox

Density: 0.997 g/cm^2 at 25^{o}C

Data for stainless steel tubes

Capillary	Head above tube inlet cms.of soln.	Pg cms.of Hg.	G gms/sec	ΔP exp. Dynes/cm^2	ΔP cal. dynes/cm^2
		0.00	0.547570	84886.5	84824.2
		3.90	0.837706	133622.0	133554.0
1S1	4.958	7.10	1.060890	172845.0	172822.0
		10.30	1.273720	211470.0	211714.0
		14.75	1.550120	264454.0	264328.0
		0.0	0.564579	64489.4	63603.0
		3.9	0.965002	111508.0	112081.0
1S2	7.105	7.6	1.302291	154617.0	155083.0
		10.9	1.578164	192148.0	191730.0
		0.0	0.566005	39835.7	40068.9
1S3	7.473	3.7	1.087320	82152.4	81906.4
		7.9	1.594582	127071.0	127156.0

.....contd...

Capillary	Head above tube inlet cms.of sol^n	Pg cms.of Hg	G gms/sec	ΔP exp. dynes/cm^2	ΔP cal dynes/cm^2
2S1	6.397	0.0	0.141363	83287	82716
		8.0	0.308897	187432	186398
		15.8	0.464539	287389	288213
		23.8	0.610696	388770	388641
		31.6	0.748328	486472	487476
		40.0	0.885605	590916	590177
2S2	7.363	0.0	0.148282	50737	49614
		8.5	0.452170	157930	159010
		16.0	0.682269	249129	248746
		24.4	0.920612	348238	347969
		32.2	1.125284	438103	438269
2S3	7.345	0	0.158029	31109	29355
		7.9	0.591210	125494	126768
		15.6	0.901733	212508	211879
		24.2	1.201045	305918	305996

.....contd/...

Data for capillary tube 3S

Head above the tube inlet = 7.098cms of sol^{n}.

Pg cms.of Hg	G gms/sec	ΔP dynes/cm^2	$\frac{8\langle u\rangle}{D}$ -1 sec.	τ_w exp. dynes/cm^2	τ_w cal. dynes/cm^2
0.15	0.034625	49248	1754.35	17.436	16.363
15.10	0.175683	244066	8901.37	86.408	86.044
30.00	0.303939	433310	15399.70	153.408	153.608
43.20	0.408939	597827	20719.80	211.653	211.905
60.40	0.536677	808613	27191.90	286.279	286.446
74.1	0.631987	974170	32021.00	344.892	344.655

Data for capillary tube 4S

Head above the tube inlet = 7.313 cms. of solution

Pg cms.of Hg	G gms/sec	ΔP dynes/cm^2	$\frac{8\langle u\rangle}{D}$ -1 sec.	τ_w exp. dynes/cm^2	τ_w cal. dynes/cm^2
15.4	0.047755	251690	6674.58	63.510	64.293
27.8	0.077337	414864	10809.20	104.685	104.795
42.3	0.111111	604457	15529.70	152.526	151.666
56.4	0.144548	784140	20203.00	198.692	198.732
71.3	0.178713	979552	24978.20	247.175	247.505
85.7	0.210634	1164200	29439.70	293.768	293.696

Data for capillary tube 5S

Head above the tube inlet = 7.022 cms. of solution

Pg cms.of Hg	G gms/sec	ΔP dynes/cm^2	$\frac{8\langle u\rangle}{D}$ $^{-1}$ sec.	τ_w exp, dynes/cm^2	τ_w cal, dynes/cm^2
13.9	0.015446	222761	5689.25	53.130	54.259
29.0	0.028826	422865	10617.30	100.856	101.761
42.7	0.040509	603824	14920.60	144.016	143.623
57.2	0.052886	794704	19479.30	189.542	188.358
70.7	0.064709	971737	23834.10	231.765	231.465
84.8	0.076937	1156030	28337.80	275.721	276.429

TABLE IIb

Data for Glass tubes (40 ppm)

Capillary	Head above tube inlet cms.of soln.	Pg cms.of Hg	G gms/sec	ΔP exp, dynes/cm^2	ΔP cal. dynes/cm^2
1G1	4.186	0.175	0.534018	86332	85373
		3.450	0.773428	127153	126918
		7.100	1.023360	171733	172450
		9.900	1.201559	205457	206261
		14.800	1.488599	263759	263084
1G2	8.141	0.0	0.546130	58333	57048
		3.7	0.950122	102161	102873
		6.3	1.200890	131913	132869
		9.3	1.458360	165673	164902
1G3	7.642	0.00	0.57317	33812	33545
		3.85	1.20596	74881	75181
		7.30	1.668115	108767	108642

.....contd/...

Capillary	Head above tube inlet cms.of sol^{n}.	Pg cms.of Hg	G gms/sec	ΔP_{exp} dynes/cm^2	$\Delta P_{cal.}$ dynes/cm^2
2G1	4.520	0.0	0.166884	85783	85711
		8.5	0.368388	195961	194098
		16.8	0.560988	301370	302704
		24.4	0.722200	396620	397372
		32.2	0.879122	493225	492815
		39.8	1.027438	586233	586009
2G2	5.858	0.125	0.173146	61177	58904
		7.900	0.452552	159708	159560
		16.100	0.716227	259967	260895
		24.000	0.947134	353982	354698
		31.700	1.15464	443793	443026
2G3	7.208	0.00	0.190418	34226	33152
		0.50	0.719718	133359	134038
		16.15	1.100830	214890	214632

.....contd/....

Data for capillary tube 3G

Head above the tube inlet = 6.116 cms. of sol^{n}.

Pg cms.of Hg	G gms/sec	ΔP dynes/cm^2	$\frac{8\langle u\rangle}{D}$ $sec.^{-1}$	τ_w exp. dynes/cm^2	τ_w cal. dynes/cm^2
0.0	0.039166	72207	1731.30	16.309	16.261
8.8	0.159832	301187	7065.25	68.028	67.671
16.1	0.257092	490700	11364.50	110.832	110.550
23.9	0.357235	689522	15791.30	155.739	156.046
32.8	0.465979	914090	20598.20	206.460	206.994
41.1	0.560614	1120340	24781.50	253.045	252.641

Data for capillary tube 4G

Head above the tube inlet = 6.766 cms. of sol^{n}.

Pg cms.of Hg	G gms/sec	ΔP dynes/cm^2	$\frac{8\langle u\rangle}{D}$ $sec.^{-1}$	τ_w exp. dynes/cm^2	τ_w cal. dynes/cm^2
14.6	0.018042	283135	3390.69	31.9435	32.196
28.6	0.029758	469358	5592.51	52.9534	53.288
42.2	0.040800	650052	7667.76	73.3396	73.300
56.2	0.052154	835837	9801.49	94.3000	94.011
70.4	0.063672	1024040	11966.10	115.5340	115.161
85.9	0.076571	1229170	14390.10	138.6760	139.013

Data for capillary tube 5G

Head above the tube inlet = 7.627 cms. of sol^{n}.

Pg cms.of Hg	G gms/sec	ΔP dynes/cm^2	$\frac{8\langle u\rangle}{D}$ $^{-1}$ sec.	τ_w exp. dynes/cm^2	τ_w cal. dynes/cm^2
21.0	0.007053	337034	4532.19	41:6649	41.4375
36.8	0.011351	547399	7294.51	67.6707	67.9110
50.9	0.015013	735011	9647.73	90.8638	90.8284
65.5	0.018730	929160	12036.10	114.8650	114.5920
85.3	0.023754	1192260	15264.60	147.3900	147.5210

TABLE IIc

Solution: 30 ppm (by wt.) polyox

Density: 0.997 gm/cm^3

Data for Stainless Steel tubes

Capillary.	Head above tube inlet (cms.of sol^n)	P_g cms. of Hg	G gms./sec	ΔP exp. $dynes/cm^2$	ΔP cal. $dynes/cm^2$
1S1	5.900	0.00	.553513	85754.1	83676.3
		3.05	.799357	123719.0	124138.0
		6.10	1.014761	161210.0	161256.0
		9.10	1.221590	197448.0	198362.0
		12.20	1.426460	234368.0	236531.0
		15.10	1.584762	269157.0	266989.0
1S2	7.603	0.00	.565713	64965.8	63156.5
		2.05	.786106	89876.6	90011.5
		4.05	.987217	113642.0	115618.0
		6.05	1.149536	137487.0	137052.0
		7.90	1.311994	158898.0	159189.0
		10.05	1.481967	183699.0	183084.0
1S3	9.266	0.00	.587954	41382.1	40143.3
		1.95	.901737	63576.5	64285.8
		4.10	1.192000	87294.1	88303.2
		6.10	1.420200	109106.0	108322.0

Capillary.	Head above tube inlet (cms.of sol^n)	Pg cms.of Hg.	G gms./sec	ΔP exp. dynes/cm^2	ΔP cal, dynes/cm^2
2S1	7.779	0.00	.140669	84644.8	82231.5
		8.30	.319778	192553.0	192322.0
		15.50	.462999	284787.0	284697.0
		23.90	.622695	390954.0	392249.0
		31.60	.759444	487256.0	488161.0
		39.80	.896452	588946.0	587782.0
2S2	8.131	0.00	.151706	51453.4	49881.0
		6.20	.379662	130046.0	129561.0
		12.15	.575416	203078.0	202516.0
		17.80	.753013	270452.0	272325.0
		23.80	.920498	340994.0	341317.0
		30.00	1.084170	412585.0	411699.0
2S3	8.683	0.00	.154738	32452.2	30319.7
		4.95	.430289	93017.9	91661.2
		10.10	.680430	152306.0	155498.0
		15.10	.865509	209196.0	208311.0
		19.80	1.038520	260855.0	260883.0

Data for capillary tube 3S

Head above the tube inlet = 7.302 cms. of sol^{n}.

Pg cms.of Hg.	G gms/sec	ΔP dynes/cm^2	$\frac{8\langle u\rangle}{D}$ sec^{-1}	τ_w exp. dynes/cm^2	τ_w cal. dynes/cm^2
0.00	0.034781	47445.3	1762.27	16.794	16.261
14.55	0.171960	237130.0	8712.73	83.953	83.494
27.75	0.285998	405132.0	14490.70	143.432	143.149
41.25	0.396409	537574.0	20084.90	203.066	204.163
56.40	0.507408	760173.0	25708.90	269.130	268.732
69.50	0.600339	919028.0	30417.50	325.370	325.280

Data for capillary tube 4S

Head above the tube inlet = 7.317 cms. of sol^{n}.

Pg cms.of Hg.	G gms/sec	ΔP dynes/cm^2	$\frac{8\langle u\rangle}{D}$ sec^{-1}	τ_w exp. dynes/cm^2	τ_w cal. dynes/cm^2
0.00	0.008961	47615.1	1252.51	12.015	11.821
13.50	0.043171	226602.0	6033.94	57.180	57.446
28.00	0.078572	417420.0	10981.70	105.330	105.493
41.30	0.110235	591239.0	15407.20	149.190	149.187
55.80	0.143970	779515.0	20122.30	196.699	196.487
70.30	0.177084	966565.0	24750.50	243.898	243.665
83.40	0.206718	1134500.0	28892.40	286.274	286.515

....contd/....

Data for capillary tube 5S

Head above the tube inlet = 8.368 cms. of sol^{n}.

Pg cms.of Hg.	G gms/sec	ΔP dynes/cm^2	$\frac{8\langle u\rangle}{D}$ sec^{-1}	τ_w exp, dynes/cm^2	τ_w cal. dynes/cm^2
14.1	0.015505	226740.0	5710.68	54.079	54.631
28.2	0.028002	413613.0	10313.70	98.650	99.181
41.7	0.039598	591962.0	14584.90	141.187	140.932
56.5	0.052326	786812.0	19272.90	187.660	187.212
71.2	0.064871	979676.0	23893.30	233.660	233.292
85.6	0.077192	1167930.0	28431.40	278.559	279.002

TABLE IId

Data for Glass tubes (30 ppm)

Capillary	Head above tube inlet (cms. of soln.)	Pg cms.of Hg.	G gms/sec.	$\Delta P_{exp.}$ dynes/cm^2	$\Delta P_{cal.}$ dynes/cm^2
		0.00	0.497516	84519.9	81819.3
		3.30	0.749540	125663.0	126805.0
		3.45	0.755913	127576.0	127974.0
1G1	4.368	7.30	1.010530	174817.0	175900.0
		9.95	1.174550	206888.0	208061.0
		12.50	1.311300	237794.0	235642.0
		14.75	1.451420	264268.0	264634.0
		0.00	0.502173	54470.1	52979.9
		2.10	0.738921	79795.3	79731.1
		4.10	0.947180	103263.0	104203.0
1G2	3.762	6.10	1.140277	126258.0	127679.0
		6.55	1.170783	131616.0	131457.0
		8.25	1.318210	150939.0	149981.0
		10.20	1.491510	172500.0	172320.0
		0.00	0.486816	29456.9	27959.6
		2.20	0.912310	53363.2	54071.3
1G3	2.333	4.10	1.219643	72721.6	73903.0
		5.95	1.466422	91343.3	90417.0

.....contd/...

Capillary	Head above tube inlet (cms.of sol^{n})	Pg cms.of Hg.	G gms/sec.	$\Delta P_{exp.}$ dynes/cm^2	$\Delta P_{cal.}$ dynes/cm^2
		0.00	0.161829	83940.1	83320.6
		8.50	0.365560	194131.0	193276.0
		16.25	0.542095	292759.0	293117.0
2G1	2.585	24.10	0.709181	391278.0	391514.0
		32.40	0.878659	494025.0	495197.0
		39.80	1.018830	584861.0	583902.0
		0.00	0.169688	56973.8	56194.0
		5.70	0.375251	129685.0	127877.0
		11.70	0.584067	203790.0	204741.0
2G2	3.228	17.90	0.776414	278748.0	279153.0
		23.80	0.951261	348512.0	349798.0
		30.60	1.134260	427929.0	426799.0
		0.00	0.169967	30575.4	29718.6
		5.15	0.504157	92605.4	92543.4
2G3	3.251	5.30	0.510386	94419.3	93769.6
		10.05	0.781600	147418.0	149124.0
		14.85	1.009350	199385.0	198569.0

.....contd/...

Data for capillary tube 3G

Head above the tube inlet = 3.416 cms. of sol^{n}.

Pg. cms.of Hg.	G gms/sec	ΔP dynes/cm^2	$\frac{8\langle u\rangle}{D}$ sec^{-1}	τ_w exp, dynes/cm^2	τ_w cal. dynes/cm^2
0.00	0.037877	69571.3	1713.86	15.714	15.973
13.60	0.133548	248857.0	5903.40	56.208	55.839
28.60	0.236261	444034.0	10443.70	100.291	100.356
41.70	0.321488	612644.0	14211.10	138.374	138.330
56.00	0.412370	794797.0	18228.40	179.516	179.861
69.60	0.494106	966665.0	21841.50	218.335	218.125

Data for capillary tube 4G

Head above the tube inlet = 2.978 cms. of sol^{n}.

Pg. cms.of Hg.	G gms/sec	ΔP dynes/cm^2	$\frac{8\langle u\rangle}{D}$ sec^{-1}	τ_w exp, dynes/cm^2	τ_w cal. dynes/cm^2
0.00	0.005262	84973.8	988.94	9.587	9.572
14.80	0.017654	282111.0	3317.81	31.828	32.160
30.20	0.030304	486964.0	5695.14	54.940	55.135
43.30	0.040962	661007.0	7698.17	74.576	74.533
61.45	0.055646	901820.0	10457.70	101.744	101.265
82.80	0.073554	1184520.0	13823.20	133.639	133.876

.....contd/....

Data for capillary tube 5G

Head above the tube inlet = 4.516 cms. of sol^{n}.

Pg. cms. of Hg.	G gms/sec.	ΔP dynes/cm^2	$\frac{8\langle u\rangle}{D}$ sec^{-1}	τ_w exp. dynes/cm^2	τ_w cal. dynes/cm^2
15.60	0.005251	262073.0	3374.64	32.398	32.551
30.30	0.009172	457870.0	5894.11	56.603	57.043
45.95	0.013194	666185.0	8478.74	82.355	82.337
61.50	0.017196	873021.0	11050.30	107.925	107.672
75.60	0.020765	1060460.0	13344.10	131.096	130.413
86.40	0.023732	1203890.0	15250.70	148.828	149.417

TABLE IIe

Solution: 20 ppm. (by wt.) polyox

Density: 0.997 gm/cm^3

Data for stainless steel tubes

Capillary	Head above tube inlet cms.of sol^n	Pg cms. of Hg.	G gms/sec.	ΔP exp. dynes/cm^2	ΔP Cal. dynes/cm^2
		0.0	0.578790	85559.7	84385.5
		4.3	0.917467	138776.0	139119.0
1S1	5.940	7.4	1.143620	176318.0	177870.0
		10.9	1.364628	218476.0	217442.0
		0.00	0.593410	63671.5	63320.4
		4.40	1.050278	116229.0	116751.0
IS2	6.547	6.70	1.260671	142938.0	142725.0
		10.35	1.582390	184158.0	184113.0
		0.0	0.599710	39229.7	38998.7
1S3	7.181	4.0	1.183633	84083.9	84385.5
		7.1	1.554455	117147.0	117007.0

.....contd/...

Capillary	Head above tube inlet cms.of sol^{n}	Pg. cms. of Hg	G gms/sec.	ΔP exp. dynes/cm^2	ΔP Cal. dynes/cm^2
		0.0	.155893	83633.6	88039.3
		7.9	.320048	186354.0	185066.0
		14.5	.456785	270785.0	269271.0
2S1	6.901				
		22.6	.620000	372871.0	373807.0
		30.5	.765145	471433.0	470452.0
		40.6	.946740	595622.0	596246.0
		0.0	.154166	50110.0	49739.9
		6.9	0.406036	137363.0	136227.0
2S2	6.783	15.2	0.680470	237975.0	237842.0
		22.4	0.899460	322299.0	324448.0
		30.6	1.117610	416779.0	415594.0
		0.0	.164358	31267.1	30294.4
2S3	7.577	6.7	.541889	111607.0	112175.0
		16.3	0.946992	219241.0	219086.0

.....contd/...

Data for capillary tube 3S.

Head above the tube inlet = 7.334 cms. of sol^{n}

Pg cms.of Hg	G gms/sec	ΔP dynes/cm^2	$\frac{8\langle u\rangle}{D}$ sec^{-1}	τ_w exp. dynes/cm^2	τ_w cal. dynes/cm^2
0.0	0.036722	47455.2	1860.60	16.8009	16.6889
14.9	0.180976	241339.0	9169.52	85.4429	85.1956
30.2	0.316587	435000.0	16040.60	154.0060	153.8860
42.6	0.419251	588739.0	21242.30	208.4360	208.6500
61.4	0.563585	817620.0	28555.30	289.4680	289.6700
80.3	0.697913	1043580.0	35361.30	369.4670	369.3010

Data for capillary tube 4S

Head above the tube inlet = 7.43 cms of solution

Pg cms.of Hg	G gms/sec	ΔP dynes/cm^2	$\frac{8\langle u\rangle}{D}$ sec^{-1}	τ_w exp. dynes/cm^2	τ_w cal. dynes/cm^2
0.00	0.009353	47721.3	1307.24	12.0418	12.0468
14.10	0.045683	234582.0	8384.98	59.1932	59.4543
29.90	0.084775	442267.0	11848.80	111.5990	111.5570
44.65	0.120341	634640.0	16819.70	160.1420	159.9410
61.80	0.160876	856576.0	22485.20	216.1440	216.2260
82.80	0.208686	1126120.0	29167.40	284.1600	284.1740

.....contd/...

Data for capillary tube 5S

Head above the tube inlet = 6.64 cms. of sol^{n}.

Pg cms.of Hg.	G gms/sec	ΔP dynes/cm^2	$\frac{8\langle u\rangle}{D}$ sec.$^{-1}$	τ_w exp. dynes/cm^2	τ_w cal. dynes/cm^2
0.00	0.002731	37503.9	1005.89	8.9449	9.1421
10.70	0.013004	179859.0	4789.62	42.8976	43.8060
27.40	0.028140	401237.0	10364.70	95.6975	95.6738
48.15	0.046712	674964.0	17205.00	160.9830	160.6050
65.20	0.061727	898828.0	22735.60	214.3760	214.1440
83.20	0.077333	1134190.0	28483.80	270.5110	270.7740

TABLE IIf.

Data for Glass tubes (20 ppm)

Data for Glass capillary tube 1G

Head above the tube inlet = 4.516 cms. of sol^{n}.

Pg. cms.of Hg.	G gms/sec	ΔP dynes/cm^2	$\frac{8\langle u\rangle}{D}$ sec^{-1}	τ_w exp. dynes/cm^2	τ_w cal. dynes/cm^2
0.0	0.552090	85539.7	3359.64	30.1233	30.1858
4.3	0.864561	13848.0	5261.13	48.8960	48.6670
8.1	1.132690	184639.0	6892.78	65.0218	65.3304
12.4	1.401880	235759.0	8530.89	83.0241	82.8075
14.8	1.552855	263695.0	9449.62	92.8620	92.9371

Data for capillary tube 2G

Head above the tube inlet = 4.096 cms. of sol^{n}.

Pg cms.of Hg	G gms/sec	ΔP dynes/cm^2	$\frac{8\langle u\rangle}{D}$ sec^{-1}	τ_w exp. dynes/cm^2	τ_w cal. dynes/cm^2
0.0	0.174800	85288.4	2566.41	22.4816	22.6202
7.4	0.357710	181105.0	5251.88	47.7383	47.4928
14.8	0.533271	275178.0	7829.46	72.5353	72.5218
22.8	0.710040	375381.0	10424.80	98.9484	98.8673
30.7	0.878576	472834.0	12899.20	124.6360	125.0550
39.4	1.048106	579216.0	15388.20	152.678	152.4510

.....contd/...

Data for capillary tube 3G

Head above the tube inlet = 4.356 cms. of sol^{n}.

Pg cms.of Hg	G gms/sec	ΔP dynes/cm^2	$\frac{8\langle u\rangle}{D}$ $^{-1}$ sec.	τ_w exp, dynes/cm^2	τ_w cal., dynes/cm^2
0.00	0.039678	70481.2	1753.92	15.9192	15.8655
15.20	0.148708	270566.0	6573.51	61.1112	60.6665
24.90	0.215546	396808.0	9528.02	89.6249	89.0035
41.05	0.325473	604563.0	14387.30	136.5490	137.0520
53.30	0.404160	760567.0	17865.60	171.7850	172.5490
71.80	0.514848	994237.0	22758.40	224.5630	224.0380

Data for capillary tube 4G

Head above the tube inlet = 8.85 cms of sol^{n}

Pg cms.of Hg	G gms/sec	ΔP dynes/cm^2	$\frac{8\langle u\rangle}{D}$ $^{-1}$ sec.	τ_w exp, dynes/cm^2	τ_w cal, dynes/cm^2
0.0	0.005805	90709.7	1090.88	10.2340	10.1301
16.7	0.020290	313104.0	3813.16	35.3247	35.5252
33.0	0.034136	529831.0	6415.28	59.7761	59.9535
49.4	0.047830	747565.0	8988.83	84.3411	84.2619
64.3	0.060175	945107.0	11308.90	106.6280	106.3020
84.6	0.077324	1213760.0	14531.70	136.9380	137.1180

.....contd/...

Data for capillary tube 5G

Head above the tube inlet = 9.082 cms. of Hg

Pg cms. of Hg	G gms/sec	P dynes/cm^2	$\frac{8\langle u\rangle}{D}$ sec^{-1}	τ_w exp. dynes/cm^2	τ_w cal. dynes/cm^2
15.30	0.005501	262524	3535.02	32.4539	32.6490
30.10	0.009795	471616	6294.08	58.3023	58.4384
46.25	0.013874	674566	8915.62	83.3915	83.1917
62.75	0.018314	893976	11768.80	110.5150	110.4090
83.00	0.023710	1163020	15236.40	143.7750	143.8730

TABLE III

Coefficients of the equations 3.B.11 & 3.B.10

Concentration ppm.	Capillary	A_1	B_1	A	B x 10^6
40	3S	468.369	121.810	0.630456	3.23613
	4S	1332.230	294.899	0.911718	1.44395
	5S	3492.590	1304.130	1.252790	1.27007
	3G	412.513	68.030	0.608155	2.26890
	4G	1774.960	529.314	0.997101	1.58221
	5G	5774.250	18359.600	1.429160	7.07138
30	3S	462.945	131.397	0.623155	3.49082
	4S	1316.040	338.532	0.900639	1.65759
	5S	3500.710	1473.070	1.255710	1.43460
	3G	409.474	64.724	0.603675	2.15865
	4G	1818.870	16.883	1.021770	0.05047
	5G	6170.870	5269.650	1.527330	2.02966
20	3S	450.317	112.956	0.606156	3.00090
	4S	1284.560	369.801	0.879095	1.81070
	5S	3341.890	2062.430	1.198730	2.00855
	1G	51.821	5.170	0.286552	4.69780
	2G	126.197	18.372	0.387922	3.84653
	3G	396.911	74.278	0.585153	2.47729
	4G	1742.900	392.994	0.979091	1.17473
	5G	5894.940	7300.330	1.459040	2.81179

TABLE IV

IVa

Solution: 40 ppm (by wt.) Polyox

Coefficients of the equation 3.B.15

Concentration ppm.	Capillary	Length cms.	A_L	B_L
40	1S1	84.364	146384	15571.10
	1S2	61.513	107735	8715.48
	1S3	35.943	65867	8701.56
	2S1	79.479	569696	109209.0
	2S2	45.291	326259	56177.3
	2S3	25.337	175299	66171.6
	1G1	84.389	150434	17666.70
	1G2	54.304	99300	9444.80
	1G3	30.008	55069	6030.65
	2G1	84.059	502585	65964.8
	2G2	55.914	332522	44316.4
	2G3	28.894	169739	22922.8

TABLE IVb

Solution : 30 ppm (by wt.) polyox

Coefficients of the equation 3.B.15

Concentration ppm.	Capillary	Length cms.	A_L	B_L
30	1S1	84.364	141888	16775.4
	1S2	61.513	104293	12988.3
	1S3	35.943	62627	9608.2
	2S1	79.479	571340	94078.2
	2S2	45.291	320515	54623.3
	2S3	25.337	186350	61987.8
	1G1	84.389	155135	18735.0
	1G2	54.304	100409	10141.0
	1G3	30.008	55334	4312.1
	2G1	84.059	503872	67957.4
	2G2	55.914	323224	46776.8
	2G3	28.894	170419	26067.2

TABLE IVc

Solution: 20 ppm. (by wt.) polyox

Coefficients of the equation 3.B.15

Concentration ppm.	Capillary	Length cms.	A_L	B_L
20	1S1	84.364	135820	17236.6
	1S2	61.513	100918	9753.1
	1S3	39.943	58596	10728.1
	2S1	79.479	551923	82246.1
	2S2	45.291	314761	51089.4
	2S3	25.337	17447	60086.9

TABLE V

Coefficients of equations 3.B.16, 3.B.17 & 3.B.10

Concentration (ppm)	Capillary	A_2	A_3	B_2	B_3	A	B x 10^6
40	1S	1662.35	5913.10	139.081	2566.86	.297266	4.44748
	2S	7266.76	-6511.54	876.714	33319.10	.447179	3.32006
	1G	1751.54	3105.91	216.293	-1115.50	.287830	5.84084
	2G	6033.70	-4680.72	780.166	486.76	.410960	3.61930
30	1S	1636.77	3737.34	147.707	4171.98	.292691	4.72332
	2S	7135.20	2388.54	653.437	37534.70	.439084	2.47452
	1G	1834.58	461.12	266.008	-3895.63	.301476	7.18336
	2G	6047.24	-7886.48	759.315	4192.92	.411882	3.52257
	1S	1623.21	-363.53	131.008	4632.67	.290266	4.18933
	2S	6968.18	-1612.77	463.592	41278.00	.428806	1.75559

TABLE VI

VIa

Value of n for Stainless Steel tubes at a given $\frac{8\langle u\rangle}{D}$

Concentration	τ_w dynes/cm^2	1S		2S	
		$\frac{8\langle u\rangle}{D}$ sec^{-1}	n	$\frac{8\langle u\rangle}{D}$ sec^{-1}	n
	310	24865.6	124.264	26964.8	130.545
	250	20947.8	116.336	22380.4	108.462
	190	16724.9	106.960	17548.9	83.752
40 ppm.	130	12111.9	95.570	12425.4	55.775
	100	9620.5	88.848	9735.9	40.294
	70	6975.6	81.214	6949.2	23.633
	30	3152.8	69.161	3062.2	-0.731
	310	24757.9	158.579	28410.7	191.785
	250	20896.4	144.439	23474.9	163.558
	190	16723.5	127.599	18311.5	132.507
30 ppm.	130	12148.6	106.957	12886.0	98.063
	100	9668.7	94.666	10061.6	79.343
	70	7027.2	80.601	7154.0	59.472
	30	3189.0	58.135	3134.2	30.950
	310	25531.1	153.070	30052.3	222.890
	250	21503.0	134.198	24716.4	186.080
	190	17162.8	111.896	19179.2	146.305
20 ppm.	130	12424.0	84.841	13415.9	103.089
	100	9865.8	68.889	10440.7	80.017
	70	7151.3	50.794	7396.9	55.846
	30	3230.6	37.255	3223.6	21.740

TABLE VIb

Value of n for Glass tubes at a given $\frac{8\langle u\rangle}{D}$

Concentration	τ_w dynes/cm2	Capillary tube 1G $\frac{8\langle u\rangle}{D}$ sec^{-1}	1G n	Capillary tube 2G $\frac{8\langle u\rangle}{D}$ sec^{-1}	2G n
	310	24279.2	-8.653	27421.6	-11.362
	250	20608.5	-4.550	22854.6	-12.214
	190	16612.2	0.436	18009.3	-13.182
40 ppm.	130	12185.0	6.178	12827.4	-14.300
	100	9758.4	10.561	10085.9	-14.930
	70	7147.0	15.065	7227.2	-15.615
	30	3287.8	22.541	3204.1	-16.639
	310	22518.5	-85.274	27500.0	0.010
	250	19158.3	-76.104	22906.0	-4.197
	190	15489.9	-64.869	18036.7	-8.843
30 ppm.	130	11408.7	-50.554	12835.5	-14.193
	100	9161.6	-41.798	10087.1	-17.196
	70	6732.9	-31.206	7223.8	-20.466
	30	3117.0	-13.491	3199.6	-25.326

APPENDIX (b)

SAMPLE CALCULATIONS USING

COMPUTER PROGRAMS

Program 1

Program to evaluate coefficients A_L & B_L in the equation 3.B.15 (using the method of least square curve fitting)

NOTATIONS

B & C - A_L & B_L, coefficients in the equation 3.B.15

B(I) - ΔP_{cal}, dynes/cm^2

D - $\Delta P_{exp.}$, dynes/cm^2

P - $P_{gas} - P_a$, cms of Hg.

U - <u> , Average velocity, cm/sec

V - Volumetric flow rate, cc/sec

W - G, Average mass rate of flow, gms/sec

X - $\frac{8<u>}{D}$, sec^{-1}

Y - τ_w, dynes/cm^2

L_1 - Length of the tube, cm

L_2 - Head above the tube inlet, cm

Sample calculations for #1 Stainless steel tube (84.364 cms)

```
10  DIM W[10],P[10],Q[10],U[10],D[10],V[10],X[10],Y[10],B[10],T[10]
20  READ N,R1,D1,L1,L2
30  FOR I=1 TO N
40    READ W[I]
50  NEXT I
60  FOR I=1 TO N
70    READ P[I]
80  NEXT I
90  FOR I=1 TO N
95    LET V[I]=W[I]/R1
100    LET U[I]=4*W[I]/(3.14*R1*D1↑2)
110  NEXT I
120  FOR I=1 TO N
130    LET Q[I]=(((13.6*P[I])/L1)+((L1+L2)*R1/L1))
140    LET D[I]=(Q[I]-((1.12*R1*U[I]↑2)/(L1*980.665)))*(L1*980.665)
150  NEXT I
160  FOR I=1 TO N
170    LET X[I]=8*U[I]/D1
180  NEXT I
190  FOR I=1 TO N
200    LET Y[I]=D1*D[I]/(4*L1)
210  NEXT I
220  FOR I=1 TO N
240  NEXT I
250  LET S1= 0
260  LET S2= 0
270  LET S3= 0
280  LET S5= 0
290  LET S6= 0
300  FOR I=1 TO N
310    LET S1=S1+((W[I]↑2)*D[I])
320    LET S2=S2+W[I]*W[I]
330    LET S3=S3+(W[I]↑4)
340    LET S5=S5+(W[I]↑3)
350    LET S6=S6+W[I]*D[I]
360  NEXT I
370  LET B=(S3*S6-S1*S5)/(S3*S2-S5*S5)
380  LET C=(S5*S6-S2*S1)/(S5*S5-S3*S2)
390  LET R2= 0
400  LET R3= 0
405  PRINT "P(I)","W(I)","D(I)","B(I)"
410  FOR I=1 TO N
420    LET B[I]=B*W[I]+C*(W[I]↑2)
430    LET T[I]=D[I]-B[I]
440    PRINT P[I],W[I],D[I],B[I]
450    LET R2=R2+T[I]
460    LET R3=R3+T[I]*T[I]
470  NEXT I
480  LET R2=R2/N
490  LET R3=((R3/N)↑(1/2))
495  PRINT "B","C"
500  PRINT B,C
510  END
```

```
520 DATA 5,.997,.122269,84.364,4.958
530 DATA .54757,.837706,1.06089,1.27372,1.55012
540 DATA 0,3.9,7.1,10.3,14.75
RUN
P(I)            W(I)            D(I)            B(I)
 0               .54757          84886.5         84824.2
 3.9             .837706         133622          133554
 7.1             1.06089         172845          172822
 10.3            1.27372         211470          211714
 14.75           1.55012         264454          264328
B   ≡  A_L      C    ≡   B_L
 146384          15571.3


*READY
```

Program 2

Program to evaluate coefficients A_2, A_3, B_2 and B_3 in the equations 3.B.16 and 3.B.17 (using the method of least square curve fitting)

NOTATIONS

X - L, Length, cm

Y - A_L or B_L coefficients in the equation 3.B.15

C(1) - A_3 or B_3

C(2) - A_2 or B_2

Coefficients in the equations 3.B.16 & 3.B.17

Sample calculations for #1 Stainless steel tubes

```
10  DIM X[200],Y[200],A[11,11],B[11],C[11],P[20]
20  READ M,Z,Q
30  FOR I=1 TO Z
40    READ Y[I]
50  NEXT I
60  FOR I=1 TO Q
70    READ X[I]
80    IF X[I]= 0 GOTO  780
90    IF X[I]=99999 GOTO  110
100 NEXT I
110 LET N9=I-1
120 LET M2=M*2
130 FOR I=1 TO M2
140   LET P[I]= 0
150   FOR J=1 TO N9
160     LET P[I]=P[I]+X[J]↑I
170   NEXT J
180 NEXT I
190 LET N=M+1
200 FOR I=1 TO N
210   FOR J=1 TO N
220     LET K=I+J-2
230     IF K<= 0 GOTO  260
240     LET A[I,J]=P[K]
250     GOTO  270
260     LET A[1,1]=N9
270   NEXT J
280 NEXT I
290 LET B[1]= 0
300 FOR J=1 TO N9
310   LET B[1]=B[1]+Y[J]
320 NEXT J
330 FOR I=2 TO N
340   LET B[I]= 0
350   FOR J=1 TO N9
360     LET B[I]=B[I]+Y[J]*X[J]↑(I-1)
370   NEXT J
380 NEXT I
390 LET N1=N-1
400 FOR K=1 TO N1
410   LET K1=K+1
420   LET L=K
430   FOR I=K1 TO N
440     IF (ABS (A[I,K])- ABS (A[L,K]))<= 0 GOTO  460
450     LET L=I
460   NEXT I
470   IF (L-K)<= 0 GOTO  560
480   FOR J=K TO N
490     LET T1=A[K,J]
500     LET A[K,J]=A[L,J]
510     LET A[L,J]=T1
520   NEXT J
530   LET T1=B[K]
```

```
540     LET B[K]=B[L]
550     LET B[L]=T1
560     FOR I=K1 TO N
570       LET F9=A[I,K]/A[K,K]
580       LET A[I,K]= 0
590       FOR J=K1 TO N
600         LET A[I,J]=A[I,J]-F9*A[K,J]
610       NEXT J
620       LET B[I]=B[I]-F9*B[K]
630     NEXT I
640   NEXT K
650   LET C[N]=B[N]/A[N,N]
660   LET I=N1
670   LET I1=I+1
680   LET S= 0
690   FOR J=I1 TO N
700     LET S=S+A[I,J]*C[J]
710   NEXT J
720   LET C[I]=(B[I]-S)/A[I,I]
730   LET I=I-1
740   IF (I)> 0 GOTO  670
750   FOR I=1 TO N
760     PRINT "C(";I;")=";C[I]
765   NEXT I
770   GOTO  60
780   END
790   DATA  1, 3, 5
800   DATA  146384, 107735, 65867.4
810   DATA  84.364, 61.513, 35.943, 99999, 0

RUN
C( 1 )= 5913.1
C( 2 )= 1662.35


*READY
800   DATA 15571.1,8715.48,8701.56
RUN
C( 1 )= 2566.86
C( 2 )= 139.081


*READY
```

Program 3

Program to evaluate coefficients A and B in the equation 3.B.10 knowing A_2 & B_2 and to evaluate $\frac{8\langle u\rangle}{D}$ for a given τ_w

NOTATIONS

A_1 - A_2 Coefficients in the equations 3.B.16 & 3.B.17

B_1 - B_2

D - Diameter, cm

R_1 - ρ, Density gms/c.c

T - τ_w, dynes/cm^2

X - $\frac{8\langle u\rangle}{D}$, sec^{-1}

Sample calculations for #1 Stainless Steel tube

```
10   DIM T[25],X[25]
20   READ N,A1,B1,D,R1
30   FOR I=1 TO N
40     READ T[I]
50   NEXT I
60   LET A=(A1*3.14*(D↑3)*R1)/32
70   LET B=(B1*((3.14*(D↑3)*R1/32)↑2))
80   PRINT A1,B1,D,A,B
90   FOR I=1 TO N
100     LET X[I]=(-A+((A*A+(16*T[I]*B/D))↑(1/2)))/(2*B)
110     PRINT T[I],X[I]
120   NEXT I
130   END
140   DATA  12, 1662.35, 139.Ø81, .122269, .997
190   DATA  1Ø, 3Ø, 5Ø, 7Ø, 1ØØ, 13Ø, 16Ø, 19Ø, 22Ø, 25Ø, 28Ø, 31Ø
RUN   A1                B1                D              A              B
 1662.35               139.Ø81   8<u>  .122269        .297266        4.44748E-6
 1Ø = τw               1Ø82.97 = ---
                                  D
 3Ø                    3152.81
 5Ø                    5111.63
 7Ø                    6975.63
 1ØØ                   962Ø.52
 13Ø                   12111.9
 16Ø                   14474
 19Ø                   16724.9
 22Ø                   18879
 25Ø                   2Ø947.8
 28Ø                   2294Ø.8
 31Ø                   24865.6

*READY
```

Program 4

Program to evaluate ΔP, $\frac{8\langle u\rangle}{D}$ and τ_w for tubes with high l/D ratio

NOTATIONS

D - $\Delta P_{exp.}$, dynes/cm^2

L_1 - Length of the tube, cm

L_2 - Head above the tube inlet, cm

R_1 - ρ, Density, gm/c.c

U - $\langle u\rangle$, Average velocity, cm/sec

W - G, Average mass rate of flow, gms/sec

X - $\frac{8\langle u\rangle}{D}$, sec^{-1}

Y - τ_w, dynes/cm^2

Sample calculations for #5 Stainless Steel tube

```
10  DIM W[10],P[10],Q[10],U[10],D[10],V[10],X[10],Y[10],B[10],T[10]
20  READ N,R1,D1,L1,L2
30  FOR I=1 TO N
40    READ W[I]
50  NEXT I
60  FOR I=1 TO N
70    READ P[I]
80  NEXT I
90  FOR I=1 TO N
95    LET V[I]=W[I]/R1
100    LET U[I]=4*W[I]/(3.14*R1*D1↑2)
110  NEXT I
120  FOR I=1 TO N
130    LET Q[I]=(((13.6*P[I])/L1)+((L1+L2)*R1/L1))
140    LET D[I]=(Q[I]-((1.12*R1*U[I]↑2)/(L1*980.665)))*(L1*980.665)
150  NEXT I
160  FOR I=1 TO N
170    LET X[I]=8*U[I]/D1
180  NEXT I
190  FOR I=1 TO N
200    LET Y[I]=D1*D[I]/(4*L1)
210  NEXT I
215  PRINT "P(I)","W(I)","D(I)","X(I)","Y(I)"
220  FOR I=1 TO N
230    PRINT P[I],W[I],D[I],X[I],Y[I]
240  NEXT I
510  END
520  DATA  6, .997, .030276, 31.735, 7.022
530  DATA  .015446, .028826, .040509, .052886, .064709, .076937
540  DATA  13.9, 29, 42.7, 57.2, 70.7, 84.8
RUN
P(I)          W(I)          D(I)          X(I)          Y(I)
 13.9          .015446       222761        5689.14       53.1298
 29            .028826       422865        10617.3       100.856
 42.7          .040509       603825        14920.5       144.016
 57.2          .052886       794704        19479.2       189.542
 70.7          .064709       971737        23833.9       231.765
 84.8          .076937       1.15603E+6    28337.8       275.721

*READY
```

Program 5

Program to evaluate A_1 & B_1 coefficients in the equation 3.B.11 (using the method of least square curve fitting)

NOTATIONS

B(I) - $\tau_{w_{cal.}}$, dynes/cm^2

B - A_1

C - B_1

Coefficients in the equation 3.B.11

T(I) - $\tau_{w_{exp.}} - \tau_{w_{cal.}}$, dynes/cm^2

R_2 - Standard deviation

Sample calculations for #5 Stainless Steel tube

```
10  DIM X[100],Y[100],B[100],T[100]
20  READ N
25  FOR I=1 TO N
30    READ Y[I]
40  NEXT I
50  FOR I=1 TO N
60    READ X[I]
70  NEXT I
80  LET S1= 0
90  LET S2= 0
100  LET S3= 0
110  LET S5= 0
120  LET S6= 0
150  FOR I=1 TO N
170    LET S1=S1+((X[I]↑2)*Y[I])
180    LET S2=S2+X[I]*X[I]
190    LET S3=S3+(X[I]↑4)
200    LET S5=S5+(X[I]↑3)
210    LET S6=S6+X[I]*Y[I]
240  NEXT I
340  LET B=(S3*S6-S1*S5)/(S3*S2-S5*S5)
350  LET C=(S5*S6-S2*S1)/(S5*S5-S3*S2)
360  LET R1= 0
370  LET R2= 0
375  PRINT "X(I)","Y(I)","B(I)","T(I)"
380  FOR I=1 TO N
385    LET B[I]=B*X[I]+C*(X[I]↑2)
390    LET T[I]=Y[I]-B[I]
395    PRINT X[I],Y[I],B[I],T[I]
400    LET R1=R1+T[I]
410    LET R2=R2+T[I]*T[I]
420  NEXT I
430  LET R1=R1/N
440  LET R2=((R2/N)↑(1/2))
445  PRINT "B","C","R1","R2"
450  PRINT B,C,R1,R2
460  END
470  DATA  6
480  DATA  53.1289, 100.856, 144.016, 189.542, 231.765, 275.721
490  DATA  1.54463E-2, .028826, 4.05095E-2, 5.28862E-2, 6.47095E-2, .076
```

```
RUN
X(I)              Y(I)              B(I)              T(I)
 1.54463E-2        53.1289           54.2587          -1.1298
 .028826           100.856           101.761          -.905014
 4.05095E-2        144.016           143.623           .392822
 5.28862E-2        189.542           188.357           1.18451
 6.47095E-2        231.765           231.465           .300201
 .076937           275.721           276.429          -.708374
B                 C                 R1                R2
 3492.59           1304.25          -.144276           .841107

*READY
```

Program 6

Program to evaluate coefficient A & B in the equation 3.B.10 knowing A_1 & B_1 and to evaluate $\frac{8\langle u\rangle}{D}$ for a given τ_w

NOTATIONS

A_2 - A_1 Coefficients in the equation 3.B.11

B_2 - B_1

D - Diameter, cm

R_1 - ρ, Density gms/c.c

T - τ_w, dynes/cm^2

X - $\frac{8\langle u\rangle}{D}$, sec^{-1}

Sample calculations for #5 Stainless Steel tube

```
NEW
10  DIM T[25],X[25]
20  READ N,A2,B2,D,R1
30  FOR I=1 TO N
40    READ T[I]
50  NEXT I
52  LET A1=A2*4/D
54  LET B1=B2*4/D
60  LET A=(A1*3.14*(D↑3)*R1)/32
70  LET B=(B1*((3.14*(D↑3)*R1/32)↑2))
76  PRINT A2,B2
80  PRINT A1,B1,D,A,B
90  FOR I=1 TO N
100    LET X[I]=(-A+((A*A+(16*T[I]*B/D))↑(1/2)))/(2*B)
110    PRINT T[I],X[I]
120  NEXT I
130  END
140  DATA  12, 3492.59, 1304.13, .030276, .997
190  DATA  10, 30, 50, 70, 100, 130, 160, 190, 220, 250, 280, 310
RUN
 A1            B1            D             A             B
 3492.59       1304.13
 461433        172299        .030276       1.25279       1.27006E-6
 10            1053.12
 30            3153.45
 50            5244.67
 70            7327.36
 100           10435
 130           13524.1
 160           16593.6
 190           19645.3
 220           22678.8
 250           25694.3
 280           28693.2
 310           31674.1

*READY
```

Program 7

Program to evaluate coefficients in the equation 3.C.10 and to recalculate τ_w for a given $\frac{8(\langle u \rangle - U_w)}{D}$

NOTATIONS

X(I) - $\frac{8(\langle u \rangle - U_w)}{D}$, sec^{-1}

Y(I) - τ_w, $dynes/cm^2$

B - α

C - β

, coefficients in the equation 3.C.10

Sample calculations for #1 Stainless Steel tube

```
10  DIM X[100],Y[100],T[100],K[100],P[100],Q[100]
20  READ N,M
25  FOR I=1 TO N
30    READ Y[I]
40  NEXT I
50  FOR I=1 TO N
60    READ X[I]
70  NEXT I
72  FOR J=1 TO M
74    READ P[J]
76  NEXT J
80  LET S1= 0
90  LET S2= 0
100  LET S3= 0
110  LET S5= 0
120  LET S6= 0
150  FOR I=1 TO N
170    LET S1=S1+((X[I]↑2)*Y[I])
180    LET S2=S2+X[I]*X[I]
190    LET S3=S3+(X[I]↑4)
200    LET S5=S5+(X[I]↑3)
210    LET S6=S6+X[I]*Y[I]
240  NEXT I
340  LET B=(S3*S6-S1*S5)/(S3*S2-S5*S5)
350  LET C=(S5*S6-S2*S1)/(S5*S5-S3*S2)
360  LET R1= 0
370  LET R2= 0
380  FOR I=1 TO N
385    LET K[I]=B*X[I]+C*(X[I]↑2)
390    LET T[I]=Y[I]-K[I]
395    PRINT X[I],Y[I],K[I],T[I]
400    LET R1=R1+T[I]
410    LET R2=R2+T[I]*T[I]
420  NEXT I
421  FOR J=1 TO M
422    LET Q[J]=B*P[J]+C*(P[J]↑2)
424    PRINT P[J],Q[J]
426  NEXT J
430  LET R1=R1/N
440  LET R2=((R2/N)↑(1/2))
450  PRINT B,C,R1,R2
460  END
```

.....contd/....

```
470  DATA  8, 10
480  DATA  310, 250, 190, 130, 100, 70, 50, 30
490  DATA  22389.4, 19406.4, 16129.4, 12105.4, 9721.6, 7271.07
500  DATA  5387.42, 3442.93
510  DATA  1100, 1500, 2200, 3500, 5000, 7000, 10000, 14000, 20000
520  DATA  30000
```

RUN $\frac{8(\langle u\rangle - U_w)\tau_w}{D}$	τ_w	$\tau_{w_{cal.}}$	
22389.4	310	308.008	1.99158
19406.4	250	250.558	-.558167
16129.4	190	193.261	-3.26114
12105.4	130	131.233	-1.23288
9721.6	100	98.8192	1.18085
7271.07	70	68.8572	1.14281
5387.42	50	48.1415	1.85848
3442.93	30	28.8674	1.1326
1100	8.49221		
1500	11.7504		
2200	17.6706		
3500	29.4025		
5000	44.1303		
7000	65.7521		
10000	102.438		
14000	159.293		
20000	261.588		
30000	477.447		
7.40828E-3	2.83559E-7	.281765	1.72735
B	C		

```
*READY
```

Program 8

Program to calculate n for various $\frac{8\langle u\rangle}{D}$ at a given shear stress, knowing A_2, B_2, A, & B.

NOTATIONS

A_1 - A_2 Coefficients in the equations 3.B.16 & 3.B.17

B_1 - B_2

A - A Coefficients in the equation 3.B.10

B - B

D - Diameter, cm

R_1 - ρ, Density, gm/c.c

T(I) - τ_w, Dynes/cm^2

X(I) - $\frac{8\langle u\rangle}{D}$, sec^{-1}

M(I) - n, entrance length correction factor

Sample calculations for #1 Stainless Steel tube

```
10  DIM T[25],X[25],M[25]
20  READ N,A1,B1,D,R1,A2,B2
30  FOR I=1 TO N
40    READ T[I]
50  NEXT I
60  LET A=(A1*3.14*(D↑3)*R1)/32
70  LET B=(B1*((3.14*(D↑3)*R1/32)↑2))
72  LET A3=A2*3.14*(D↑3)*R1/32
74  LET B3=B2*((3.14*(D↑3)*R1/32)↑2)
80  PRINT A1,B1,D,A,B,A3,B3
90  FOR I=1 TO N
100    LET X[I]=(-A+((A*A+(16*T[I]*B/D))↑(1/2)))/(2*B)
105    LET M[I]=(A3*X[I]+B3*(X[I]↑2))/(2*T[I])
110    PRINT T[I],X[I],M[I]
120  NEXT I
130  END
140  DATA  12, 1662.35, 139.081, .122269, .997, 5913.1, 2566.86
190  DATA  10, 30, 50, 70, 100, 130, 160, 190, 220, 250, 280, 310
RUN  A1              B1              D               A               B
 1662.35          139.081          .122269          .297266         4.44748E-6
 1.05739 - A3     8.20821E-5 - B3
 10               1082.97          62.0699
 30               3152.81          69.1613
 50               5111.63          75.4968
 70               6975.63          81.2143
 100  τw          9620.52 8<u>/D   88.8483  M(I)=n
 130              12111.9          95.5704
 160              14474            101.563
 190              16724.9          106.96
 220              18879            111.858
 250              20947.8          116.336
 280              22940.8          120.455
 310              24865.6          124.264

*READY
```

Program 9

Program to evaluate of U_w, δ and η_w for a given shear stress, knowing α, β, A, &B.

NOTATIONS

A - α
B - β
Coefficients in the equation 3.C.10

A_1 - A
B_1 - B
Coefficients in the equation 3.B.10

D - Diameter, cm

T - τ_w, dynes/cm^2

Z(I) - Non-Newtonian viscosity, gm/cm.sec

D(I) - ,Anomalous layer thickness, cm

U(I) - U_w, cm/sec

W(I) - $\frac{8U_w}{D}$, sec^{-1}

X(I) - $8(<u>-U_w)/D$, sec^{-1}

Y(I) - $8<u>/D$, sec^{-1}

Sample calculations for #1 Stainless Steel tube

```
10  DIM X[20],T[20],Y[20],W[20],U[20],Z[20],D[20]
20  READ N,D,V,A,B,A1,B1
30  FOR I=1 TO N
40    READ T[I]
50  NEXT I
60  FOR I=1 TO N
70    LET X[I]=(-A+((A*A+4*B*T[I])↑(1/2)))/(2*B)
75    LET Z[I]=(A+B*X[I])*(4*A+8*B*X[I])/(4*A+7*B*X[I])
80    LET Y[I]=(-A1+((A1*A1+(16*B1*T[I]/D))↑(1/2)))/(2*B1)
90    LET W[I]=Y[I]-X[I]
100    LET U[I]=(W[I]*D)/8
102    IF U[I]<= 0 GOTO 106
104    LET D[I]=(U[I]*V*Z[I])/(T[I]*(Z[I]-V))
105    GOTO 110
106    LET D[I]=-(U[I]*Z[I]/T[I])
110    PRINT T[I],Y[I],X[I],W[I],U[I],Z[I],D[I]
120  NEXT I
130  END
140  DATA  8, .122269, .008937, 7.40828E-3, 2.83559E-7, .297266, 4.4474E
150  DATA  310, 250, 190, 130, 100, 70, 30, 10
```

RUN	$8\langle u\rangle/D$	$\frac{8\langle u\rangle - U_w)}{D}$	$8U_w/D$	U_w
310	24865.6	22488.2	2377.36	36.3346
τ_w				
1.49686E-2	2.59956E-3			
$-\eta_w$		δ		
250	20947.8	19376	1571.72	24.0216
1.39436E-2	2.39158E-3			
190	16724.9	15931.8	793.082	12.1212
1.28054E-2	1.88731E-3			
130	12111.9	12018.9	93.0176	1.42165
1.15055E-2	4.37789E-4			
100	9620.5	9812.79	-192.295	-2.93896
1.07682E-2	3.16472E-4			
70	6975.62	7369.95	-394.334	-6.02685
9.94654E-3	8.56376E-4			
30	3152.82	3563.52	-410.702	-6.27701
8.6505E-3	1.80997E-3			
10	1082.96	1286.52	-203.561	-3.11115
7.86118E-3	2.44573E-3			

```
*READY
```